Tel1p and Mec1p Regulate Chromosome Segregation and Chromosome Rearrangements in *Saccharomyces cerevisiae*

by

Jennifer Lynn McCulley

Department of Pharmacology and Cancer Biology
Duke University

Date:_____
Approved:

_____
Dr. Thomas D. Petes, Chair

_____
Dr. Sue Jinks-Robertson

_____
Dr. Daniel J. Lew

_____
Dr. Steven B. Haase

_____
Dr. Christopher M. Counter

Dissertation submitted in partial fulfillment of
the requirements for the degree of Doctor
of Philosophy in the Department of
Pharmacology and Cancer Biology in the Graduate School
of Duke University

2010

ABSTRACT

Tel1p and Mec1p Regulate Chromosome Segregation and Chromosome Rearrangements in *Saccharomyces cerevisiae*

by

Jennifer Lynn McCulley

Department of Pharmacology and Cancer Biology
Duke University

Date:_____
Approved:

_____
Dr. Thomas D. Petes, Chair

_____
Dr. Sue Jinks-Robertson

_____
Dr. Daniel J. Lew

_____
Dr. Steven B. Haase

_____
Dr. Christopher M. Counter

An abstract of a dissertation submitted in partial
fulfillment of the requirements for the degree
of Doctor of Philosophy in the Department of
Pharmacology and Cancer Biology in the Graduate School
of Duke University

2010

Copyright by

Jennifer Lynn McCulley

2010

Abstract

Cancer cells often have elevated frequencies of chromosomal aberrations, and it is likely that loss of genome stability is one driving force behind tumorigenesis. Deficiencies in DNA replication, DNA repair, or cell cycle checkpoints can all contribute to increased rates of chromosomal duplications, deletions and translocations. The human ATM and ATR proteins are known to participate in the DNA damage response and DNA replication checkpoint pathways and are critical to maintaining genome stability. The *Saccharomyces cerevisiae* homologues of ATM and ATR are Tel1p and Mec1p, respectively. Because Tel1p and Mec1p are partially functionally redundant, loss of both Tel1p and Mec1p in haploid yeast cells (*tel1 mec1* strains) results in synergistically elevated rates of chromosomal aberrations, including terminal duplications, chromosomal duplications, and telomere-telomere fusions. To determine the effect of Tel1p and Mec1p on chromosome aberrations that cannot be recovered in haploid strains, such as chromosome loss, I investigated the phenotypes associated with the *tel1 mec1* mutations in diploid cells. In the absence of induced DNA damage, *tel1 mec1* diploid yeast strains exhibit extremely high rates of aneuploidy and chromosome rearrangements. There is a significant bias towards trisomy of chromosomes II, VIII, X, and XII, whereas the smallest chromosomes I and VI are commonly monosomic.

The telomere defects associated with *tel1 mec1* strains do not cause the high rates of aneuploidy, as restoring wild-type telomere length in these strains by expression of the Cdc13p-Est2p fusion protein does not prevent cells from becoming aneuploid. The *tel1 mec1* diploids are not sensitive to the microtubule-destabilizing drug benomyl, nor do they arrest the cell cycle in response to the drug, indicating that the spindle assembly checkpoint is functional. The chromosome missegregation phenotypes of *tel1 mec1* diploids mimic those observed in mutant strains that do not achieve biorientation of sister chromatids during mitosis.

The chromosome rearrangements in *tel1 mec1* cells reflect both homologous recombination between non-allelic Ty elements, as well as non-homologous end joining (NHEJ) events. Restoring wild-type telomere length with the Cdc13p-Est2p fusion protein substantially reduces the levels of chromosome rearrangements (terminal additions and deletions of chromosome arms, interstitial duplications, and translocations). This result suggests that most of the rearrangements in *tel1 mec1* diploids are initiated by telomere-telomere fusions. One common chromosome rearrangement in *tel1 mec1* strains is an amplification of sequences on chromosome XII between the left telomere and rDNA sequences on the right arm. I have termed this aberration a "schromosome." Preliminary evidence indicates that the schromosome exists in the *tel1 mec1* cells as an uncapped chromosome fragment that gets resected over time.

Dedication

This thesis is dedicated to my ever-supportive family and friends who were there for me every step of the way. I am especially grateful to my parents Charles Robert McCulley and Judith Ann McCulley. I could not have achieved this degree without their unwavering love and encouragement. I would also like to dedicate this thesis to my late grandfather, George Robert Stewart, who was always supportive of all of my endeavors.

Contents

List of Tables

List of Figures

List of Abbreviations

APC	anaphase-promoting complex
A-T	Ataxia Telangiectasia
ATM	mutated in Ataxia Telangiectasia
ATR	ATM and Rad3-related
BIR	break-induced replication
CGH	comparative genome hybridization
CHEF	contour-clamped homogeneous electric field
CIN	chromosome instability
DDR	DNA damage response
DSB	double-strand break
DSBR	double-strand break repair
DRC	DNA replication checkpoint
FEAR	Cdc14p early anaphase release
GCR	gross chromosomal rearrangement
HR	homologous recombination
LOH	loss of heterozygosity
LTR	long-terminal repeat
MEN	mitotic exit network
MIN	microsatellite instability
MRX	Mre11-Rad50-Xrs2
NHEJ	non-homologous end joining
NTS	non-transcribed spacer
ORF	open reading frame
PCR	polymerase chain reaction

rDNA	ribosomal DNA
RFB	replication fork block
RNR	ribonucleotide reductase
RPA	replication protein A
S. cerevisiae	*Saccharomyces cerevisiae*
SAC	spindle assembly checkpoint
SC	sister chromatid
SDSA	synthesis-dependent strand annealing
SPB	spindle pole body
SSA	single-strand annealing
ssDNA	single-stranded DNA
TTF	telomere-telomere fusion

Acknowledgements

I am especially grateful to my advisor, Dr. Thomas Petes, who gave me a chance to pursue my doctoral degree in his lab and helped me to develop into a (more or less) competent scientist. Many of the hypotheses and experiments described in this thesis developed as the result of regular and frequent conversations about my project, often on weekends. I am very fortunate to have trained with such a supportive, motivating, experienced, and knowledgeable mentor. Dr. Petes truly cares about the achievements of his students and helps in every way possible to ensure their success.

I give many, many thanks to all members of the Petes laboratory for useful discussions, technical expertise, and for making the lab environment pleasant and fun. Patricia Greenwell helped me get started in the lab, and along with Malgorzata Dominska and Malgorzata Gawel, assisted me with technical procedures. Juan Lucas Argueso, Anne Casper, Piotr Mieczkowski, and Wei Song were invaluable colleagues who helped me plan experiments, imparted a lot of expert technical advice, and helped me trouble-shoot experimental difficulties. I credit my fellow graduate students Phoebe Lee and Jordan St. Charles with lively and engaging discussions about genome stability (and other non-scientific topics) and for empathizing when experiments were not working.

I am also indebted to my committee members Sue Jinks-Robertson, Daniel Lew, Steven Haase, and Christopher Counter for their guidance and critical thinking about my project. Stephen Elledge and Victoria Lundblad graciously supplied plasmids for my thesis research.

Finally, I would like to acknowledge the support and encouragement of all of my friends and family. They stood by me through the ups and downs of graduate school and encouraged me to keep going even when I felt like I was not making sufficient

progress. My parents, Robert and Judith, and brothers, Mark and Ryan, believed in me more than I did and would always remind me that I could achieve this goal. My boyfriend John Royal has been unbelievably supportive as well as extremely patient and understanding, especially when "date nights" consisted of reading scientific papers and writing manuscripts. I could not have made it through this long journey without all of my friends, with whom I spent hours on long runs, bike rides, or on the phone venting about hypotheses and experiments. I am also very thankful for my dog Kona and horse Flash, who required that I maintain an adequate work-life balance and could always lift my spirits with their playful antics.

1. Introduction

Although a high level of genetic instability is a characteristic of cells in most solid tumors, the mechanism that generates this instability is not well understood. In my thesis research, I investigated the roles of two yeast proteins, Tel1p and Mec1p, in regulating genome stability in diploid cells. I showed that mutations in the genes encoding these proteins result in a high level of chromosome rearrangements (primarily reflecting homologous recombination between ectopic repeats) and aneuploidy. I found that the mechanisms responsible for these two mutant phenotypes were different. The chromosome rearrangements were initiated by fusions between telomeres. The aneuploidy was unrelated to telomere dysfunction or a defective spindle assembly checkpoint, but likely reflects a role of Tel1p and Mec1p at the kinetochore. Below, I review background information concerning the relationship between genome instability and cancer, the roles of Tel1p and Mec1p in relating genome stability, and several other relevant topics.

1.1 Genome instability and cancer

Many solid tumors contain genome aberrations such as duplication or loss of entire chromosomes (aneuploidy), reciprocal or non-reciprocal translocations between chromosomes, and interstitial or terminal amplification of single genes or large regions within a chromosome (Albertson *et al.*, 2003). Since cell viability requires that genetic information be transferred faithfully between generations, cells have evolved many mechanisms to control the level of genetic deletions, duplications, and chromosome rearrangements. Deficiencies in any process involved in the duplication, transmission, or repair of the genetic material (including high-fidelity DNA replication, telomere maintenance, DNA damage repair, and functional mitotic checkpoints) may lead to genome instability and thus contribute to tumorigenesis.

1.1.1 Types of genetic instability in tumors

The rate of spontaneous mutations is too low to account for the large number of genetic changes observed in most cancers. According to the mutator hypothesis, an early step in tumorigenesis is the acquisition of a mutator phenotype, which serves to destabilize the genome and facilitate the accumulation of further mutations that directly deregulate cellular growth controls (Loeb, 1991). Cancer cells that have rapidly changing karyotypes are called CIN tumors (chromosome instability; Lengauer *et al.*, 1998). Although the causal mutation or mutations in CIN tumors have not been identified for most tumors of this class, some mutations have been observed in genes that participate in the spindle assembly checkpoint (SAC; for review see Kops *et al.*, 2005). The other type of genetic instability, microsatellite instability (MIN), is present only in a small fraction of tumors and is caused by mutations in the mismatch repair pathway (Boyer *et al.*, 1995). The identification of the causal role of mutations in the mismatch repair pathway in the generation of MIN tumors is a clear validation of Loeb's mutator hypothesis.

While most solid tumors show a high degree of aneuploidy, it is still debated as to whether the aneuploidy is a cause of tumorigenesis, or a secondary consequence of the unregulated growth associated with metastatic tumors. Several arguments support the hypothesis that aneuploidy may be linked causally to tumorigenesis. First, aneuploidy is observed early in the process of tumorigenesis (Shih *et al.*, 2001), suggesting that aneuploidy may directly influence the rate of tumor growth. Second, in a study in Chinese hamster embryo cells, the degree of aneuploidy correlated with the rate of chromosome rearrangements (deletions, duplications and translocations; (Duesberg *et al.*, 1998). Third, mathematical models describing the onset of colorectal cancer are consistent with tumor cells acquiring a CIN phenotype prior to the loss of tumor suppressors to facilitate oncogenic initiation (Nowak *et al.*, 2002).

Conversely, some research indicates that aneuploidy can act as a barrier to tumorigenesis (Williams *et al.*, 2008). In one experiment, researchers generated mouse cell lines that possessed an extra copy of a single chromosome. They demonstrated that the metabolic properties of the cells were altered; cellular proliferation decreased, and tumorigenesis was impaired in the aneuploid cells. To explain the observation that most metastatic tumors are composed of highly aneuploid cells, Williams and Amon suggested that, although most aneuploid cells are incapable of generating a tumor, the cellular stress associated with aneuploidy facilitates a higher mutation rate and tumorigenesis in a very small number of cells (Williams and Amon, 2009). These mutator cells continue to accumulate additional alterations, leading to cancer.

1.1.2 Pathways affecting genome stability are dysregulated in cancer cells

Malignant oncogenesis arises as a result of progressive dysregulation of six independent cellular pathways that control cell growth: most cancer cells activate telomerase, become insensitive to growth inhibitory signals, overproduce positive growth signals, avoid apoptosis, increase the capacity for angiogenesis, and, consequently, become metastatic (Hanahan and Weinberg, 2000). Two of these pathways relevant to my thesis will be described in detail below.

1.1.2.1 Dysfunctional telomere regulation

The state of the telomeres is particularly important in preventing oncogenesis in two different ways. First, in normal mammalian tissues, telomerase (the enzyme involved in the elongation of telomeres) is inactive and telomeres progressively shorten during each cell division. After many divisions in cell culture, telomeres reach a critically short length and the cells containing these short telomeres are eliminated through apoptosis (Linskens *et al.*, 1995). Thus, the lack of telomerase in normal cells restricts their potential for unlimited growth. In contrast, telomerase is activated in

about 90% of tumor cells (Kim *et al.*, 1994). This activation allows for the large number of cell divisions required to form a tumor.

Abnormal telomeres can also contribute to genetic instability by a different mechanism. Although most tumors have activated telomerase, telomeres in cancer cells are generally shorter than those of normal cells and are structurally abnormal as well (Feldser *et al.*, 2003; Hackett and Greider, 2002). These abnormal telomeres have an elevated frequency of telomere-telomere fusions, resulting in the creation of dicentric chromosomes. Subsequent breakage of the dicentric chromosome can result in genetic instability by repeated breakage-fusion-bridge cycles. As described below, mutations affecting telomere length also result in elevated rates of genetic instability in *Saccharomyces cerevisiae*.

1.1.2.2 Defective response to growth inhibitory signals

Aberrant expression of telomerase alone is insufficient for tumorigenesis; additional changes are required (Kendall *et al.*, 2005). For example, the DNA damage response (DDR) is activated early in carcinogenesis, most likely due to aberrant replication intermediates. This activation is thought to protect the genome from mutations or other genetic alterations that would otherwise set the cell on the path to transformation (Bartkova *et al.*, 2005; Gorgoulis *et al.*, 2005). Components of the DDR are often disabled in metastatic tumors. For example, the majority of tumors lack the p53 tumor suppressor protein; p53 responds to DNA damage to arrest the cell cycle and promote apoptosis if timely repair is not achieved (Hollstein *et al.*, 1991; Levine, 1997). In summary, the DDR plays an important role in preventing cellular transformation early in the process, but selective pressure results in suppression of the DDR in later stages of tumor growth.

1.1.3 ATM and ATR

There are many diseases that cause, among other pathophysiological conditions, a predisposition to early-onset cancer. Ataxia Telangiectasia (A-T) is one such disease. Patients with A-T develop cerebellar neurodegeneration, immunodeficiency, and are predisposed to developing lymphatic malignancies (Ahmed and Rahman, 2006; Kastan and Bartek, 2004; Renwick *et al.*, 2006). This disease is the result of homozygous mutations in the ATM (Mutated in Ataxia Telangiectasia) protein, which, along with the related protein ATR (ATM and Rad3-related), is involved in the regulation of many cellular processes, including the DNA damage response (DDR), DNA replication checkpoint (DRC), and telomere maintenance (Cimprich and Cortez, 2008; Jeggo and Lobrich, 2006; Metcalfe *et al.*, 1996). Cells from patients with A-T are radiosensitive, have very short telomeres, and often contain chromosomes with telomere-telomere fusions (Kojis *et al.*, 1989; Metcalfe *et al.*, 1996; Takagi *et al.*, 1998).

Up to 30% of individuals with A-T develop lymphoid tumors (Lavin, 2008), and heterozygous mutations in ATM increase breast cancer susceptibility (Swift *et al.*, 1987). Importantly, the estimated prevalence of heterozygous ATM mutations in the human population is approximately 1% (Renwick *et al.*, 2006). Thus, a substantial number of sporadic breast cancers may have a genetic basis related to heterozygous ATM mutations. One of the larger studies of heterozygous carriers confirmed that there was an almost 5-fold increase in relative risk for breast cancer among women under 50 years of age (Thompson *et al.*, 2005).

While ATM is not essential for growth in mammals, the lack of the related kinase ATR is lethal in both mice and humans (Brown and Baltimore, 2000; de Klein *et al.*, 2000). ATR is thought to play an important role in normal cell cycle progression as well as coordinating the cellular response to DNA damage (Cimprich and Cortez, 2008). Patients with the rare disease Seckel Syndrome have mutations in the ATR gene, and

this results in phenotypes of microcephaly and dwarfism (O'Driscoll *et al.*, 2003). Additionally, cells from Seckel patients accumulate chromosome breaks at common fragile sites in the genome, suggesting elevated levels of genome instability (Casper *et al.*, 2004). As described below, some of the phenotypes associated with human cells with ATM and ATR mutations (telomere abnormalities, sensitivity to DNA damaging agents, and elevated levels of chromosome breaks) are recapitulated in yeast strains with mutations in the homologous *TEL1* and *MEC1* genes.

1.2 Roles of Tel1p and Mec1p in regulating genome stability

1.2.1 Relationship of Tel1p and Mec1p to ATM and ATR

The *Saccharomyces cerevisiae* homologues of ATM and ATR are Tel1p and Mec1p, respectively, and these proteins are involved in maintaining genome stability in yeast as central mediators of the DNA damage and replication checkpoints and telomere maintenance (Ritchie *et al.*, 1999; Zhou and Elledge, 2000). *TEL1* was originally isolated as a mutant that had very short (50 bp) telomeres (Greenwell *et al.*, 1995; Lustig and Petes, 1986), while *MEC1* was identified as causing sensitivity to DNA damaging agents when mutated (Kato and Ogawa, 1994). Although the phenotypes associated with the *tel1* and *mec1* mutations are not identical to those associated with mutations of ATM and ATR in mammalian cells, Fritz *et al.* (2000) made the striking observation that the *TEL1* gene, when transformed into an A-T cell line, could complement many of the mutant phenotypes associated with the ATM mutation.

Tel1p and Mec1p are structurally related serine/threonine kinases that belong to the phosphatidylinositol 3 (PI3) kinase-like family. They are partially functionally redundant, as *TEL1* has been shown to partly restore the DNA damage checkpoint in cells with a *mec1* deficiency (Clerici *et al.*, 2004), and cells lacking *tel1* and *mec1* are more sensitive to DNA damaging agents than either single mutant (Morrow *et al.*, 1995).

Because of this redundancy in function, *tel1* or *mec1* mutations alone demonstrate low or moderate effects on genome stability in mutational assays in yeast, but a deficiency of both genes leads to synergistically elevated levels of genome instability events (Craven *et al.*, 2002; Mieczkowski *et al.*, 2003; Myung *et al.*, 2001b). For example, *tel1 mec1-1* cells show a synergistically high forward mutation rate, an increased rate of deletions, and formation of dicentric and circular chromosomes (Craven *et al.*, 2002). A more extended discussion of the chromosome abnormalities observed in strains lacking Tel1p and Mec1p will be given below.

1.2.2 Tel1p and Mec1p regulate the DNA damage response through multiple pathways

1.2.2.1 Activation of Tel1p and Mec1p by DNA damage

In response to DNA damage such as a double-strand break (DSB), Tel1p and Mec1p are recruited to the site of the break, where they initiate a signal transduction cascade that results in phosphorylation and activation of effector proteins, transcription of DNA repair genes, and cell cycle arrest (Putnam *et al.*, 2009b). This coordinated response of DNA repair and cell cycle arrest elicited by Tel1p and Mec1p ultimately ensures that the DNA has time to be repaired prior to mitosis. Failure to repair a DSB before chromosome segregation would result in loss of a chromosome or chromosome fragment.

Tel1p and Mec1p are directed to two different types of DNA damage, although there may be some functional overlap. Tel1p is thought to respond to an unprocessed DSB, such as that generated initially by ionizing radiation (Kitagawa and Kastan, 2005). As shown in Fig. 1.1, the Mre11-Rad50-Xrs2 (MRX) complex recognizes broken chromosome ends and recruits Tel1p to the site of the break (Nakada *et al.*, 2003). While the activation mechanism for Tel1p is not completely elucidated, it is known that the Tel1p homologue ATM exists as a dimer in human cells. DNA damage causes the

autophosphorylation of the inactive ATM dimer, which dissociates ATM into active monomers that are competent to phosphorylate target proteins (Bakkenist and Kastan, 2003). Mec1p, in contrast, is activated in response to large regions of single-stranded DNA (ssDNA) that arise due to uncoupling of the helicase from the polymerase at stalled replication forks, or through extensive resection of broken chromosome ends to generate long single-stranded overhangs (Zou and Elledge, 2003). These long single-stranded regions are coated with the ssDNA-binding replication protein A (RPA), which recruits Mec1p through its accessory protein Ddc2p (Brush *et al.*, 1996; Zou and Elledge, 2003). Localization of the specialized DNA damage clamp 9-1-1 (Rad17p-Ddc1p-Mec3p) complex to the site of DNA damage occurs independently of Mec1p-Ddc2p (Kondo *et al.*, 2001; Melo *et al.*, 2001). Colocalization of Mec1p-Ddc2p and 9-1-1 is sufficient for activation of the DNA damage response (Bonilla *et al.*, 2008). The replication protein Dpb11p can also activate Mec1p at sites of DNA damage, and this activation is synergistic with that of 9-1-1 (Mordes *et al.*, 2008; Navadgi-Patil and Burgers, 2008).

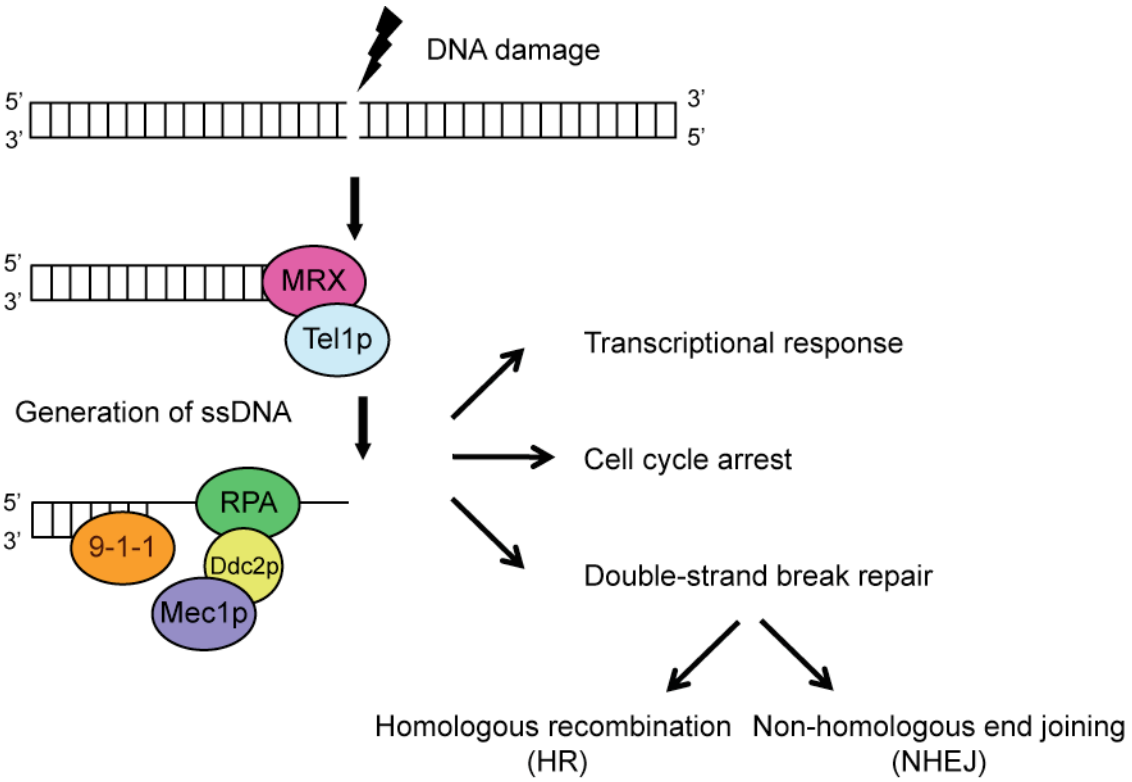

Figure 1.1 Model for the cellular response to DNA damage.

DNA damaging agents such as ionizing radiation creates DSBs within the DNA. The DSBs are detected by the Mre11p-Rad50p-Xrs2p (MRX) complex, which activates Tel1p to initiate the DNA damage response. MRX can also resect the end of the DSB, exposing regions of ssDNA which is coated with replication protein A (RPA) and subsequently recruits Mec1p-Ddc2p. Localization of the DNA damage clamp 9-1-1 also activates the DDR. In addition to resected ends, stalled replication forks can generate RPA-coated regions of ssDNA that lead to Mec1p activation.

1.2.2.2 Cell cycle arrest mediated byTel1p and Mec1p

The cell can be halted at various "checkpoints" depending on when the DNA damage occurs during the cell cycle and the type of activating lesion. The role of Telp1 and Mec1p in activating the G1/S, intra-S, and replication checkpoints has been well characterized (Elledge, 1996; Putnam *et al.*, 2009b). Once recruited to the break site, Tel1p and Mec1p phosphorylate many substrates to elicit the DDR cascade (Smolka *et al.*, 2007). In addition to RPA (Brush *et al.*, 1996), a primary target of Mec1p is Rad9p, which amplifies the DDR signal by stimulating Mec1p-dependent phosphorylation of the effector kinases Rad53p and Chk1p (Emili, 1998; Toh and Lowndes, 2003; Vialard *et*

al., 1998). The phosphorylation of Chk1p begins the process of cell cycle arrest (Schollaert *et al.*, 2004). This arrest is accomplished through Chk1p-dependent phosphorylation of Pds1p (also known as securin), which blocks the ubiquitination and degradation of Pds1p by the anaphase-promoting complex (APC; Sanchez *et al.*, 1999). Pds1p inhibits the metaphase to anaphase transition by sequestering the separase protein Esp1p, thus preventing the cleavage of cohesin and separation of sister chromatids that normally happens in anaphase (Sanchez *et al.*, 1999; Wang *et al.*, 2001). Rad53p also contributes to the prevention of Pds1p degradation by inhibiting the Pds1p-Cdc20p interaction (Agarwal *et al.*, 2003). The cell cycle arrest incurred by preventing the degradation of Pds1p through phosphorylation by Tel1p and Mec1p allows the cell time to repair the DNA damage, to complete replication, and to avoid a catastrophic mitosis.

In addition to preventing premature sister chromatid separation, Tel1p and Mec1p prevent spindle elongation through the action of downstream effector Rad53p and its phosphorylation target Cdc5p (Zhang *et al.*, 2009). In *rad53* cells, elongated spindles lead to unequal segregation of DNA (Bachant *et al.*, 2005). These elongated spindles are a consequence of aberrantly high levels of microtubule motor proteins Kip1p and Cin8p, which are negatively regulated by APC subunit Cdh1p (Zhang *et al.*, 2009). In response to DNA damage, Mec1p phosphorylates Rad53p, which inhibits Cdc5p-mediated inhibition of Cdh1p, thus keeping Kip1p and Cin8p levels low and restraining spindle elongation. Rad53p and Chk1p also regulate the mitotic exit network (MEN) and the Cdc14p early anaphase release (FEAR) pathways, respectively, to inhibit mitotic exit in response to DNA damage (Liang and Wang, 2007).

1.2.2.3 Transcriptional activation of DNA repair genes by Tel1p and Mec1p in response to DNA damage

The transcriptional response to DNA damage is largely indicative of a general stress response, but certain DNA repair-specific genes are upregulated in a Mec1p-dependent manner (Gasch *et al.*, 2001). As described above, Telp1 and Mec1p

phosphorylate Rad53p when responding to DSBs, and a phosphorylation target of Rad53p is the protein kinase Dun1p (Chen *et al.*, 2007). The transcription of DNA repair genes is elicited through the activated Dun1p, which de-represses numerous genes important in responding to DNA damage. For example, Dun1p phosphorylates the transcriptional repressor Crt1p in response to DNA damage (Fu *et al.*, 2008). Under normal circumstances, Crt1p inhibits the transcription of the four ribonucleotide reductase (*RNR*) genes that are responsible for regulating the pools of nucleotides. In response to DNA damage, elevated nucleotide levels are necessary to promote repair synthesis and to re-start stalled replication forks (Desany *et al.*, 1998). When Crt1p is phosphorylated by Dun1p, it no longer represses the transcription of the *RNR* genes and nucleotide production is elevated.

Tel1p and Mec1p also indirectly regulate the RNR inhibitor Sml1p in response to DNA damage to further elevate nucleotide levels. Phosphorylation of Sml1p by Dun1p targets Sml1p for degradation (Zhao and Rothstein, 2002). Sml1p is an inhibitor of Rnr1p, the large subunit of RNR (Zhao *et al.*, 2000). As described above, Tel1p and Mec1p are indirectly required to degrade Sml1p because they are required for Rad53p phosphorylation, which activates Dun1p. Thus, through multiple pathways, Tel1p and Mec1p ensure that there are adequate nucleotide pools to repair DNA damage.

1.2.2.4 Interactions between Tel1p and Mec1p and DSB-repair pathways

Once localized to the site of DNA damage, Tel1p and Mec1p signal to downstream effectors that recruit DNA repair proteins. One important phosphorylation target is the histone H2A, which marks damaged chromatin (Rogakou *et al.*, 1998). Phosphorylation by Tel1p and Mec1p on serine 129 of H2A occurs rapidly in response to DNA damage, and this phosphorylation is required for the efficient repair of DNA damage (Downs *et al.*, 2000); the phosphorylated form of H2A is called "γH2A." Mec1p-independent phosphorylation of H2A on serine 122 is also important for the DDR

(Harvey *et al.*, 2005). γH2A forms foci at the site of DSBs and acts to recruit repair factors such as Rad52p (Barlow and Rothstein, 2009) as well as to activate Rad9p and Rad53p (Toh and Lowndes, 2003; Toh *et al.*, 2006). γH2A is also required for damage-induced cohesin binding to prevent premature dissolution of sister chromatids while repair is ongoing (Strom *et al.*, 2007; Unal *et al.*, 2007). Finally, γH2A recruits the INO80 chromatin remodeling complex to DNA, where the Ies4p subunit is a phosphorylation substrate of Mec1p; this recruitment is also important for the efficient repair of DNA damage (Downs *et al.*, 2004; Morrison *et al.*, 2007).

1.2.3 Genetic instability observed in strains of the *tel1 mec1* genotype

Tel1p and Mec1p are related proteins with discrete functions, but which also have some functional overlap. *TEL1* was originally isolated as a mutant that had very short telomeres (Greenwell *et al.*, 1995; Lustig and Petes, 1986), while *MEC1* was identified as a gene causing sensitivity to DNA damaging agents when mutated (Kato and Ogawa, 1994). The argument that these two proteins are functionally redundant is partly based on the observations that the double mutant *tel1 mec1* strains are more sensitive to DNA damage than either single mutant strain (Morrow *et al.*, 1995) and have a more profound telomere defect (Ritchie *et al.*, 1999). In addition, the double mutant strains have synergistically elevated levels of genome instability in a variety of assays (described below) including telomere length, mitotic chromosome loss, mitotic recombination, rates of gross chromosome rearrangements (GCR), rates of *CAN1* deletions, formation of telomere-telomere fusions, and frequencies of chromosome rearrangements.

The *tel1* strain was originally described as a mutant that reduced telomere length from the wild-type length of about 400 bp to about 50 bp (Lustig and Petes, 1986). The Petes lab subsequently showed that the hypomorphic *mec1-21* allele reduced telomere

lengths by about 50 bp (Ritchie *et al.*, 1999). Double mutant *tel1 mec1* strains have very short telomeres and undergo cellular senescence (Ritchie *et al.*, 1999). Occasional survivors of the senescence process elongate their telomeres by a Rad52p-dependent recombination process (Ritchie *et al.*, 1999). This telomere phenotype of the double mutant strains mimics that observed in yeast cells deficient in the telomerase RNA *TLC1*. Subsequently, *TEL1* was shown to participate in the recruitment of telomerase proteins Est1p and Est2p to the telomeres (Goudsouzian *et al.*, 2006). In addition, the single-stranded telomere binding protein Cdc13p was identified as a phosphorylation target of Tel1p and Mec1p (Tseng *et al.*, 2006).

When strains with the temperature-sensitive *mec1-4* allele are incubated at the restrictive temperature, DSBs are observed by contour-clamped homogeneous electric field (CHEF) gel analysis; these DSBs occur in regions of the chromosome that are replicated slowly even in wild-type strains, supporting a role for *MEC1* in stabilization of the replication fork in hard-to-replicate regions of the genome (Cha and Kleckner, 2002). Most mutants that have high levels of DSBs have high levels of mitotic recombination and chromosome loss. Craven *et al.* (2002) measured mitotic recombination and chromosome loss in diploids that were wild-type, *mec1*, *tel1*, and *tel1 mec1*. Mitotic recombination and chromosome loss rates were elevated about 10-fold in *mec1* strains relative to wild-type and were not affected by the *tel1* mutation. The double mutant strains had about 100-fold elevation in the rates of both chromosome loss and recombination. These results suggest a very high level of DSBs in the double mutant strain.

The Kolodner lab has developed an assay for measuring gross chromosome rearrangements (GCR). This assay, which will be described in more detail in another section of the thesis, involves measuring the rate of deletions of two closely-linked genes (*CAN1* and *URA3*) located near the end of chromosome V. As will be discussed further

below, most of the observed deletions result in loss of all sequences centromere-distal to the marker genes. This sequence loss is accompanied by fusion of the resulting shortened chromosome to a fragment derived from a non-homologous chromosome or *de novo* addition of a telomeric repeat to the shortened chromosome (Chen and Kolodner, 1999). In this assay, *tel1* strains had a GCR rate similar to wild-type, whereas *mec1* mutants had a GCR rate about 200-fold higher than wild-type (Myung *et al.*, 2001b). Strains with the *tel1 mec1* genotype had a GCR rate about 13,000-fold higher than wild-type, one of the highest GCR rates observed in any genotype examined. In a related study, Craven *et al.* (2002) observed a rate of *CAN1* deletions in the *tel1 mec1* strain that was more than 1000-fold higher than that observed in a wild-type strain.

Another phenotype associated with the *tel1 mec1-21* genotype is an elevated rate of telomere-telomere fusions (TTFs; Mieczkowski *et al.*, 2003). TTFs were measured using a PCR assay that detected fusions between the two types of subtelomeric repeats, X and Y′ elements, located on different chromosomes (Chan and Tye, 1983; Walmsley *et al.*, 1984). X elements are present at the ends of all yeast chromosomes centromere proximal to $TG_{1\text{-}3}$ repeats, while Y′ elements are only present in a subset of chromosome ends. Two X or two Y′ elements fused together create a palindromic sequence that cannot be easily detected by PCR. However, a fusion between an X element and a Y′ element generates a structure that can be PCR amplified. Single mutant *mec1-21* and *tel1* strains have very low rates of TTFs, but the *tel1 mec1-21* haploids have an approximately 100-fold elevated level of TTFs (Mieczkowski *et al.*, 2003). Telomeres of wild-type length can be restored in *tel1 mec1* strains by expressing a Cdc13p-Est2p fusion protein that constitutively recruits telomerase to telomeres (Evans and Lundblad, 1999; Tsukamoto *et al.*, 2001). This fusion protein suppresses TTFs (Mieczkowski *et al.*, 2003), suggesting that the severe telomere defect of *tel1 mec1-21* mutants is responsible for initiating TTFs between chromosomes. In addition, expression of the fusion protein substantially

reduces the rate of *CAN1* deletions (Mieczkowski *et al.*, 2003), arguing that many of these deletions reflect breakage of the dicentric chromosomes that would be generated by a TTF.

The final phenotype that will be discussed is the elevated rate of chromosome rearrangements in *tel1 mec1* strains. These rearrangements have been detected in two different ways. First, as described above, in strains with a deletion of *CAN1*, PCR procedures were used to sequence the breakpoints of the deleted version of chromosome V with the added DNA sequence. In the *tel1 mec1* strains, all GCR events reflect fusion of chromosome V to a non-homologous chromosome or circularization of chromosome V (Craven *et al.*, 2002; Myung *et al.*, 2001b). Since these fusions have no extended sequence homology, they represent non-homologous end joining (NHEJ) events. No *de novo* telomere additions were observed, indicating a requirement of Tel1p and/or Mec1p for this process.

Chromosome rearrangements can also be detected using DNA microarrays (Comparative Genome Hybridization, CGH analysis). Unselected wild-type, *tel1*, *mec1-21* and *tel1 mec1-21* haploids were subcultured for about 200 cell generations, followed by CGH analysis (Vernon *et al.*, 2008). The wild-type and *tel1* strains had no chromosome aberrations or aneuploidy. The *mec1-21* and *tel1 mec1-21* strains were usually disomic for chromosome VIII. The disomy of chromosome VIII could be suppressed by overexpressing *DNA2* (Vernon *et al.*, 2008), an essential replication-associated helicase located on that chromosome. Thus, it is likely that acquisition of an extra copy of *DNA2* through disomy of chromosome VIII confers a growth benefit to the *mec1*-21 and *tel1 mec1-21* haploid strains.

The *tel1 mec1-21* strains, but not any of the other strains tested, had high levels of chromosome rearrangements. Of 21 sub-cultured strains, 20 had deletions, duplications, or translocations. Most of these alterations involved chromosome III and all of the well-

characterized rearrangement were a consequence of homologous recombination between repeated genes (Vernon *et al.*, 2008). Most of these events involved repetitive Ty elements.

The chromosome rearrangements in the *tel1 mec1* haploid that were selected using GCR assays involving deletions of *CAN1* and/or *URA3* were exclusively the result of NHEJ between the deleted chromosome and other chromosome fragments. However, the chromosome rearrangements that were non-selectively observed in the *tel1 mec1-21* haploid by microarrays involved homologous recombination between dispersed repeats. The reason for this difference is obvious. The events selected on chromosome V required a deletion of *CAN1* but retention of an essential gene (*PCM1*) located about 10 kb centromere-proximal to *CAN1*. There are no repeated sequences in this region. In addition, the selected events occurred at a frequency of about 10^{-5} to 10^{-6}. The unselected and much more frequent events involved ectopic recombination between repetitive elements, a mechanism that would not be detectable with the GCR/*CAN1* deletion system. In support of this interpretation (Vernon *et al.*, 2008), when a repeated gene is placed between the *CAN1*-*URA3* markers and *PCM1*, translocations reflecting homologous recombination between repeated genes are more common than NHEJ events (Putnam *et al.*, 2009a).

While these previous studies have established that haploid *tel1 mec1* strains have very elevated rates of genome instability, certain types of chromosome aberrations, such as large deletions or chromosome loss, cannot be recovered in haploid cells. For this reason, I investigated the genetic instability associated with the *tel1 mec1* mutations in diploid cells. I show that *tel1 mec1* diploid strains have extremely high rates of chromosome rearrangements and aneuploidy (Chapters 3 and 4). Furthermore, these two types of chromosome aberrations occur through independent mechanisms, as fixing

the telomere defect of *tel1 mec1* strains has no effect on aneuploidy, but reduces the frequency of chromosome rearrangements.

1.3 Pathways of DNA lesion repair by recombination

As described above, one important source of DNA damage in *tel1 mec1* cells is likely to be DSBs induced by breakage of a dicentric chromosome. There are two general pathways of repair of DSBs, homologous recombination (HR) and non-homologous end joining (NHEJ). Characteristics of each of these pathways will be described below.

1.3.1 Homologous recombination (HR)

The two pathways employed to repair DSBs are shown in Fig. 1.2. In *Saccharomyces cerevisiae*, the high-fidelity homologous recombination (HR) pathway of DSB repair is favored over non-homologous end joining (NHEJ) under most circumstances (Paques and Haber, 1999). There are four different HR pathways (to be discussed further below) that are abbreviated SSA, SDSA, DSBR, BIR (Fig. 1.2). All of these HR pathways begin with 5'-3' end resection by the exonucleases Mre11p, Sae2p, Dna2p, and/or Exo1p (Friedel *et al.*, 2009). If the resection reveals flanking homologous sequences between the two broken ends, they can re-anneal at the regions of homology; this pathway (single-strand annealing or SSA) always results in loss of information between the two homologous regions (Fig. 1.2). The SSA pathway is Rad51p-independent (Ivanov *et al.*, 1996; Malkova *et al.*, 1996; Sugawara and Haber, 1992).

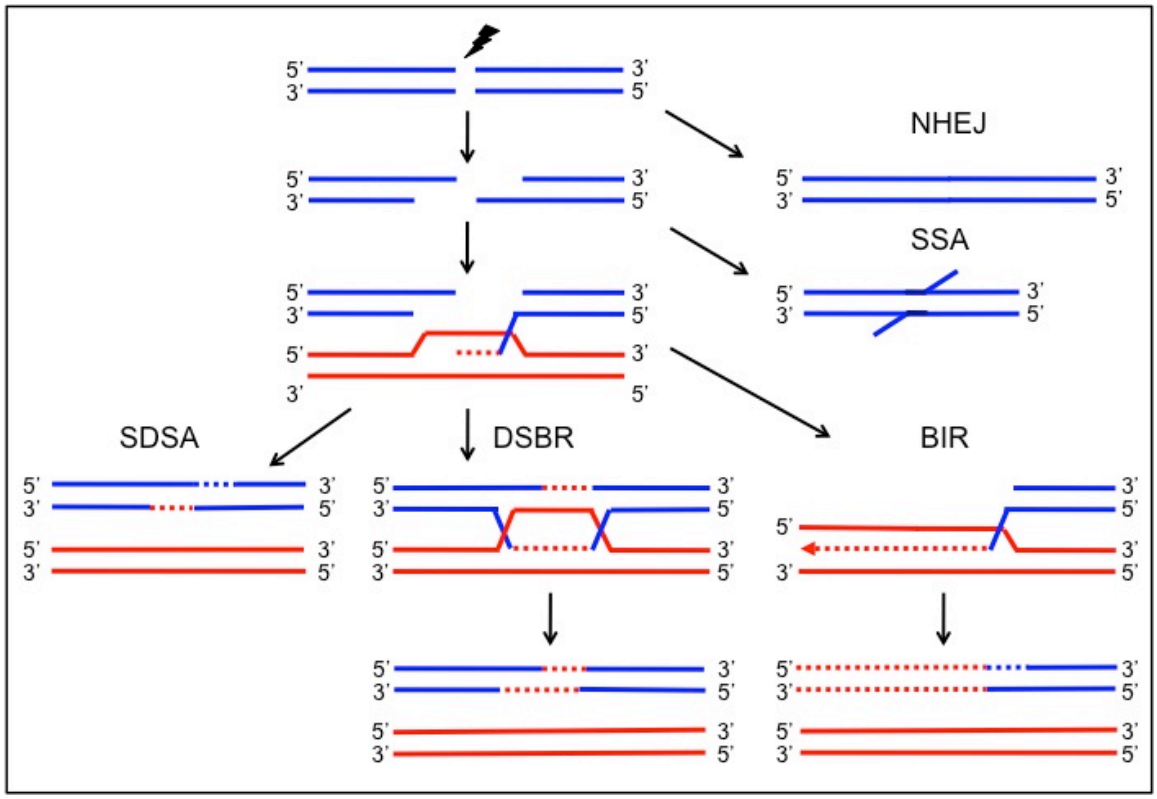

Figure 1.2 Model for the repair of double-strand breaks (DSBs).

DSBs generated through endogenous or exogenous sources utilize non-homologous end joining (NHEJ) or homologous recombination (HR) pathways for repair. Details are described in the text. DSBR, double-strand break repair; SDSA, synthesis-dependent strand annealing; BIR, break-induced replication; SSA, single-strand annealing. Solid lines indicate one DNA strand; the orientation of each strand is shown by 5′ or 3′. Newly synthesized DNA is indicated by dotted lines. This figure is adapted from Krogh and Symington, 2004.

5′-3′ end resection generates a single-stranded 3′ overhang that can also invade sequences of homology on a sister chromatid (if the cell is in the G2 phase of the cell cycle), homologue (if the cell is diploid), or non-allelic regions of homology (such as the repetitive Ty elements dispersed throughout the genome, described below). After the DSB has been resected to expose ssDNA, replication protein A (RPA) coats the region of ssDNA until it is displaced by Rad51p with the help of Rad52p (Sung, 1997). Together with Rad54p and Rdh54p, the Rad51p nucleoprotein filament then invades the homologous region to generate a "D-loop" structure (Petukhova *et al.*, 1998; Petukhova *et al.*, 2000).

Following processing of the broken DNA ends, the DNA can be repaired through several different mechanisms (Fig 1.2; Moynahan and Jasin; Paques and Haber, 1999). Synthesis-dependent strand annealing (SDSA) occurs when the invading DNA strand dissociates from the homologous template after a short amount of DNA synthesis and religates to the other side of the DNA break (McGill *et al.*, 1989). This repair event results in gene conversion events that are not associated with crossovers. Alternatively, second-end capture of the other broken DNA strand by the homologous template generates a double Holliday junction that can be resolved to generate crossovers or non-crossovers in the double-strand break repair model (DSBR; non-crossover outcome pictured in Fig. 1.2; Szostak *et al.*, 1983). Finally, the invading strand can set up a stable replication fork and copy the DNA from the site of the break through the end of the chromosome. This event (break-induced replication or BIR) is inherently non-reciprocal (Malkova *et al.*, 1996). If the BIR event involves an interaction of two homologues, it results in loss of heterozygosity (LOH) for all markers distal to the DSB. Although some proteins are required for all HR pathways, some proteins are specific to individual HR pathways (Krogh and Symington, 2004). For example, one protein that is important for BIR, but not other HR pathways, is Pol32p, a non-essential subunit of the Polδ replication complex (Lydeard *et al.*, 2007).

1.3.2 Chromosome rearrangements generated by homologous recombination (HR) between ectopic repeated genes

Homologous recombination usually repairs DSBs using allelic sequences on the sister chromatid or, in diploid cells, on the homologue (Paques and Haber, 1999). However, if a DSB occurs in a repeated gene, HR can occur between non-allelic sequences; such events are called "ectopic recombination" (Paques and Haber, 1999). For example, translocations involving ectopic repeats have been observed in yeast strains with low levels of DNA polymerase alpha (Lemoine *et al.*, 2005) or IR radiation (Argueso

et al., 2008). Most of these translocations reflect BIR events between the Ty retrotransposons located on non-homologous chromosomes. Intrachromosomal recombination events involving non-allelic Ty elements have also been observed (Argueso *et al.*, 2008). Ty elements are repetitive 6.1 kb DNA sequences randomly dispersed throughout the genome (Kim *et al.*, 1998). There are at least 30-50 Ty elements per haploid genome in *Saccharomyces cerevisiae*, depending on the specific strain (Gabriel *et al.*, 2006). Ty elements, which are structurally related to retroviruses, have long-terminal repeats (LTRs) of 330 bp called delta elements. In addition to intact Ty elements, there are more than 200 solo delta elements. Chromosome rearrangements involving solo delta elements have also been observed (Argueso *et al.*, 2008).

Another highly repetitive region in the *Saccharomyces cerevisiae* genome is the large array of tandemly repeated ribosomal DNA (rDNA) units on chromosome XII (Petes, 1979). The rDNA array consists of 100-150 copies of a 9.1 kb sequence that encodes the 35S and 5S rRNA genes (Fig. 4.1). Due to the repetitive nature of the rDNA gene cluster, the number of rDNA repeats per cluster is highly variable even in wild-type cells. This variability is a consequence of unequal mitotic crossovers within the rRNA gene cluster (Andersen *et al.*, 2008; Casper *et al.*, 2008; Szostak and Wu, 1980). The rRNA genes have a polar replication fork barrier (RFB) that prevents DNA polymerase from colliding with RNA polymerase transcribing the 35S gene; the Fob1p binds to the RFB and is required for this barrier to function (Kobayashi, 2003). Spontaneous crossovers within the rRNA gene cluster are likely to be initiated by DSBs occurring at the barrier because deleting the *FOB1* gene reduces recombination between the rDNA repeats (Defossez *et al.*, 1999; Johzuka and Horiuchi, 2002; Kobayashi *et al.*, 1998).

1.3.3 Non-homologous end joining (NHEJ)

In conditions in which repair of a DSB by homologous recombination is difficult or impossible (for example, a DSB in a single-copy region of a haploid strain in G1),

yeast cells will perform non-homologous end joining (NHEJ). NHEJ is an error-prone recombination pathway in which two broken ends of DNA are joined without extensive processing of the broken ends (Fig. 1.2). NHEJ often results in the deletion or insertion of a small number (<10) of bases close to the break site. The NHEJ pathway requires certain proteins that are not required for HR including Ku70p and Ku80p, Lig4p, Lif1p, and Nej1p (Dudasova *et al.*, 2004). In diploid cells that express both *MAT***a** and *MATα* information, the expression of *NEJ1* is repressed, resulting in inefficient NHEJ (Kegel *et al.*, 2001; Lee *et al.*, 1999; Valencia *et al.*, 2001). Interestingly, Nej1p is a target of the DDR and Nej1p phosphorylation is Dun1p-dependent (Ahnesorg and Jackson, 2007). This observation indicates that NHEJ is also directly regulated by the DDR.

While HR is the predominant repair pathway in diploid yeast, NHEJ is very efficient in higher eukaryotes such as mammals (Shrivastav *et al.*, 2008). One possible reason is that yeast lack homologues of the NHEJ-promoting mammalian proteins DNA-PKcs, BRCA1, and Artemis. Furthermore, since imprecise NHEJ is required to generate antibody diversity during V(D)J recombination (Jung *et al.*, 2006), there may have been selective pressure favoring NHEJ pathways in mammals. HR is also more problematic in higher eukaryotes whose genomes contain a lot of repetitive DNA.

In wild-type yeast strains, the telomeres are not a substrate for NHEJ (Marcand *et al.*, 2008); NHEJ events between different chromosomes would result in dicentric chromosomes. In strains with various defects in telomere structure, however, telomere-telomere fusions (TTFs) occur by NHEJ. In yeast, TTFs are found in cells that lack *TEL1* and *MEC1* (Mieczkowski *et al.*, 2003) and the efficient production of these events is dependent on Lig4p. End-to-end chromosome fusions have also been documented in mammalian cells that lack telomere-associated proteins ATM, Ku, DNA-PK, or TRF2 (de Lange, 2002; Kojis *et al.*, 1989; Pandita, 2002). TTFs are also common in cancer cells prior to telomerase activation (Hackett and Greider, 2002).

1.4 Genetic regulation of the frequency of gross chromosome rearrangements (GCR) and chromosome losses/gains in yeast

As discussed above, there are many genes involved in regulating genetic stability in yeast. In this section of the Introduction, I will first describe assays used to detect these genes and the screens that have performed with these assays. I will then discuss some of the pathways that have been identified in these screens, including genes involved in sister chromatid cohesion, kinetochore structure, spindle pole body structure and the spindle assembly checkpoint.

1.4.1 Screens identifying mutants with elevated rates of genetic instability

One extensively-used assay for detecting genome-destabilizing mutants is the gross chromosome rearrangement (GCR) assay developed in the Kolodner lab (described above). These researchers introduced a *URA3* marker next to the *CAN1* gene located near the end of chromosome V in a haploid strain (Chen and Kolodner, 1999); there are no essential genes between these markers and the telomere of V and the first essential gene (*PCM1*) centromere-proximal to *CAN1* is about 10 kb away. They then selected strains that simultaneously became resistant to both canavanine and 5-fluoro-orotate. Such strains have a terminal deletion in which both reporter genes and all sequences distal to the reporter have been lost. The breakpoint of the deletion on chromosome V is between the reporters and *PCM1*. Chromosomes with a deletion that includes the telomere would be expected to be very unstable. In the strains that lost the two reporter markers, the deletion derivative of chromosome V was fused to telomere-containing fragments of other chromosomes or acquired a telomere by *de novo* addition (Chen and Kolodner, 1999).

In wild-type strains, the frequency of simultaneous loss of both *CAN1* and *URA3* was very low, about 10^{-10}/division (Chen and Kolodner, 1999). The frequency of loss

was greatly elevated (>100-fold) in certain mutants affecting DNA replication (*rfa1*, *rfa3*, *rfa5*, *rad27*), recombination (*rad52*, *rad50*, *mre11*, *xrs2*, *sgs1*), telomere addition or regulation (*pif1*, *rif1*, *rif2*), chromatin assembly (*cac1*, *asf1*, *cac2*), and DNA damage checkpoints (*mec1*, *rad53*, *dun1*, *chk1*, *ddc2*, *pds1*, *rad17*, *rad24*, *rad9*; Chen and Kolodner, 1999; Schmidt *et al.*, 2006). In addition to studies of the frequencies of GCR in single mutant strains, these researchers also investigated some combinations of double and triple mutations. When these mutations affected different pathways, striking elevations in the frequencies of GCR were observed. For example, strains that lacked Rad52p (required for homologous recombination) and Lig4p (required for NHEJ) and had the *pif1-m2* mutation (which increases the frequency of telomere additions) had GCR rates that were 10,000-fold elevated compared to wild-type (Myung *et al.*, 2001a).

In addition to the GCR studies described above, Yuen *et al.* (2007) screened 4,700 different "knock out" yeast strains for mutations that elevated the frequency of chromosome loss or chromosome recombination. They identified about 130 genes that, when mutated, increased the frequency of chromosome loss or chromosome rearrangements. Many of these genes overlapped with those characterized by the GCR assays, affecting DNA replication, DNA repair, or some other aspect of DNA metabolism. However, they also identified mutants affecting chromosome loss that were not detected in the GCR assays. One large class of such mutations affected the spindle assembly checkpoint (SAC) including *bub1*, *mad2*, and *mad1*. Another class was mutations involved in assembling the spindle (*ase1* and *cin2*). One important caveat in this type of screen is that genes encoding essential functions important for maintaining genetic stability, such as *MEC1*, would not be identified. Since many of the genes involved in kinetochore and spindle structure, as well components of the cohesin complex, are essential, many genes were missed in the Yuen *et al.* screen. In a screen of 45 temperature-sensitive alleles of essential genes, Ben-Aroya *et al.* (2004) identified nine

mutants that had elevated levels of chromosome loss or rearrangements; four of these (*yor262W*, *dre2*, *swc4*, and *yhr122w*) had defects in sister chromatid cohesion.

In contrast to large studies identifying mutants with elevated chromosome loss, a number of small searches for mutations that result in increased rates of chromosome gain have also been done. Chan and Botstein (1993) identified two *increase-in-ploidy* mutants, *ipl1* and *ipl2*. Ipl1p regulates kinetochore-microtubule attachments and Ipl2p is involved in the organization of the cytoskeleton. Howlett and Schiestl (2004) showed that mutations affecting nucleotide excision repair (*rad1*, *rad2*, and *rad4*) resulted in elevated rates of chromosome loss, although these effects were small (about 5-fold). Finally, by examining 230 haploid strains from the "knock-out" collection with DNA microarrays, Hughes *et al.* (2000) identified twenty-two mutants that were aneuploid for one or more chromosomes. Among those aneuploid strains were several mutants (*bub1*, *bub3*, and *bim1*) affecting the structure of the spindle or the spindle assembly checkpoint.

1.4.2 Regulation of genetic stability by sister chromatid (SC) cohesion

A genetic screen looking for elevated levels of chromosome loss identified mutants (*smc1*, *smc3*, *scc1*, *scc2*) in the sister chromatid (SC) cohesion pathway (Michaelis *et al.*, 1997). In addition to having high rates of chromosome loss, these mutants were capable of separating sister chromatids in the absence of APC function. In a second screen, Warren *et al.* (2004) identified mutants that were synthetically lethal with *chl1*. Chl1p is a helicase-like protein that helps establish SC cohesion following DNA replication (Skibbens, 2004). This screen identified numerous genes involved directly with DNA replication or the DNA replication checkpoint including *rad53*, *mrc1*, *rrm3*, *csm3*, *tof1*, and *xrs2*. These mutants also had high levels of chromosome loss, suggesting that a loss of SC cohesion results in genome instability. From these data, Skibbens (2004) concluded that the MRX complex and components of the DNA replication checkpoint are important in ensuring SC cohesion.

In response to DNA damage, cohesin is recruited to approximately 100 kb surrounding the site of a DSB (Unal *et al.*, 2004). In addition to enhanced cohesion on the broken molecule, damage-induced cohesion is generated on undamaged chromosomes (Strom *et al.*, 2007; Unal *et al.*, 2007). As described above, this response is due to DDR signaling from Tel1p and Mec1p through γH2A. Interestingly, Mec1p is required for the damage-induced cohesion to a much greater extent than Tel1p or γH2A. This preference for Mec1p is due to the direct role for Chk1p, a substrate of the Mec1p kinase, in phosphorylating the cohesin subunit Scc1p (Heidinger-Pauli *et al.*, 2008).

There is also evidence for cohesion being important for genome stability in higher eukaryotes. Cohesin subunit SMC1 is a target of ATM in human cells and is recruited to the site of DNA damage (Kim *et al.*, 2002; Yazdi *et al.*, 2002). Additionally, Barber, *et al.* (2008) demonstrated that 10 of 11 mutations identified in a panel of 132 colorectal cancers were in genes that functioned in cohesion, and down-regulation of some cohesion-related genes such as *Smc1l1* and *Mre11a* resulted in chromosome instability.

1.4.3 Regulation of genetic stability by kinetochores

The accurate segregation of chromosomes requires the proper function of many proteins that compose the kinetochore (the proteinaceous complex assembled on the centromere; Tanaka *et al.*, 2005), the microtubules attached to the kinetochore, and the spindle pole body (the microtubule organizing center of the yeast cell). Below, I discuss some of the proteins that compose these various structures and the evidence that mutations in these proteins lead to genetic instability (primarily chromosome mis-segregation).

Each yeast kinetochore is comprised of over 60 proteins (Tanaka *et al.*, 2005). The proteins bind in specific complexes to the centromere, an approximately 130 bp conserved region of DNA in each yeast chromosome. The protein complex that binds

directly to the centromere DNA is the CBF3 complex, and all of these proteins are essential for growth (Lechner and Carbon, 1991). The Dam1 complex directly interacts with microtubules, and the Ndc80, MIND, and COMA complexes are located between the internal (CBF3) and external (Dam1) kinetochore complexes. These complexes bridge the gap between the inner and outer kinetochore (Cheeseman *et al.*, 2001; De Wulf *et al.*, 2003; Ortiz *et al.*, 1999; Pinsky *et al.*, 2003; Wigge and Kilmartin, 2001).
Many of these kinetochore proteins are important for the segregation of sister chromatids. For example, proteins comprising the inner kinetochore CBF3 complex, such as Ncd10p, have greatly elevated rates of chromosome mis-segregation when mutated (Hyman and Sorger, 1995). Each yeast kinetochore also contains a variant histone H3 protein (Cse4p), and disruption of the proper localization pattern of this histone variant results in elevated levels of genome instability (Au *et al.*, 2008).

1.4.4 Regulation of genetic stability by spindle structure or by the spindle assembly checkpoint (SAC)

1.4.4.1 Proteins of the microtubules and the spindle pole body

The spindle is composed of microtubules attached to the spindle pole body at one end and to the kinetochore at the other. Microtubules are composed of polymerized alpha/beta-tubulin dimers; *TUB1* and *TUB3* encode alpha tubulin and *TUB2* encodes beta tubulin (Carminati and Stearns, 1999). Mutants defective in beta-tubulin or beta-tubulin folding genes (*CIN1*, *CIN2*, and *CIN4*) have high rates of chromosome mis-segregation (Hoyt *et al.*, 1990). Associated with the microtubules are many plus and minus end-directed motor proteins, such as Cin8p and Kip1p, that are involved in moving chromosomes along the microtubules towards the spindle poles, ensuring proper chromosome segregation. Mec1p-dependent inhibition of Cin8p is known to restrain spindle elongation in response to DNA replication blocking agents such as

hydroxyurea, and loss of this inhibition results in premature spindle elongation and unequal partitioning of DNA into each daughter cell (Bachant *et al.*, 2005).

The spindle pole body (SPB), which organizes microtubules in *S. cerevisiae* contains at least 17 proteins (Jaspersen and Winey, 2004). The SPB is integrated in the nuclear envelope with microtubules extending into the cytoplasm (cMTs) and into the nucleus (nMTs); the nuclear microtubules are also called kinetochore microtubules (kMTs). The SPB core proteins (Spc110p, Spc42p and Spc29p) interact with gamma tubulin (encoded by *TUB4*) and the gamma tubulin-associated proteins Spc97p and Spc98p. The gamma tubulin complex nucleates the kMTs. The complete details of the assembly of the SPB have not yet been worked out. Since many of the proteins of the SPB are encoded by essential genes, the effect of null mutations on chromosome segregation have not been examined. However, a mutation in *SPC105* is associated with elevated levels of chromosome non-disjunction (Nekrasov *et al.*, 2003).

1.4.4.2 Spindle assembly checkpoint proteins

The SAC is required for ensuring the correct attachment of kinetochores to microtubules and for the proper biorientation of the chromosomes at metaphase through the action of Bub1p, Bub3p, Mad2p, Mad3p, and Mps1p (Kadura and Sazer, 2005; Lew and Burke, 2003; Musacchio and Salmon, 2007). There are two types of kinetochore defects that can activate the spindle assembly checkpoint: a lack of kinetochore attachment to microtubules (Rieder *et al.*, 1995) and a lack of tension between sister kinetochores (Li and Nicklas, 1995; Stern and Murray, 2001). Significantly, mutants defective in the SAC are known to have elevated rates of aneuploidy (Bernard *et al.*, 1998; Hughes *et al.*, 2000; Warren *et al.*, 2002) and have been implicated in oncogenesis in mammals (Baker *et al.*, 2005; Burds *et al.*, 2005; Cahill *et al.*, 1998; Draviam *et al.*, 2004; Jallepalli and Lengauer, 2001). More specifically, decreased expression of *Mad2* is found

in breast cancer and mutations in *Bub1* and *Bubr1* have been identified in colorectal cancers.

1.4.4.3 Interplay between the DNA damage response (DDR) and the spindle assembly checkpoint (SAC)

Researchers have found multiple connections between the DDR and the SAC, both of which function to halt the cell cycle in response to cellular insults. First, the Mad2p is required for a complete cell cycle arrest in response to DNA damaging agents such as MMS and hydroxyurea in fission yeast, baker's yeast, and human cells (Collura *et al.*, 2005; Garber and Rine, 2002; Kim and Burke, 2008; Mikhailov *et al.*, 2002; Sugimoto *et al.*, 2004). Second, defective telomeres activate both the DDR and the SAC in baker's yeast and fruit flies (Maringele and Lydall, 2002; Musaro *et al.*, 2008). Third, both the DNA damage checkpoint and the spindle assembly checkpoint halt the cell cycle by preventing Pds1p degradation (Cohen-Fix and Koshland, 1997). In the DDR, Chk1p phosphorylates and stabilizes Pds1p (Searle *et al.*, 2004), whereas Mad2p interacts with Cdc20p to prevent the ubiquitination and destruction of Pds1p by the APC (Fang *et al.*, 1998). Fourth, Rad53p and Rad9p are phosphorylated in the presence of the SAC-eliciting agent nocodazole (Clemenson and Marsolier-Kergoat, 2006). Interestingly, this phosphorylation is independent of Tel1p and Mec1p but is abolished in strains lacking *BUB1* or *MAD2*. Finally, it has been shown that cells from A-T patients and heterozygous carriers have a defective SAC (Shigeta *et al.*, 1999; Takagi *et al.*, 1998). In summary, the DDR and the SAC are activated by some of the same conditions and arrest the cell cycle through some of the same mechanisms.

1.5 Rationale for my thesis research

In most of the studies described above, genetic instability was examined in haploid strains using assays that were specific to certain loci. In my research, I used two assays that would allow detection of chromosome rearrangements throughout the

genome. These assays were CHEF (contour-clamped homogeneous electric field) gel electrophoresis and comparative genome hybridization (CGH) microarrays. In addition, I examined diploid strains, allowing the detection of large deletions that would be lethal in a haploid strain. I concentrated my analysis of diploids that were homozygous for mutations in the related *TEL1* and *MEC1* genes because previous studies from the Petes and Kolodner labs had shown that this mutant background was likely to have a very high level of chromosome aberrations.

Since the cells of metastatic tumors usually have high levels of aneuploidy and chromosome rearrangements, one important question is whether these two phenotypes reflect the same mutational defect or arise as independent genetic defects. In my thesis research, I show that one genetic background can give rise to both changes in chromosome number and changes in chromosome structure. Furthermore, these two types of genome instability events are mechanistically separable, as repairing the telomere defect in *tel1 mec1* strains reduces the frequency of translocations without affecting the frequency of aneuploidy.

2. Materials and Methods

2.1 Strain construction and subculturing of yeast strains

Chemicals were purchased from Sigma, St. Louis, MO, unless otherwise noted. All strains were constructed in the MS71 background (*MATα ade5-1 leu2-3 trp1-289 ura3-52 his7-2 LEU2*; Strand *et al.*, 1995) using standard gene-replacement techniques (Goldstein and McCusker, 1999; Schiestl and Gietz, 1989). Gene deletions were verified via PCR. When the essential gene *MEC1* is deleted, the viability can be rescued by a concurrent deletion of *SML1*, which elevates nucleotide pools and allows for viability (Zhao *et al.*, 1998). All *mec1::NAT* strains described in this paper contain a *sml1::HYG* deletion as well. Genotypes and strain construction methods can be found in Table 2.1 for haploids and Table 2.2 for diploids; oligonucleotide sequences can be found in Table 2.3.

Because *tel1 mec1* strains have an extremely unstable genotype, the diploid strains were constructed while expressing a complementing wild-type copy of *MEC1* on a *TRP1*-marked plasmid (pSAD3-3b/*MEC1*; Desany *et al.*, 1998) so the cells were not Mec1p-deficient until the start of the analysis. To begin the analysis, the *tel1 mec1* strains were streaked on non-selective YPD media to facilitate loss of the complementing plasmid. These plates were replicated to SD-trp to identify colonies that had lost the wild-type copy of *MEC1*, which was a very rare event. The *trp1*-deficient colonies were streaked to YPD to create "subculture zero," the first time the strains were deficient in Mec1p. In the initial analysis, five individual colonies from the subculture zero plate were streaked again to YPD to create subculture one. For subcultures two through five, cells from the heavy growth area of the plate (not single colonies) were restreaked on YPD. Each subculture equals approximately 20 cell divisions; hence, five subculturings equals approximately 100 generations of growth.

Plasmid pVL1107-*URA3* was constructed by replacing the *LEU2* gene of plasmid pVL1107 (Evans and Lundblad, 1999) with a wild-type copy of *URA3*. The wild-type *URA3* gene was PCR-amplified using genomic DNA from yeast strain S25 and the oligonucleotides LEU-URA-UP and LEU-URA-DN (Table 2.2) to create a PCR product containing the wild-type *URA3* gene with 50 bp of flanking *LEU2* homology on either side. This PCR product was transformed into a wild-type yeast strain containing plasmid pVL1107 to replace the *LEU2* gene in the plasmid with *URA3*. The transformed plasmid was then recovered and confirmed via PCR.

Plasmids pRS316-*SRL2* and pRS426-*SRL2* were constructed by PCR-amplifying *SRL2* along with 500 bp of its native promoter and 300 bp of its native terminator using the primers JLMo220 and JLMo221. JLMo220 contained a *Sac*I restriction enzyme site, while JLMo221 contained a *Kpn*I restriction enzyme site. Plasmids pRS316 (Sikorski and Hieter, 1989) and pRS426 (Christianson *et al.*, 1992) were digested with *Sac*I and *Kpn*I along with the *SRL2* PCR product and the *SRL2* insert was ligated into each vector. The plasmids were confirmed with restriction digestion and sequencing.

2.2 Contour-clamped homogeneous electric field (CHEF) analysis and Southern blotting

Contour-clamped homogeneous electric field (CHEF) analysis and Southern blotting techniques were performed as previously described (Narayanan *et al.*, 2006). Briefly, yeast strains were inoculated into two 10 ml volumes of YPD, or selective SD-trp media if the strain contained the pSAD3-3b/*MEC1* plasmid. The cultures were grown for two days until fully saturated. The OD_{600} of each strain was measured, and 5×10^7 to 1×10^8 cells were harvested in an eppendorf tube. The samples were spun down, and resuspended in 200 μl of melted 0.5% lowmelt agarose (FMC BioProducts, Rockland, ME) in 0.1 M EDTA pH 7.5. 4 μl of 25 mg/ml Zymolase 20T (MP Biomedical, Solon, OH) in 10 mM KPO_4 were added, the samples were vortexed, and used to fill two plug

molds. Plugs were solidified at 4°C for 10 minutes and then incubated in a solution of 0.5 M EDTA, 10 mM Tris pH 7.5. The plugs were incubated at 37°C overnight. To this solution, 200 μl of a solution containing 5% sarcosyl, 5 mg/ml proteinase K, and 0.5 M EDTA pH 7.5 was then added. The plugs were incubated at 50°C 5 hours to overnight. To prepare the CHEF gel, the plugs were incubated in 0.5X TBE buffer for an hour and then loaded onto a 1% agarose gel (Bio-Rad, Hercules, CA). The CHEF gels were run on a BioRad CHEF Mapper for 32 hours and 47 minutes, with a size range of 400 kilobases to 1700 kilobases, an angle of 120 degrees, an initial switch time of 46.67 seconds, and a final switch time of 2 minutes and 49.31 seconds. The ramping was linear, and the power was 5.0 V/cm.

For Southern blots, the CHEF gel was transferred to a Hybond membrane (Amersham Biosciences, Little Chalfont, Buckinghamshire) for 48 hours using high-salt wicking conditions. The DNA was crosslinked to the membrane using UV irradiation, and then the membrane was pre-hybridized with a solution containing 6X SSC, 0.5% SDS, and 5X Denhardt's for an hour at 65°C. PCR products of specific loci were used as probes. 50 ng of PCR DNA was denatured, then incubated with a Ready-To-Go™ DNA Labeled Beads (GE Healthcare, Little Chalfont, Buckinghamshire) and 0.5 μCi of ^{32}P-dCTP for 24 hours at 65°C. The membrane was washed for 30 minutes and exposed to a PhosphoImager screen (Molecular Probes) for 1 hour to 10 days depending on signal strength. The PhosphoImager screen was scanned with a Typhoon 9200 scanner (Molecular Dynamics).

2.3 Comparative genome hybridization (CGH) microarray analysis

Comparative genome hybridization (CGH) microarray analysis followed the techniques of Lemoine *et al.* (2005). Genomic DNA was isolated from control and experimental yeast strains following standard techniques. The DNA was then sonicated

in 500 μl water using 40 x 1 sec pulses of a Branson Digital Sonifier set to 20% amplitude. Zymocolumns (Zymo Research) were used to concentrate 5 μg of DNA in 10.5 μl water. A Bio Prime Array CGH kit (Invitrogen, Carlsbad, CA) was used to label control DNA with Cy3 and experimental DNA with Cy5 (Cyanine Smart Pack dUTP, PerkinElmer Life Sciences, Boston, MA). The labeled DNA was purified again with Zymocolumns, then combined and hybridized to a microarray containing all 6,000 yeast ORFs and 6,000 intergenic regions (Lemoine *et al.*, 2005). Each locus was represented in duplicate on the microarray for a total of 24,000 spots. The hybridization was carried out at 65°C for at least 16 hours. The arrays were washed for 30 minutes, and then scanned using a GenePix 4000B scanner (Axon Instruments). GenePix Pro 5.0, the UNC Microarray Database (www.genome.unc.edu, Chapel Hill, NC) and CGH Miner (http://www-stat.stanford.edu/~wp57/CGH-Miner/) were used to analyze the data. The normalized ratio of red to green signal was used to determine the relative copy number of the experimental sample. A yellow spot indicates an equivalent level of hybridization between the wild type control and experimental strain, a green spot indicates a deletion of that particular locus in the experimental strain, and a red spot indicates an amplification. Plotting these data can identify regions of chromosomal amplifications and deletions. CGH microarray analysis can differentiate between trisomic chromosomes and higher order aneuploidies. *tel1 mec1* diploids demonstrated a few tetrasomic chromosomes after 100 generations of growth; these were identified as having a normalized probe intensity across the chromosome of twice the amount of a normalized probe intensity across a trisomic chromosome.

Band arrays (Argueso *et al.*, 2008) were performed by running DNA from the strain of interest across 5 lanes of a 1% lowmelt agarose CHEF gel. The aberrant band was excised, purified with a Quiagen gel purification kit, and then labeled with Cy5

DNA and hybridized to the microarray as described. A CHEF plug containing all of the DNA from a wild-type strain was treated similarly and labeled with Cy3 DNA.

2.4 Analysis of aneuploidy frequency

Chi-square analysis was performed to determine whether the amount of trisomy for any particular genotype was significantly different than that of the *te11 mec1* strains. The number of independently subcultured strains for each genotype was multiplied by 16 (the number of different chromosomes in a yeast cell) to get a total number of chromosomes analyzed for that genotype (for example, 20 strains analyzed x 16 = 320 total chromosomes). Then, the number of trisomies for each genotype was added together (for example, 50 trisomic chromosomes identified, out of 320 total chromosomes that each had the potential to become trisomic) and this ratio was compared between different genotypes using the Fisher exact probability test or chi-square analysis tool on the VassarStats website (http://faculty.vassar.edu/lowry/VassarStats.html).

2.5 Benomyl assays

For the benomyl spot assay, cultures were grown in YPD overnight to saturation, then reinnoculated to OD_{600}=0.2. After 3 hours, the ODs were again measured, and all of the cultures, except for the *tel1 mec1* strain, were normalized to an OD_{600} of 0.5. Because *tel1 mec1* strains grow poorly even in YPD, a 6-fold excess of cells was collected for the experiment. Three ten-fold serial dilutions were made and then 3 μl of each dilution was spotted on YPD plates or YPD plates containing 10 μg/ml, 20 μg/ml, 40 μg/ml, or 70 μg/ml benomyl (Sigma, St. Louis, MO).

When following the morphology of individual cells over time to monitor the cell cycle, the protocol from Hoyt *et al.* (1991) was minimally modified. A culture of cells in YPD was inoculated overnight such that the cells would be in log phase in the morning

(OD_{600} between 0.2 – 0.6). The cultures were washed twice in water, reinnoculated to an OD_{600} of 0.2 in 5 ml of YPD pH 3.5, and incubated with 5 μg/ml alpha factor (Sigma, St. Louis, MO; 5 mg/ml stock in DMSO). The cells were arrested with alpha factor for 2.5 to 3 hours at 30°C, then washed twice in water and resuspended in YPD containing 50 μg/ml pronase (10 mg/ml stock in water; Sigma P5147, St. Louis, MO). 500 μl of released cells were sonicated for 10 x 1 second pulses on a Branson Digital Sonifier at 20% amplitude. 150 μl of cells were spread on a YPD or a YPD + 70 μg/ml benomyl plate. Pictures were taken at 100X magnification immediately after the cells were plated (time zero) and after 8 hours at room temperature using a Sony Cybershot DSC-H10 digital camera with a microscope attachment (manual setting, F8.0 aperture, 200, 0.5m set focus, no flash). Unbudded cells at time zero were compared with the 8 hour time point, and the number of cells derived from each single cell after 8 hours was recorded. Because the alpha factor arrest was nearly complete (at least 94% for wild-type, 90% for *mad2*, and 80% for *tel1 mec1* strains), any single cell at time zero was considered unbudded, and any small projections from the cell were considered shmoos. Occasionally the shmoos were still visible on the original cell after 8 hours, but these could be differentiated from buds by comparing the cell morphology at time zero. At least 100 cells were counted for each strain, and the experiments were repeated in duplicate.

Table 2.1 Description of the haploid strains used in this study.

Strain name	Relevant Genotype	Construction details
MS71	*α ade5-1 his7-2 leu2-3 LEU2 trp1-289 ura3-52*	(Strand *et al.*, 1995)
JMY314-1a	*α ade2-1 leu2-3,112 his3-11 trp1-1 ura3-1 can1-100 RAD5 sml1::HIS3*	Spore colony from JMY314 (Mallory and Petes, 2000)
JAY82	*α ade2-1 leu2-3,112 his3-11 trp1-1 ura3-1 can1-100 RAD5 sml1::HPH*	Transformation of JAY60 with *sml1::HPH*; pAG32 (hphMX4) template (Goldstein and McCusker, 1999); primers JAO19 and JAO20
LDY2B	*a sml1::HPH*	Transformation of MS71 *MAT a* with *sml1::HPH*; JAY82 template; primers JAO21 and JAO22
PG256	*α tel1::KANMX*	Transformation of MS71 with *tel1::KANMX;* pFA6-kanMX4 template (Wach *et al.*, 1994); primers Tel1KanMXF and Tel1KanMXR
JLMy62-2b	*a tel1::KANMX mec1::NAT sml1::HPH* + pSAD3-3b/*MEC1*	Spore colony from JLMy62
JLMy62-4d	*α mec1::NAT sml1::HPH* + pSAD3-3b/*MEC1*	Spore colony from JLMy62
JLMy62-6b	*α tel1::KANMX mec1::NAT sml1::HPH* + pSAD3-3b/*MEC1*	Spore colony from JLMy62
JLMy62-7c	*a* + pSAD3-3b/*MEC1*	Spore colony from JLMy62
JLMy62-9a	*α tel1::KANMX sm1l::HPH* + pSAD3-3b/*MEC1*	Spore colony from JLMy62
JLMy62-10b	*a tel1::KANMX* + pSAD3-3b/*MEC1*	Spore colony from JLMy62
JLMy62-10c	*a mec1::NAT sml1::HPH* + pSAD3-3b/*MEC1*	Spore colony from JLMy62
JLMy62-15c	*α tel1::KANMX* + pSAD3-3b/*MEC1*	Spore colony from JLMy62
JLMy62-17c	*α tel1::KANMX mec1::NAT sml1::HPH* + pSAD3-3b/*MEC1*	Spore colony from JLMy62
JLMy62-18c	*a tel1::KANMX mec1::NAT sml1::HPH* + pSAD3-3b/*MEC1*	Spore colony from JLMy62
JLMy62-20c	*a tel1::KANMX sml1::HPH* + pSAD3-3b/*MEC1*	Spore colony from JLMy62
JLMy62-21c	*α* + pSAD3-3b/*MEC1*	Spore colony from JLMy62
JLMy148-1a	*a bub1::NAT*	Spore colony from JLMy148
JLMy148-4d	*α bub1::NAT*	Spore colony from JLMy148
JLMy149-1a	*a bub1::NAT*	Spore colony from JLMy149
JLMy149-4b	*α bub1::NAT*	Spore colony from JLMy149
JLMy176	*a mec1::NAT sml1::HPH* + pSAD3-3b/*MEC1* + pVL1107-*URA3*	Transformation of JLMy62-10c with pVL1107-*URA3* ((Evans and Lundblad, 1999) and Chapter 2)
JLMy195	*a fob1::NAT tel1::KANMX sml1::HPH* + pSAD3-3b/*MEC1*	Transformation of JLMy62-20c with *fob1::NAT*; pAG25 template (natMX4) (Goldstein and McCusker, 1999); primers AMC065 and AMC066 (Casper *et al.*, 2008)

Table 2.1 Continued.

Strain name	Relevant Genotype	Construction details
JLMy213	α *fob1::NAT tel1::KANMX sml1::HPH* + pSAD3-3b/*MEC1*	Transformation of JLMy62-9a with *fob1::NAT*; template AMC156 (Casper *et al.*, 2008); primers JLMo104 and JLMo105. This creates a PCR product with over 500 bp of homology on either side of the *fob1::NAT* locus in AMC156 to facilitate transformation into JLMy62-9a.
JLMy214-10b	α *fob1:: NAT tel1::KANMX mec1::NAT sml1::HPH* + pSAD3-3b/*MEC1*	Spore colony from JLMy214
JLMy214-19c	*a fob1:: NAT tel1::KANMX mec1::NAT sml1::HPH* + pSAD3-3b/*MEC1*	Spore colony from JLMy214
JLMy214-22d	*a fob1:: NAT tel1::KANMX mec1::NAT sml1::HPH* + pSAD3-3b/*MEC1*	Spore colony from JLMy214
JLMy217-17d	*a fob1:: NAT tel1::KANMX mec1::NAT sml1::HPH* + pSAD3-3b/*MEC1*	Spore colony from JLMy217
JLMy240-3b	α *pol32::NAT tel1::KANMX sml1::HPH*	Spore colony from JLMy240
JLMy248-1b	α *pol32::NAT tel1::KANMX mec1::NAT sml1::HPH* + pSAD3-3b/*MEC1*	Spore colony from JLMy248
JLMy248-2b	α *pol32::NAT tel1::KANMX mec1::NAT sml1::HPH* + pSAD3-3b/*MEC1*	Spore colony from JLMy248
JLMy250-21c	*a pol32::NAT tel1::KANMX mec1::NAT sml1::HPH* + pSAD3-3b/*MEC1*	Spore colony from JLMy250; pVL1107-*URA3* plasmid not retained
JLMy250-41c	*a pol32::NAT tel1::KANMX mec1::NAT sml1::HPH* + pSAD3-3b/*MEC1*	Spore colony from JLMy250; pVL1107-*URA3* plasmid not retained
JLMy271	α *CEN2::pCORE tel1::KANMX mec1::NAT sml1::HPH* + pSAD3-3b/*MEC1*	Transformation of JLMy62-6b with *CEN2::pCORE*; pCORE template (Storici *et al.*, 2001); primers JLMo191 and JLMo192
JLMy281	*a CEN2::pCORE*	Transformation of JLMy62-7c with *CEN2::pCORE*; pCORE template; primers JLMo191 and JLMo192; *pRS314-MEC1* plasmid not retained
JLMy283 JLMy284	*a cen2::CEN14*	Transformation of JLMy281 with *cen2::CEN14*; MS71 template; primers JLMo193 and JLMo194
JLMy288-14a	*a tel1::KANMX mec1::NAT sml1::HPH cen2::CEN14 + pRS314-MEC1*	Spore colony from JLMy288
JLMy288-21a	*a tel1::KANMX mec1::NAT sml1::HPH cen2::CEN14 + pRS314-MEC1*	Spore colony from JLMy288
JLMy290-31c	*a tel1::KANMX mec1::NAT sml1::HPH cen2::CEN14 + pRS314-MEC1*	Spore colony from JLMy290

Table 2.1 Continued.

Strain name	Relevant Genotype	Construction details
JLMy290-40a	*α tel1::KANMX mec1::NAT sml1::HPH cen2::CEN14 + pRS314-MEC1*	Spore colony from JLMy290
JLMy309	*a mad2::NAT*	Transformation of JLMy62-7c with *mad2::NAT*; pAG25 template (natMX4) (Goldstein and McCusker, 1999); primers JLMo216 and JLMo217; pSAD3-3b/*MEC1* plasmid not retained
JLMy317 JLMy319	*α mad2::NAT*	Transformation of JLMy62-21c with *mad2::NAT*; pAG25 template (natMX4) (Goldstein and McCusker, 1999); primers JLMo216 and JLMo217; pSAD3-3b/*MEC1* plasmid not retained
JLMy394	*a bub1-ΔK::KANMX*	Transformation of JLMy62-7c with *bub1-ΔK::KANMX*; pFA6a-GFP(S65T)-kanMX6 template (Longtine *et al.*, 1998; Wach *et al.*, 1994); primers JLMo231 and JLMo232; pSAD3-3b/*MEC1* plasmid not retained. This truncation deletes the C-terminal amino acids 609-1021 of Bub1p (Fernius and Hardwick, 2007).
JLMy401-2b	*α bub1-ΔK::KANMX tel1::KANMX mec1::NAT sml1::HPH* + pSAD3-3b/*MEC1*	Spore colony from JLMy401
JLMy401-16c	*α bub1-ΔK::KANMX*	Spore colony from JLMy401; pSAD3-3b/*MEC1* plasmid not retained
JLMy401-18c	*a bub1-ΔK::KANMX tel1::KANMX mec1::NAT sml1::HPH* + pSAD3-3b/*MEC1*	Spore colony from JLMy401
JLMy438	*a chk1::NAT*	Transformation of JLMy62-7c with *chk1::NAT*; pAG25 template (natMX4) (Goldstein and McCusker, 1999); primers JLMo247 and JLMo248; pSAD3-3b/*MEC1* plasmid not retained
JLMy440	*α chk1::NAT*	Transformation of JLMy62-21c with *chk1::NAT*; pAG25 template (natMX4) (Goldstein and McCusker, 1999); primers JLMo247 and JLMo248; pSAD3-3b/*MEC1* plasmid not retained
JLMy464	*a sgo1::KANMX*	Transformation of JLMy62-7c with *sgo1::KANMX*; pFA6-kanMX4 template (Wach *et al.*, 1994); primers JLMo251 and JLMo261; pSAD3-3b/*MEC1* plasmid not retained
JLMy466	*α sgo1::KANMX*	Transformation of JLMy62-21c with *sgo1::KANMX*; pFA6-kanMX4 template (Wach *et al.*, 1994); primers JLMo251 and JLMo261; pSAD3-3b/*MEC1* plasmid not retained

Table 2.2 Description of the diploid strains used in this study.

Strain name	Relevant Genotype	Construction details
JLMy39.1	*a/α TEL1/tel1::KANMX sml1:HPH/SML1*	LDY2B x PG256
JLMy43.2	*a/α TEL1/tel1::KANMX mec1::NAT/MEC1 sml1::HPH/SML1*	Transformation of JLMy39.1 with *mec1:NAT*; pAG25 template (natMX4) (Goldstein and McCusker, 1999); primers JLMo26 and JLMo27
JLMy62	*a/α TEL1/tel1::KANMX mec1::NAT/MEC1 sml1::HPH/SML1* + pSAD3-3b/*MEC1*	Transformation of JLMy43.2 with plasmid pSAD3-3b/*MEC1* (Desany *et al.*, 1998)
JLMy80 JLMy81	*a/α tel1::KANMX/tel1::KANMX mec1::NAT/mec1::NAT sml1::HYG/sml1::HYG* + pSAD3-3b/*MEC1*	JLMy62-2b x JLMy62-6b
JLMy82 JLMy83	*a/α tel1::KANMX/tel1::KANMX mec1::NAT/mec1::NAT sml1::HYG/sml1::HYG* + pSAD3-3b/*MEC1*	JLMy62-17c x JLMy62-18c
JLMy100	*a/α* + pSAD3-3b/*MEC1*	JLMy62-7c x JLMy62-21c
JLMy101	*a/α*	JLMy62-7c x JLMy62-21c; pSAD3-3b/*MEC1* plasmid not retained
JLMy102 JLMy104	*a/α tel1::KANMX/tel1::KANMX* + pSAD3-3b/*MEC1*	JLMy62-10b x JLMy62-15c
JLMy111 JLMy112 JLMy113	*a/α mec1::NAT/mec1::NAT sml1::HPH/sml1::HPH* + pSAD3-3b/*MEC1*	JLMy62-10c x JLMy62-4d; in JLMy112 the pSAD3-3b/*MEC1* plasmid was not retained
JLMy1262	*a/α tel1::KANMX/tel1::KANMX mec1::NAT/mec1::NAT sml1::HYG/sml1::HYG* + pSAD3-3b/*MEC1*+ pVL1107-*URA3*	Transformation of JLMy80 with plasmid pVL1107-*URA3* (Evans and Lundblad, 1999)
JLMy1271 JLMy1272	*a/α tel1::KANMX/tel1::KANMX mec1::NAT/mec1::NAT sml1::HYG/sml1::HYG* + pSAD3-3b/*MEC1*+ pVL1107-*URA3*	Transformation of JLMy82 with plasmid pVL1107-*URA3* (Evans and Lundblad, 1999)
JLMy1301	*a/α tel1::KANMX/tel1::KANMX mec1::NAT/mec1::NAT sml1::HYG/sml1::HYG* + pSAD3-3b/*MEC1 + pRS316*	Transformation of JLMy80 with plasmid pRS316 (Sikorski and Hieter, 1989)
JLMy1311	*a/α tel1::KANMX/tel1::KANMX mec1::NAT/mec1::NAT sml1::HYG/sml1::HYG* + pSAD3-3b/*MEC1 + pRS316*	Transformation of JLMy82 with plasmid pRS316 (Sikorski and Hieter, 1989)
JLMy148 JLMy149	*a/α bub1::NAT/BUB1*	Transformation of JLMy100 with *bub1::NAT;* pAG25 template (natMX4) (Goldstein and McCusker, 1999); primers JLMo59 and JLMo60; pSAD3-3b/*MEC1* plasmid not retained

Table 2.2 Continued.

Strain name	Relevant Genotype	Construction details
JLMy148-19 JLMy148-48 JLMy148-108 JLMy148-112 JLMy148-132	*a/α bub1::NAT/bub1::KANMX*	Transformation of JLMy148 with *bub1::KANMX;* JLMy208 template; primers JLMo167 and JLMo169. This creates over 600 bp of homology on either side of *bub1::KANMX,* and *bub1::KANMX* is targeted to the only remaining wild-type copy of *BUB1* in JLMy148. Transformants were not purified to limit the number of cell divisions prior to analysis.
JLMy149-34 JLMy149-45 JLMy149-93	*a/α bub1::NAT/bub1::KANMX*	Transformation of JLMy149 with *bub1::KANMX;* JLMy208 template; primers JLMo167 and JLMo169. This creates over 600 bp of homology on either side of *bub1::KANMX,* and *bub1::KANMX* is targeted to the only remaining wild-type copy of *BUB1* in JLMy149. Transformants were not purified to limit the number of cell divisions prior to analysis.
JLMy156	*a/α bub1::NAT/bub1::NAT*	JLMy149-1a x JLMy149-4b
JLMy200 JLMy202	*a/α* + pRS316	Transformation of JLMy101 with pRS316 (Sikorski and Hieter, 1989)
JLMy208	*a/α bub1::KANMX/BUB1*	Transformation of JLMy101 with *bub1::KANMX;* pFA6-kanMX4 template (Wach *et al*., 1994); primers JLMo100 and JLMo101. This deletes all but 50 bp inside either end of *BUB1* so the transformation to knock out the second copy of *BUB1* in strains JLMy148 and JLMy149 is facilitated.
JLMy214	*a/α fob1::NAT/FOB1 tel1::KANMX/TEL1 MEC1/mec1::NAT sml1::HPH/sml1::HPH* + pSAD3-3b/*MEC1*	JLMy195 x JLMy62-4d
JLMy217	*a/α FOB1/fob1::NAT TEL1/tel1::KANMX mec1::NAT/MEC1 sml1::HPH/sml1::HPH* + pSAD3-3b/*MEC1,*	JLMy62-10c x JLMy213
JLMy229 JLMy230	*a/α fob1::NAT/fob1::NAT tel1::KANMX/tel1::KANMX mec1::NAT/mec1::NAT sml1::HYG/sml1::HYG* + pSAD3-3b/*MEC1*	JLMy214-19c x JLMy214-10b
JLMy233	*a/α fob1::NAT/fob1::NAT tel1::KANMX/tel1::KANMX mec1::NAT/mec1::NAT sml1::HYG/sml1::HYG* + pSAD3-3b/*MEC1*	JLMy214-22d x JLMy214-10b

Table 2.2 Continued.

Strain name	Relevant Genotype	Construction details
JLMy237	*a/α fob1::NAT/fob1::NAT tel1::KANMX/tel1::KANMX mec1::NAT/mec1::NAT sml1::HYG/sml1::HYG* + pSAD3-3b/*MEC1*	JLMy217-17d x JLMy214-10b
JLMy240	*a/α pol32::NAT/POL32 TEL1/tel1::KANMX sml1::HPH/SML1*	Transformation of JLMy39.1 with *pol32::NAT*; pAG25 template (natMX4) (Goldstein and McCusker, 1999); primers JLMo163 and JLMo164
JLMy248	*a/α POL32/pol32::NAT TEL1/tel1::KANMX mec1::NAT/MEC1 sml1::HPH/sml1::HPH* + pSAD3-3b/*MEC1*	JLMy62-10c x JLMy240-3b
JLMy250	*a/α POL32/pol32::NAT TEL1/tel1::KANMX mec1::NAT/MEC1 sml1::HPH/sml1::HPH* + pSAD3-3b/*MEC1* + pVL1107-*URA3*	JLMy176 x JLMy240-3b
JLMy254 JLMy255 JLMy256	*a/α pol32::NAT/pol32::NAT tel1::KANMX/tel1::KANMX mec1::NAT/mec1::NAT sml1::HYG/sml1::HYG* + pSAD3-3b/*MEC1*	JLMy250-21c x JLMy248-1b
JLMy258	*a/α pol32::NAT/pol32::NAT tel1::KANMX/tel1::KANMX mec1::NAT/mec1::NAT sml1::HYG/sml1::HYG* + pSAD3-3b/*MEC1*	JLMy250-41c x JLMy248-2b
JLMy288	*a/α cen2::CEN14/CEN2 TEL1/tel1::KANMX MEC1/mec1::NAT SML1/sml1::HPH* + pSAD3-3b/*MEC1*	JLMy283 x JLMy62-6b
JLMy290	*a/α cen2::CEN14/CEN2 TEL1/tel1::KANMX MEC1/mec1::NAT SML1/sml1::HPH* + pSAD3-3b/*MEC1*	JLMy284 x JLMy62-17c
JLMy294 JLMy295	*a/α cen2::CEN14/cen2::CEN14 tel1::KANMX/tel1::KANMX mec1::NAT/mec1::NAT sml1::HPH/sml1::HPH* + pSAD3-3b/*MEC1*	JLMy288-14a x JLMy290-40a
JLMy296 JLMy297 JLMy298	*a/α cen2::CEN14/cen2::CEN14 tel1::KANMX/tel1::KANMX mec1::NAT/mec1::NAT sml1::HPH/sml1::HPH* + pSAD3-3b/*MEC1*	JLMy290-31c x JLMy290-40a

Table 2.2 Continued.

Strain name	Relevant Genotype	Construction details
JLMy327 JLMy328 JLMy329 JLMy330 JLMy366 JLMy367	*a/α mad2::NAT/mad2::NAT*	JLMy309 x JLMy317
JLMy376 JLMy377	*a/α mad2::NAT/mad2::NAT*	JLMy309 x JLMy319
JLMy342	*a/α tel1::KANMX/tel1::KANMX mec1::NAT/mec1::NAT sml1::HYG/sml1::HYG* + pSAD3-3b/*MEC1* + pRS316-*DNA2*	Transformation of pRS316-*DNA2* (Lee *et al.*, 2000) into JLMy80
JLMy344	*a/α tel1::KANMX/tel1::KANMX mec1::NAT/mec1::NAT sml1::HYG/sml1::HYG* + pSAD3-3b/*MEC1* + pRS316-*DNA2*	Transformation of pRS316-*DNA2* (Lee *et al.*, 2000) into JLMy81
JLMy346	*a/α tel1::KANMX/tel1::KANMX mec1::NAT/mec1::NAT sml1::HYG/sml1::HYG* + pSAD3-3b/*MEC1* + pRS316-*DNA2*	Transformation of pRS316-*DNA2* (Lee *et al.*, 2000) into JLMy82
JLMy348	*a/α tel1::KANMX/tel1::KANMX mec1::NAT/mec1::NAT sml1::HYG/sml1::HYG* + pSAD3-3b/*MEC1* + pRS316-*DNA2*	Transformation of pRS316-*DNA2* (Lee *et al.*, 2000) into JLMy83
JLMy350	*a/α tel1::KANMX/tel1::KANMX mec1::NAT/mec1::NAT sml1::HYG/sml1::HYG* + pSAD3-3b/*MEC1* + pRS316-*SRL2*	Transformation of pRS316-*SRL2* into JLMy80
JLMy354	*a/α tel1::KANMX/tel1::KANMX mec1::NAT/mec1::NAT sml1::HYG/sml1::HYG* + pSAD3-3b/*MEC1* + pRS316-*SRL2*	Transformation of pRS316-*SRL2* into JLMy81
JLMy356	*a/α tel1::KANMX/tel1::KANMX mec1::NAT/mec1::NAT sml1::HYG/sml1::HYG* + pSAD3-3b/*MEC1* + pRS426-*SRL2*	Transformation of pRS426-*SRL2* into JLMy81
JLMy360	*a/α tel1::KANMX/tel1::KANMX mec1::NAT/mec1::NAT sml1::HYG/sml1::HYG* + pSAD3-3b/*MEC1* + pRS426-*SRL2*	Transformation of pRS426-*SRL2* into JLMy82
JLMy401	*a/α bub1-ΔK::KANMX/BUB1 CEN2/CEN2::pCORE TEL1/tel1::KANMX MEC1/mec1::NAT SML1/sml1::HPH* + pSAD3-3b/*MEC1*	JLMy394 x JLMy271

Table 2.2 Continued.

Strain name	Relevant Genotype	Construction details
JLMy405 JLMy406 JLMy407 JLMy408 JLMy409 JLMy410 JLMy411 JLMy412 JLMy448 JLMy449 JLMy450 JLMy451	*a/α bub1-ΔK::KANMX/ bub1-ΔK::KANMX*	JLMy394 x JLMy401-16c
JLMy413 JLMy414 JLMy415 JLMy416	*a/α bub1-ΔK::KANMX/ bub1-ΔK::KANMX tel1::KANMX/ tel1::KANMX mec1::NAT/ mec1::NAT sml1::HPH/ sml1::HPH* + pSAD3-3b/*MEC1*	JLMy401-18c x JLMy401-2b
JLMy444 JLMy445 JLMy460 JLMy461	*a/α chk1::NAT/chk1::NAT*	JLMy438 x JLMy440
JLMy468 JLMy469 JLMy470	*a/α sgo1::KANMX/sgo1::KANMX*	JLMy464 x JLMy466
JLMy479	*a/α bub1-ΔK::KANMX/ bub1-ΔK::KANMX + pRS316*	Transformation of JLMy405 with pRS316 (Sikorski and Hieter, 1989)
JLMy481	*a/α bub1-ΔK::KANMX/ bub1-ΔK::KANMX tel1::KANMX/ tel1::KANMX mec1::NAT/ mec1::NAT sml1::HPH/ sml1::HPH + pSAD3-3b/MEC1 + pRS316*	Transformation of JLMy413 with pRS316 (Sikorski and Hieter, 1989)

Table 2.3 Sequences of oligonucleotides used in strain construction, plasmid construction, and breakpoint mapping.

Oligonucleotide Name	Sequence
AMC065	GGA GAA CAA TTT AAC GAT TGT GTG AGT GTG AAT TTG TGC TGA GGA TAA CAC GTA CGC TGC AGG TCG AC
AMC066	AAC CGC GTA CAT TAA ATA CAG GGT CAT ATA CAG GAA GAG CTT TCA ACA CCA TCG ATG AAT TCG AGC TCG
CAN1 F	AGT GGA ACT TTG TAC G
CAN1 R	CTT CAA CGC TGT TAT CTT AAC AAC C
CHA1 F, CHA1 R	(Casper *et al.*, 2009)
CUP1 F, CUP1 R	(Vernon *et al.*, 2008)
DOT1 F	CTT AGA CTC TCA GGA ATC TTC
DOT1 R	CAG AGG AAG TGT CGT TAT CTG
JAO19	TCT TAC GGT CTC ACT AAC CTC TCT TCA ACT GCT CAA TAA TTT CCC GCT AAT TAA GGC GCG CCA GAT CTG
JAO20	AGA GTA TGA AAG GAA CTT TAG AAG TCC ATT TCC TCG ACC TTA CCC TGG GCA TAG GCC ACT AGT GGA T
JAO21	GAA CAT CGC CCG TTT CGC CCG
JAO22	TAG TAG GAC GAG AGT CCC TGA
JLMo26 mec1::NAT KO F	AGG CTG GAC AAC AAG AAC GAC ATA CAC CGC GTA AAG GCC CAC AAG ACT GCC GTA CGC TGC AGG TCG AC
JLMo27 mec1::NAT KO R	TGG TTA GAT CAA GAG GAA GTT CGT CTG TTG CCG AAA ATG GTG GAA AGT CGA TCG ATG AAT TCG AGC TCG
JLMo36 ASP3 F	CTC TCT TTG TCG CAA TGT CCA G
JLMo37 ASP3 R	TTA ACC ACC GTA GAC GCC
JLMo59 bub1::NAT KO F	GAA AGA TTA TTG ACG GTT CCT ATT GTT TGA ATG TTA ACG CTG ACC AGG AAC GTA CGC TGC AGG TCG AC
JLMo60 bub1::NAT KO R	CAG GAC ACC AAA AAG TCA CCT ATG CGG GAG ATG AAG GCA TAT TTA TTC ACA TCG ATG AAT TCG AGC TCG
JLMo67 NEJ1 F	ATG GAT TCT GAG TTG AAA GGG C
JLMo68 NEJ1 R	TCT GTG GGT ATT CTT CGA CC
JLMo98 JLP1 F	TCT GTG GGT ATT CTT CGA CC
JLMo99 JLP1 R	CTT TAG ATC TTC CAC GGG CC
JLMo100 bub1::KANMX KO F	CAC ATT TCC GCA ATC GAA AGG CGT TAG CTC ATC TCA AAA AGA GCA GCC GTA CGC TGC AGG TCG AC
JLMo101 bub1::KANMX KO R	GCT TCA TAA CTC CAT GGC TTG CCC GCA CGC ATT TCC CAG CAA TCA TCG ATG AAT TCG AGC TCG
JLMo104 FOB1 - P520 F	CGA GAA ATC GAG GTT TCC TG
JLMo105 FOB1 + T546 R	GGG ACT TAT CAT GTG CGA AC
JLMo106 II; 812868 F	GGT AGA ACA ACA GTA CAG TGA G
JLMo119 XII; 545091 R	CTA TTT CCT CAC CTG CCA TGG
JLMo149 III; 113259 F	GCT AGC ACC AGT GAA CAT C

Table 2.3 Continued.

Oligonucleotide Name	Sequence
JLMo158 XII; 941098 F	CGT TGA ACC CTT AGA CGA GC
JLMo163 pol32::NAT KO F2	ATG GAT CAA AAG GCG TCA TAT TTT ATC AAT GAG AAG CTC TTC ACT GAG GTA AAG CCG TAC GCT GCA GGT CGA C
JLMo164 pol32::NAT KO R2	CA CGG GTG ATG GCT TGC GTG GTG GTG TTG AAG TTG CGG GTC TCT TTG TCA CAA TAT ATC ATC GAT GAA TTC GAGCTCG
JLMo167 BUB1 - P657 F	CTA GAG ACA TCG ACG CTG TAC
JLMo169 BUB1 + T679 R	CAG GTT GTG GTG AAT GCA G
JLMo191 CEN2::pCORE F	GAG AAT TCT ATC ACA CGG TAA TGA TAG TGT TCC CGA TGT CAA GCA GTC TTG AGC TCG TTT TCG ACA CTG G
JLMo192 CEN2::pCORE R	TAG CTT GCC AGA TCT TCT TGC TTA TTC TTA AGC TCT TGG GTA GTA CTG TAT TCC TTA CCA TTA AGT TGA TC
JLMo193 cen2::CEN14 F	TTT GAC GAT GTC AGT GAA TCC CGG TTA ATG ATA TTC TGT TTT TCA CGG GAT AAA ATT TGC AAC CCT ATA ATA AAT CGG
JLMo194 cen2::CEN14 R	ACC TAT AAT ATT GAC GAA CAT ATG TAA ATA AGA TAT ATG TTA TAT TCT TCT GGT ATG CGA CTA TTC AAA CAC G
JLMo205 APT1 F	GTG GGT TCT TGT TCG GAC CAA C
JLMo206 APT1 R	GAG CGT TCA GTA AAG TGA ACA CTG G
JLMo216 mad2::NAT KO F	CTC GTA CAA GAG TAT TGA AAA CCA CTT CAA AGG GGC CCA ATA GCA CAT TTA CGT ACG CTG CAG GTC GAC
JLMo217 mad2::NAT KO R	GTA TAG TAT AAT ATA GTT CAT AAA TCT ATA TTC TTT CTA AAC ATC GAA AAC GAG ATC GAT GAA TTC GAG CTC G
JLMo220 SRL2 – P500F	TAT ATA GAG CTC CTA TAT GTT GGG TTA GGG CG
JLMo221 SRL2 + T300R	TAT ATA GGT ACC CAT GCT CTG CCA TCC TTT G
JLMo227 I; 166916 R	GCG GTA TCA TCA GCA AGC
JLMo229 I; 159688 F	GTG CAA GAC TAG GAA CGA CTG
JLMo231 bub1-ΔK::KANMX F	CAA CCA TTC AAA GTT CTC CAT TTC TCA CAC AAC CTG AAC CAC AAG CAG AAA AGT GAG GCG CGC CAC TTC TAA A
JLMo232 bub1-ΔK::KANMX R	GGC AGG ACA CCA AAA AGT CAC CTA TGC GGG AGA TGA AGG CAT ATT TAT TCA GAA TTC GAG CTC GTT TAA AC
JLMo245 XVI; 55314 F	GCA TAG CAT CTG TGT GCA GTG
JLMo246 XVI; 63360 R	GCT TGT CAT ACT TCG ATT CCG
JLMo247 chk1::NAT KO F	CAA ACA TAA GAG TAT ATC ATA AGT TGC TGT ATA TGG GCA GCA CGT ATT ACT CGT ACG CTG CAG GTC GAC
JLMo248 chk1::NAT KO R	CAA TAA TAA AAT CTC TCG AAA CAA TAT ATA GTT ACG ATG ACA CAC TAG AAA TCG AGA GAG ATC GAT GAA TTC GAG CTC G
JLMo251 sgo1::KANMX KO F	ACA CAC GCA TAT ATA TGT TTA ATT GGG TAT AGA GGG GTT ATT GTT TGA CCC GTA CGC TGC AGG TCG AC
JLMo261 sgo1::KANMX KO R2	GAC GAC TTG GAG GGT CGC GTA GTA GAA TTT TCA TCA GAT AAA TTA TTG ACA TCG ATG AAT TCG AGC TCG

Table 2.3 Continued.

Oligonucleotide Name	Sequence
LEU2-URA-UP	ATG TCT GCC CCT AAG AAG ATC GTC GTT TTG CCA GGT GAC CAC GTT GGT CAA GAG ATA GTG ATG ATA TTT CAT A
LEU2-URA-DN	TTA AGC AAG GAT TTT CTT AAC TTC TTC GGC GAC AGC ATC ACC GAC TTC GGT GGT ATT CTG GCG AGG TAT TGG ATA
LYS20 F	CGG GCG ACT ATC TTT CTA ATG
LYS20 R	CAA TGT CTC TGA TCT TGT GCA AC
PDR3 F	TTG CCT ACT ACA GCT GTT G
PDR3 R	CAG ATG CCG TCG TAG TAG G
RAD24 F	GAG CTC ATC TAG ACC GAC TTC GC
RAD24 R	GTC GTA ATG GCC GAC CTA ATA TC
rDNA probe	rDNA plasmid clone pY1rG12 (Petes *et al.,* 1978)
Tel1KanMX F	TCG AAA AAA AAG CCT TCA AAG AAA AGG GAA ATC AGT GTA ACA TAG ACG CTG ACG CTG CAG GTC GAC
Tel1KanMX R	CGT ATT TCT ATA AAC AAA AAA AAG AAG TAT AAA GCA TCT GCA TAG CAA ATC GAT GAA TTC GAG CTC G
Y′ F/R	(Ritchie *et al.,* 1999)
YJR030C F	CAT GAT GAC ATG TCT CTA ACA CAA TCC ATA GTG
YJR030C R	GAT CTA TGC AGT GTG CGA CCA TTG TGT TAT TG

3. High rates of chromosome rearrangements and aneuploidy in yeast strains lacking both Tel1p and Mec1p reflect deficiencies in two different mechanisms

3.1 Introduction

Two types of genetic instability are associated with cells derived from solid tumors (Lengauer *et al.*, 1998), elevated rates of small genetic alterations (single-base changes and microsatellite alterations) and high frequencies of chromosome rearrangements and aneuploidy. The first type of instability is associated with tumors deficient in nucleotide excision repair (NIN tumors) and DNA mismatch repair (MIN tumors). Cells with elevated rates of chromosome aberrations (deletions, duplications, and translocations) and/or aneuploidy have been termed "CIN" (chromosome instability) tumors (Lengauer *et al.*, 1997). Although some CIN tumors have mutations in genes affecting the spindle assembly checkpoint pathway (Rajagopalan *et al.*, 2003) or chromatid cohesion (Barber *et al.*, 2008), the relevant genome-destabilizing mutations have not been characterized in most CIN tumors (Teixeira da Costa and Lengauer, 2002).

Many yeast mutants have been identified that have elevated rates of chromosome alterations and/or aneuploidy. One widely-employed assay designed to detect gross chromosomal rearrangements (GCR) involves selecting for the deletion of two closely-linked markers near the end of chromosome V (Putnam *et al.*, 2009a; Putnam *et al.*, 2005). Mutations that elevate GCR are found in genes controlling S-phase DNA damage checkpoints (Myung *et al.*, 2001b), DNA replication (Chen and Kolodner, 1999), telomere length regulation (Craven *et al.*, 2002; Myung *et al.*, 2001a), chromatin assembly (Myung *et al.*, 2003), as well as other pathways. Importantly, strains with mutations in the spindle assembly checkpoint pathway (which result in elevated levels of chromosome non-disjunction) do not necessarily have elevated rates of GCR (Myung *et al.*, 2004), indicating that these two phenotypes are not intrinsically linked.

In *Saccharomyces cerevisiae*, the related kinases Tel1p (orthologous to the mammalian ATM gene) and Mec1p (orthologous to the mammalian ATR gene) have somewhat overlapping roles in the DNA damage/S-phase checkpoint and in telomere length regulation (Harrison and Haber, 2006). In response to DNA damage such as a double-strand break (DSB), Tel1p and Mec1p are recruited to the site of the break, where they initiate a signal transduction cascade that results in phosphorylation and activation of effector proteins, transcription of DNA repair genes, and cell cycle arrest (Chapter 1). Strains with the *tel1 mec1* genotype are more sensitive to DNA damaging agents than either single mutant strain (Morrow *et al.*, 1995). Similarly, the single mutant *tel1* and *mec1* strains have short but stable telomeres whereas *tel1 mec1* double mutant strains have a phenotype similar to a telomerase-negative strain (Ritchie *et al.*, 1999).

Mec1p, but not Tel1p, is an essential protein, but the lethality of the *mec1* mutation can be suppressed by a mutation in *SML1* that results in elevated nucleotide pools (Zhao *et al.*, 1998). In addition, *mec1* strains have elevated levels of DSBs in hard-to-replicate regions of the genome (Cha and Kleckner, 2002). These and other results suggest that the essential role of Mec1p may be to stabilize stalled replication forks (Cimprich and Cortez, 2008).

Haploid yeast strains lacking both Tel1p and Mec1p have very high rates of chromosome rearrangements (Craven *et al.*, 2002; Myung *et al.*, 2001b). In haploid strains, the rate of deletions of *CAN1* is elevated about 10,000-fold in the *tel1 mec1* strain relative to wild-type. In some *can1* strains, the deletion derivative of chromosome V (the location of *CAN1*) was fused to the telomere of a non-homologous chromosome by a non-homologous end joining (NHEJ) event (Craven *et al.*, 2002). In addition, the *tel1 mec1* strains had very high rates of telomere-telomere fusions relative to *tel1* or *mec1* strains (Mieczkowski *et al.*, 2003). Expression of a Cdc13p-Est2p fusion protein allows extension of telomeres to wild-type length in a *tel1 mec1* strain (Tsukamoto *et al.*, 2001). This

extension reduces the rate of *CAN1* deletions about 10-fold, arguing that many chromosome rearrangements are likely to reflect breakage of dicentric chromosomes formed by telomere-telomere fusions (Mieczkowski *et al.*, 2003). In addition, we previously observed a high frequency of chromosome rearrangements in haploid *tel1 mec1* strains subcultured for about 200 cell divisions (Vernon *et al.*, 2008). All of these rearrangements reflected homologous recombination between non-allelic repeated sequences, involving mostly Ty elements.

As described above, CIN tumors have elevated rates of aneuploidy in addition to high rates of chromosome rearrangements. Large genetic screens for mutations resulting in elevated rates of chromosome loss were done in *S. cerevisiae* (Spencer *et al.*, 1990; Yuen *et al.*, 2007). In a systematic screen of about 4,700 different deletion strains, 130 mutants had elevated rates of chromosome loss (Yuen *et al.*, 2007). Many of these mutants affected proteins directly involved with the mechanics of chromosome disjunction (the spindle pole body, microtubules, and the kinetochore), whereas others affected the spindle assembly checkpoint (SAC). Since this study was done with deletion alleles, mutants in essential genes, such as *SMC1* (encoding a cohesin subunit), would not be detected, although hypomorphic *smc1* alleles are known to elevate chromosome non-disjunction (Strunnikov *et al.*, 1993).

Yeast strains with high rates of aneuploidy often have a defect in the SAC. This checkpoint is required to ensure that chromosomes establish bipolar orientation on the spindle prior to anaphase. There are two types of kinetochore defects that activate the checkpoint: lack of kinetochore occupancy by microtubules and lack of tension between sister kinetochores (reviewed by Lew and Burke, 2003; Musacchio and Salmon, 2007). Although most SAC proteins (Mad1p-Mad3p, Bub1p, and Bub3p) are required to respond to both types of defect, separation-of-function alleles of *bub1* have been

obtained; strains that lack the kinase domain of Bub1p (*bub1-ΔK*) are defective only in the tension-sensing function of the SAC (Fernius and Hardwick, 2007).

Although mutants affecting the DNA damage response (DDR) usually have elevated levels of gross chromosome rearrangements and mutants affecting the SAC have elevated levels of aneuploidy, connections between these two pathways exist. First, the elimination of the delay of the cell cycle in response to DNA damaging agents such as methyl-methane sulfonate (MMS) and hydroxyurea (HU) in *S. pombe*, *S. cerevisiae*, and human cells requires mutations in both the DNA damage checkpoint pathway and the SAC (Collura *et al.*, 2005; Garber and Rine, 2002; Kim and Burke, 2008; Mikhailov *et al.*, 2002; Sugimoto *et al.*, 2004). Second, the DNA damage checkpoint and the SAC are both activated by certain types of chromosome damage (for example, defective telomeres; Maringele and Lydall, 2002; Musaro *et al.*, 2008) and certain drugs (for example, nocodazole; Clemenson and Marsolier-Kergoat, 2006).

Most of the connections between the DNA damage checkpoint and the SAC described above are observed in the presence of DNA damage. Below, we show that *tel1 mec1* diploid strains have a very high rate of aneuploidy and chromosome rearrangements in the absence of induced DNA damage, but the SAC remains functional in these strains. We also show that these two phenotypes reflect two different cellular defects, since the frequency of chromosome rearrangements, but not the frequency of aneuploidy, is reduced by correcting the telomere defect of the *tel1 mec1* mutant strain.

3.2 Results

3.2.1 Rationale

As discussed in Chapter 1, previous studies of *tel1 mec1* haploid yeast strains demonstrated high rates of chromosome aberrations. Since some genetic alterations are haploid-lethal (deletions removing essential genes, for example), in this study we examined genomic alterations in *tel1 mec1 sml1* diploids. The *sml1* mutation is necessary to suppress the lethality of *mec1* null alleles (Zhao *et al.*, 1998); in our subsequent discussion, the *tel1 mec1 sml1* genotype will be abbreviated to *tel1 mec1*.

The *tel1 mec1* diploids were constructed to contain a plasmid-borne *MEC1* gene (details in Tables 2.1-2.3). The strains JLMy80-JLMy83 are isogenic *tel1 mec1* diploids constructed by crossing isogenic haploids. We then selected derivatives that lost the *MEC1* plasmid to initiate our genomic instability analysis. Independent derivatives were subcultured for about 100 cell divisions and then re-transformed with the *MEC1*-containing plasmid. We examined the frequency of aneuploidy and other changes in gene dosage in these strains by Comparative Genome Hybridization (CGH) microarrays, and alterations in the sizes of chromosomal DNA molecules by Contour-clamped Homogeneous Electric Field (CHEF) gel analysis. No alterations were observed in the starting strain relative to the wild-type diploid in either assay, but the subcultured *tel1 mec1* diploids had high rates of aneuploidy and chromosome rearrangements.

3.2.2 Aneuploidy in *tel1 mec1* diploids

We used microarrays containing all ORFs and intergenic regions as PCR fragments on glass slides (DeRisi *et al.*, 1997). For each CGH experiment, we labeled DNA from the subcultured strain and from the control strain with different fluorescent nucleotides, and examined the ratio of hybridization to the two DNA samples for each gene and

intergenic region on the array (Chapter 2). From this analysis, it was clear that the *tel1 mec1* diploids had very high frequencies of aneuploidy and other changes in gene dosage that reflected chromosome rearrangements. For example, strain JLMy80-1s (Fig. 3.1A) was monosomic for chromosome I and trisomic for chromosomes X, XII, and XVI, whereas strain JLMy81-1L was trisomic for chromosome VIII and had an interstitial deletion on IV (Fig. 3.1B). Of the 20 subcultured diploids analyzed, 18 were trisomic for one or more chromosomes and half were monosomic for chromosomes I and/or VI (Table 3.1; Appendices A and B).

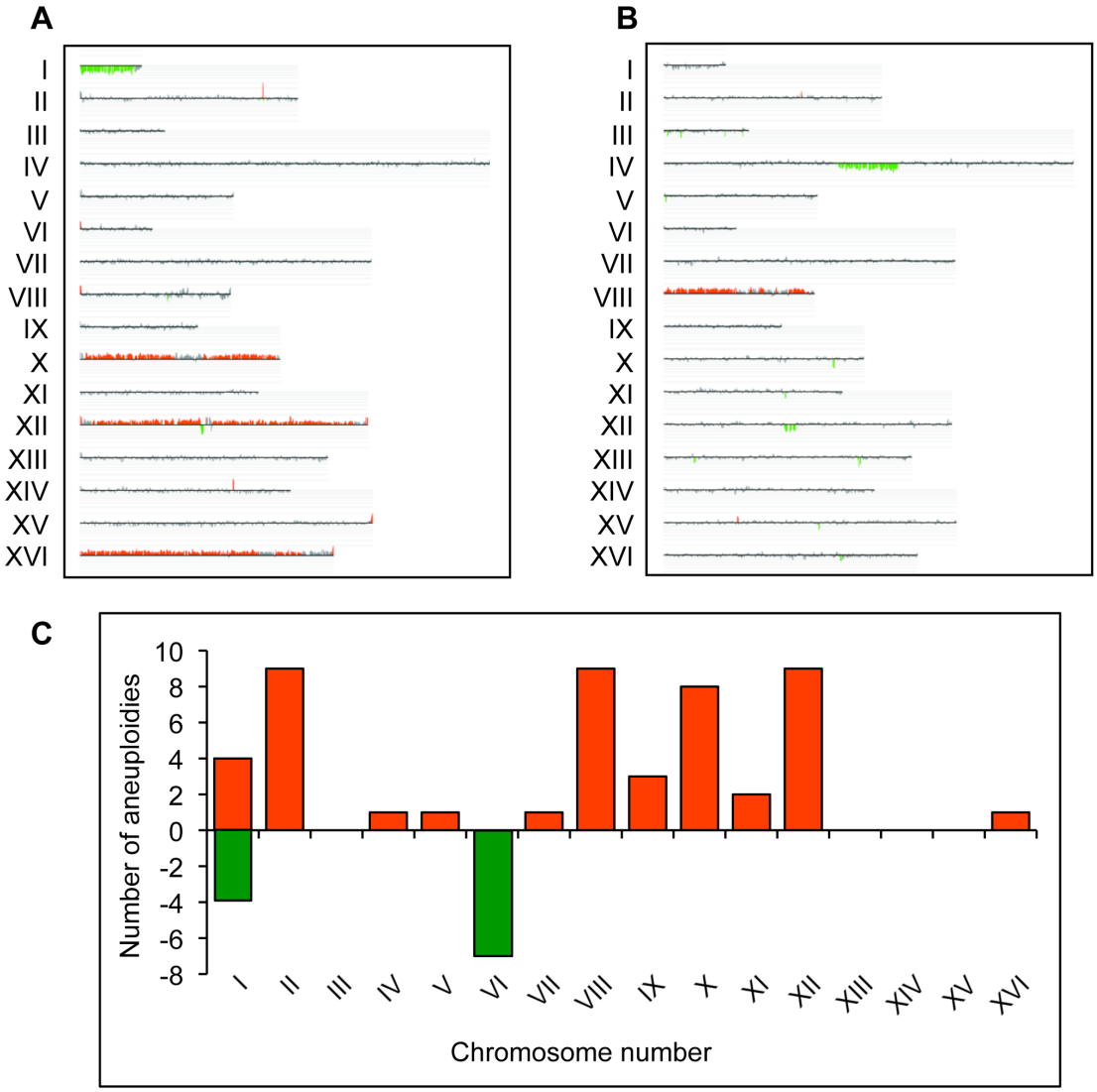

Figure 3.1 Microarray analysis of aneuploidy and chromosome rearrangements in *tel1 mec1* diploids.

Representative microarrays of two subcultured strains are shown (CGH Miner depiction). Each chromosome is shown as a single line with losses and gains of chromosomes or chromosome segments indicated in green and red, respectively. (A) The *tel1 mec1* diploid JLMy80-1s is monosomic for chromosome I and trisomic for chromosomes X, XII, and XVI. (B) The strain JLMy81-1L is trisomic for chromosome VIII and contains an interstitial deletion on chromosome IV. (C) The distribution of trisomies (red) and monosomies (green) in 20 independently subcultured *tel1 mec1* strains. Chromosomes II, VIII, X, and XII became trisomic with the highest frequencies.

Chromosomes II, VIII, X, and XII accounted for three-quarters of the trisomies, and chromosomes I and VI accounted for all of the monosomies (Fig. 3.1C). By Chi-square goodness of fitness tests (with Yates correction), the distributions of trisomies and monosomies were very significantly ($p<0.001$) different from random. Since chromosomes I and VI are the smallest chromosomes, it is likely that strains monosomic for other chromosomes have a selective growth disadvantage or the small chromosomes have a lower rate of re-duplication. Possible explanations for the non-random pattern of trisomic chromosomes will be addressed in Section 3.3.

We also examined the frequencies of aneuploid chromosomes in subcultured wild-type, *tel1*, and *mec1* diploids and in *tel1 mec1* haploids (Table 3.1, Appendix B). The *tel1 mec1* diploid strain had significantly more aneuploidy than any of these other strains. Thus, as for a number of other phenotypes, the *tel1* and *mec1* mutations have a synergistic or additive interaction for the aneuploidy phenotype. It is likely that the higher frequency of trisomy in the diploid *tel1 mec1* strains compared to the frequency of disomy in the haploid *tel1 mec1* strain reflects an ability of the cell to tolerate a 1.5-fold imbalance in gene expression of chromosomes more readily than a two-fold imbalance.

Table 3.1: Number of trisomic and monosomic (in parentheses) chromosomes in strains with mutations in the DNA damage checkpoint after five cycles of subculturing.

Chromosome number	*tel1 mec1* diploids	Wild-type diploids	*tel1* diploids	*mec1* diploids	*tel1 mec1* haploids	*tel1 mec1* + pVL1107-*URA3* diploids
I	4 (4)	0	1	0	0	4 (1)
II	9	0	0	1	3	4
III	0	0	0	0	1	0 (1)
IV	1	0	0	0	0	1
V	1	0	0	0	0	2
VI	0 (7)	0	0 (1)	0	0	0
VII	1	0	0	1	0	5
VIII	9	0	1	1	1	8
IX	3	0	0	1	0	4
X	8	0	0	2	0	2
XI	2	0	0	0	0	2
XII	9	0	0	0	2	5
XIII	0	0	0	0	0	3
XIV	0	0	0	1	0	0
XV	0	0	0	0	0	0
XVI	1	0	0	1	0	2
Total # trisomic (monosomic) chromosomes[1]	48 (11)	0 (0)	2 (1)	8 (0)	7 (0)	42 (2)
Total # chromosomes analyzed[2]	320	64	64	160	144	192
Aneuploid/euploid chromosomes	59/261	0/64[3]	3/61[4]	8/152[5]	7/137[6]	44/148

Table 3.1 Continued.

[1]Following sub-culturing strains for about 100 generations, we examined aneuploidy using CGH microarrays. The numbers outside parentheses represent the number of strains in which trisomy (or, rarely, tetrasomy) was observed for a given chromosome; the numbers inside parentheses represent the number of times we observed monosomy. The strain names for each genotype are in Appendix B.
[2]The total number of chromosomes was calculated by multiplying the number of independent strains examined by 16, the number of homologues in *S. cerevisiae*.
[3]Significant ($p<0.001$) reduction in the frequency of aneuploidy compared to the *tel1 mec1* diploid (Fisher exact test).
[4]Significant ($p<0.05$) reduction in the frequency of aneuploidy compared to the *tel1 mec1* diploid (Fisher exact test).
[5]Significant ($p<0.0001$) reduction in the frequency of aneuploidy compared to the *tel1 mec1* diploid (Fisher exact test).
[6]Significant ($p<0.005$) reduction in the frequency of disomy compared to the frequency of trisomy in *tel1 mec1* diploid (Fisher exact test).

3.2.3 Chromosome rearrangements in *tel1 mec1* diploids

By CHEF gel analysis, 19 of 20 subcultured *tel1 mec1* strains had at least one chromosome different in size from the progenitor parental strain (Fig. 3.2). Chromosome II in the wild-type strain (lanes 1 and 12) is larger than chromosome II in all of the *tel1 mec1* strains, since these strains were constructed by replacing the very large *TEL1* and *MEC1* genes (both located on chromosome II) with smaller drug resistance markers. Chromosome XII (containing the 150-repeat rRNA gene cluster) and chromosome VIII (containing the *CUP1* gene cluster) were particularly unstable. Changes in the sizes of these chromosomes were confirmed by Southern analysis using rDNA or *CUP1* hybridization probes (data not shown). Additionally, some changes in chromosome size were due to amplification of the tandem Y′ elements located at the telomeres on most chromosomes (Appendix A).

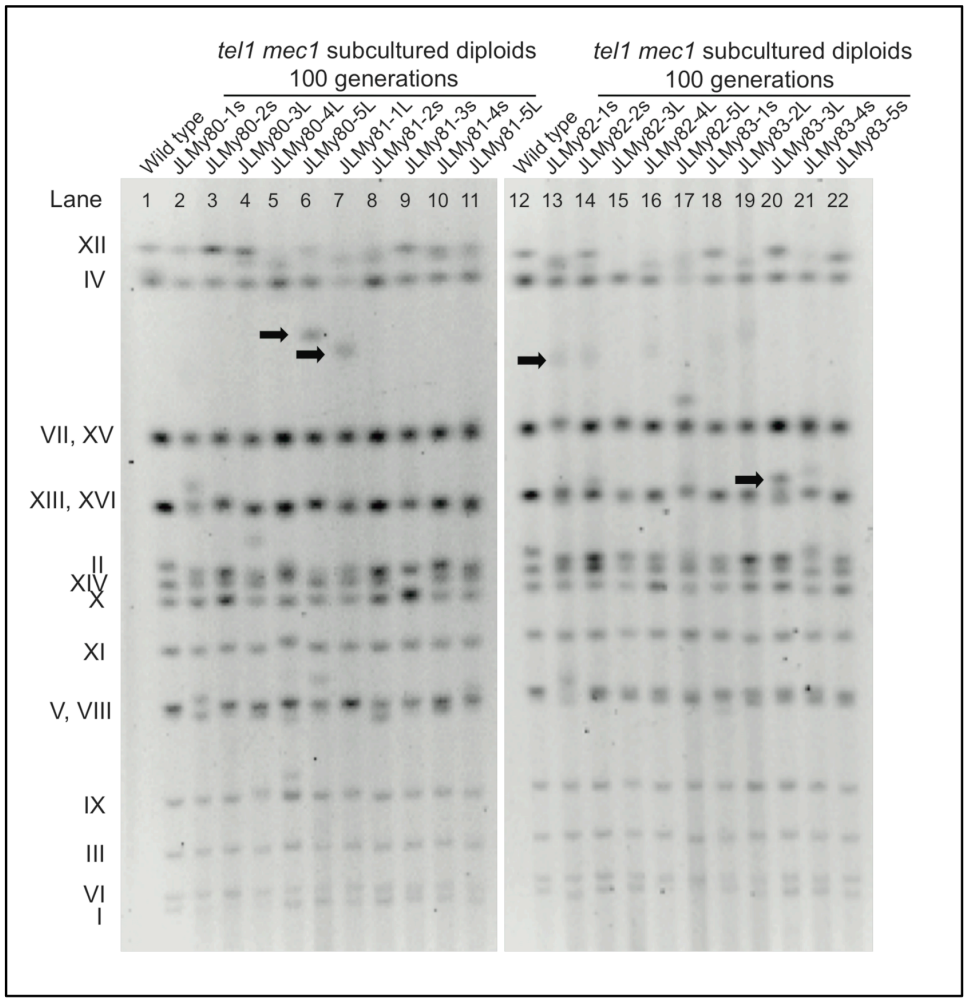

Figure 3.2 CHEF gel analysis of DNA derived from subcultured *tel1 mec1* diploids.

Separated yeast chromosomes were visualized by staining of the gel with ethidium bromide and exposure to UV. Relative to the wild-type strains (lanes 1 and 12), *tel1 mec1* diploids often had chromosomes of altered size. Chromosomes indicated with arrows are discussed in the text.

As described above, we also diagnosed chromosome rearrangements using microarrays. For example, the strain JLMy81-1L was heterozygous for a large interstitial deletion (Fig. 3.1B). The subcultured *tel1 mec1* diploid JLMy80-5L had a deletion and duplication on chromosome III, and a duplication of sequences from chromosome XII, in addition to having three copies of chromosome II and being monosomic for chromosome VI (Fig. 3.3A). Not including aneuploidy or changes involving the rRNA,

CUP1, or Y' genes, we found 20 large (>10 kb) genomic deletions or duplications among the 20 subcultured strains (Table 3.2, Appendix A).

Some of the chromosome rearrangements resulting in altered gene dosages were characterized in detail (Appendix A) and a few of these are indicated by arrows in Figure 3.2. The strain JMY80-5L had a novel chromosome of about 1350 kb. By both band microarray analysis (excision of the chromosome from a CHEF gel followed by hybridization to a microarray; Fig. 3.3B) and by Southern analysis of the CHEF gel (Fig. 3.3C), we showed that this chromosome had all of the DNA of chromosome II, a portion of the left arm of III, and an interstitial segment of XII. We used standard Southern analysis to determine the orientation and connectivity of the chromosome fragments and PCR analysis to amplify the fusion junctions. Primers were designed to amplify the fusion junctions, and the resulting PCR fragments were sequenced (Fig. 3.3D). The breakpoint on chromosome II is within 50 bp of the end of the chromosome. In addition, the sequence junctions share no homology, indicating that the tripartite chromosome was a consequence of two NHEJ events. Although NHEJ events are suppressed in *MAT***a**/*MAT*α diploids (Kegel *et al.*, 2001), JLMy80-5L is hemizygous at the mating type locus (Fig. 3.3A).

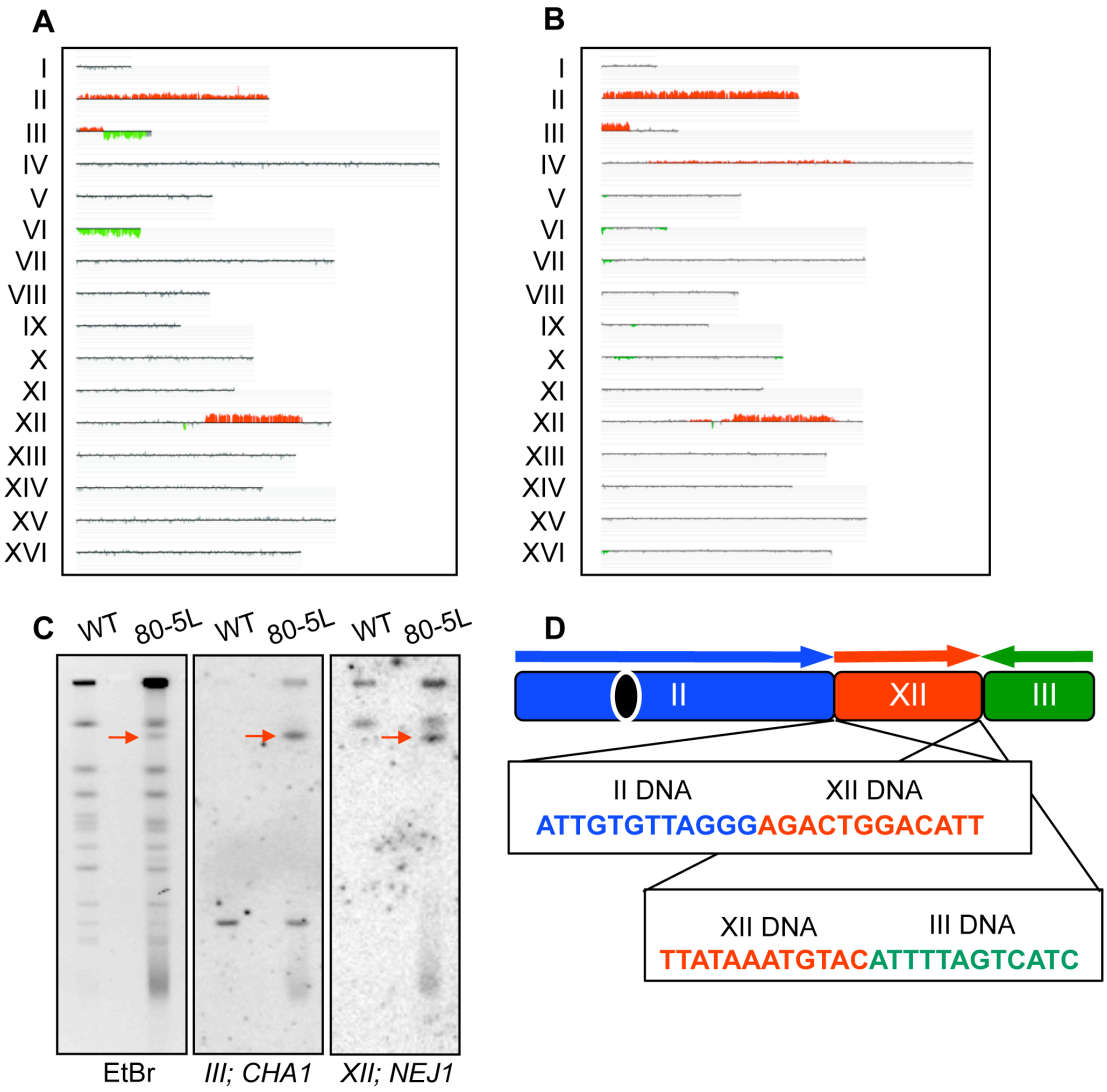

Figure 3.3 Mapping of a tripartite chromosome rearrangement.

(A) Genomic microarray analysis showed that the strain JLMy80-5L had an interstitial duplication on chromosome XII, a tandem deletion-duplication on III, trisomy for II, and monosomy for VI. (B) The 1350 kb altered chromosome was excised from the CHEF gel (indicated by an arrow in lane 6, Fig. 3.2) and analyzed by a microarray, delimiting the regions derived from chromosomes II, III, and XII. (C) The novel chromosome hybridized to probes derived from chromosomes III (*CHA1*), XII (*NEJ1*), and II (*PDR3*, data not shown). (D) PCR amplification and sequencing of the breakpoint junctions revealed that the tripartite chromosome was formed through two NHEJ events.

With the exception of JLMy80-5L, most chromosome rearrangements reflected intrachromosomal or interchromosomal exchanges between dispersed Ty retrotransposons similar to those observed in *tel1 mec1-21* haploid strains (Vernon *et al.*,

2008). Strain JLMy81-1L (Fig. 3.1B) had a large interstitial deletion on chromosome IV. We found that the breakpoints for the deletion were *YDRCTy1-1* and the *YDRWTy2-2*/*YDRCTy1-2* pair of Ty elements. Recombination between these elements would result in a 230 kb deletion, generating a novel chromosome of about 1300 kb as observed (Fig. 3.2, lane 7). Strain JLMy82-1s had a terminal deletion on the left arm of chromosome VII at an unannotated Crick-oriented Ty element (Casper *et al.*, 2009) near *YGLWdelta3* and a terminal amplification on the right arm of chromosome VII at *YGRWTy2-2*. We showed by a band array that the novel 1235 kb chromosome in this strain (Fig. 3.2, lane 13) was likely formed as a consequence of a DSB at or near the Ty element on the left arm that was repaired by break-induced replication (BIR) using *YRGWTy2-2* (Appendix A).

We also observed translocations involving Ty elements. The strain JLMy83-3L had a terminal amplification of the right end of chromosome I (breakpoint at *YARCTy1-1*) and a terminal deletion of the left end of chromosome XVI (breakpoint at *YPLWTy1-1*) (Fig. 3.4A). The expected size of a I-XVI translocation involving these breakpoints is about 960 kb, the size of a novel chromosome in this strain (Fig. 3.2, lane 20). We used a band array (Fig. 3.4B) and PCR analysis (Fig. 3.4C) to confirm the translocation. This chromosome was likely the result of a DSB in the Ty element on chromosome XVI that was repaired by a BIR event utilizing the Ty element on chromosome I.

As expected from previous studies (Craven *et al.*, 2002; Myung *et al.*, 2001b), deletions and duplications of chromosomal sequences were observed more frequently in the *tel1 mec1* diploid than in wild-type, *tel1*, or *mec1* diploids (Table 3.2). In contrast, the isogenic *tel1 mec1* haploid had approximately the same frequency of chromosome rearrangements as the diploid.

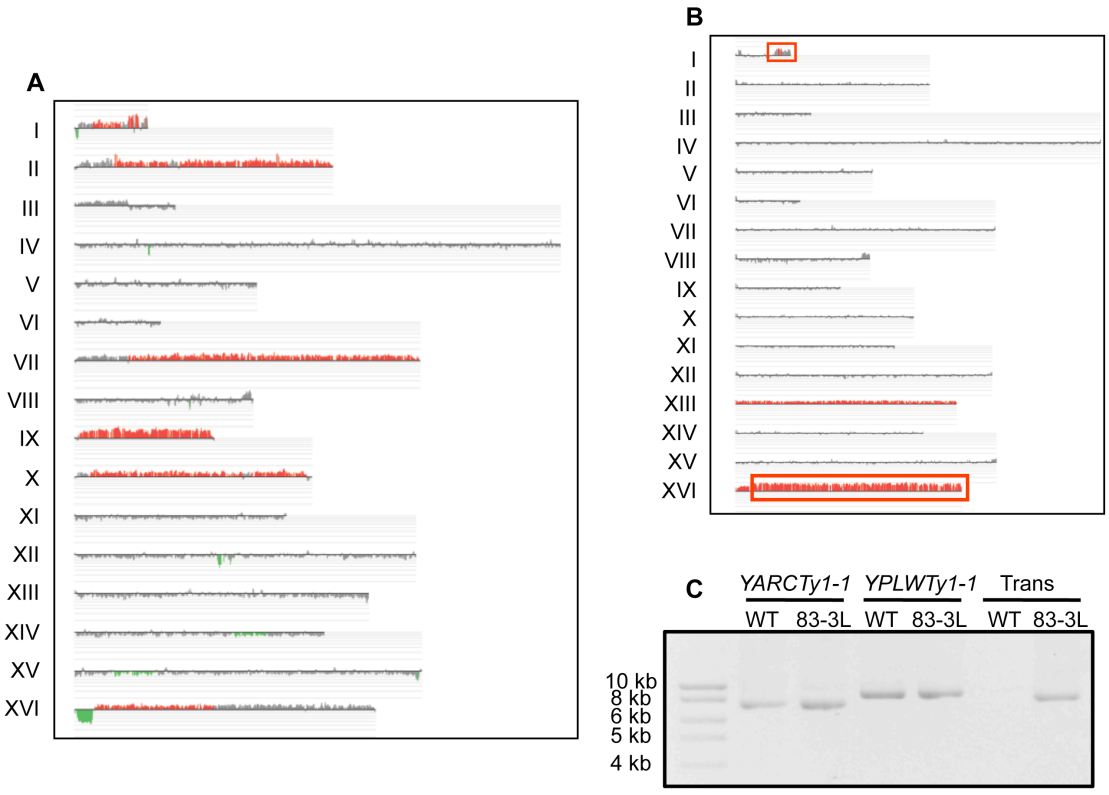

Figure 3.4 Translocation in JLMy83-3L between two Ty elements, one located on chromosome I and one located on chromosome XVI.

(A) Genomic microarray analysis of JLMy83-3L indicated multiple trisomic chromosomes in addition to a terminal amplification of chromosome I, a terminal deletion on chromosome XVI, and an amplification of part of chromosome III. (B) JLMy83-3L had a novel chromosome 960 kb in size (Fig. 3.2, lane 20). This band was purified using a CHEF gel, and a band microarray analysis was done. This analysis confirmed that the rearranged chromosome contained most of the DNA from chromosome XVI and a small piece of the right arm of chromosome I. The DNA sample for the band array was contaminated with small amounts of the unrearranged chromosomes XIII and XVI. The genomic and band microarrays indicated Ty1 elements at the breakpoints of the XIII-XVI translocation in the orientation allowing formation of a monocentric 960 kb chromosome. (C) Additional evidence that the translocation was a consequence of homologous recombination between Ty elements was achieved through PCR analysis. Primers were designed that flanked *YARCTy1-1* on chromosome I (primers JLMo227 and JLMo229 in Table 2.3) and *YPLWTy1-1* on chromosome XVI (primers JLMo245 and JLMo246 in Table 2.3). These primers resulted in a product of the expected size in the progenitor strain (JLMy83) and JLMy83-3L, as expected since JLMy83-3L contains unrearranged copies of chromosome I and XVI in addition to the translocation. When we used one primer located telomere-proximal to *YARCTy1-1* (JLMo227) and one primer telomere-proximal to *YPLWTy1-1* (JLMo246) in the "Trans" PCR reactions in the last two lanes, we observed the expected product from the strain with the translocation and no product in the progenitor strain.

Table 3.2 Number of duplications and deletions in strains with mutations in the DNA damage checkpoint.

Chromosome number	*tel1 mec1* diploids	Wild-type diploids	*tel1* diploids	*mec1* diploids	*tel1 mec1* haploids	*tel1 mec1* + pVL1107-*URA3* diploids[2]
I	2	0	0	1	2	1
II	2	0	0	0	0	0
III	2	0	0	0	1	0
IV	3	0	0	0	1	1
V	2	0	0	0	0	0
VI	1	0	0	0	0	0
VII	1	0	0	1	0	0
VIII	0	0	0	0	0	0
IX	0	0	0	0	0	0
X	3	0	0	0	2	0
XI	0	0	0	0	0	0
XII (excluding rDNA)	2	0	0	1	5	0
XIII	0	0	0	0	0	0
XIV	1	0	0	0	1	0
XV	0	0	0	0	0	0
XVI	1	0	0	1	0	0
Total # chromosomes with duplications and/or deletions[1,3]	20	0	0	4	12	2
Total # strains analyzed	20	4	4	10	9	12
# strains with del. or dup./# strains without del. or dup.	10/10	0/4	0/4	2/8	9/0	1/11[4]

Table 3.2 Continued.

[1]Following sub-culturing strains for about 100 generations, we examined deletions and duplications using CGH microarrays. The numbers represent the number of strains in which duplications or deletions were observed for a given chromosome. Only deletions/duplications >10 kb were considered significant. In addition to the alterations listed in the table, we found frequent changes (usually deletions) in the tandem array (150 repeats) of ribosomal RNA genes. The number of these changes for each strain were: *tel1 mec1* diploid (16 deletions), wild-type diploid (two deletions), *tel1* diploid (no changes), *mec1* diploid (two deletions), *tel1 mec1* haploid (one expansion), and *tel1 mec1* diploid with the pVL1107-*URA3* plasmid (two deletions and three expansions). In addition, we observed amplification of the sub-telomeric Y′ repeats in five *tel1 mec1* diploids and in none of the other strains. Amplifications of the Y′ repeats (which are found in about two-thirds of the telomeres) cannot be assigned to a specific chromosome by the microarrays.
[2]The plasmid pVL1107-*URA3* contains a *CDC13-EST2* fusion gene (Evans and Lundblad, 1999) that allows the telomeres of *tel1 mec1* strains to be elongated to wild-type lengths or greater (Tsukamoto *et al.*, 2001).
[3]Excluding changes in the rRNA gene cluster and Y′ copy variation.
[4]Significant ($p<0.01$) reduction in the frequency of deletions/duplications compared to the *tel1 mec1* diploid without the pVL1107-*URA3* plasmid (Fisher exact test).

3.2.4 Restoring wild-type length telomeres to *tel1 mec1* strains reduces the frequency of chromosome rearrangements, but does not reduce the frequency of aneuploidy

Previously, we showed that restoring wild-type length telomeres in a *tel1 mec1* haploid strain reduced the rate of *CAN1* deletions and telomere-telomere fusions (TTFs; Mieczkowski *et al*., 2003), arguing that some chromosome alterations in the haploid *tel1 mec1* strain reflected breakage of the dicentric chromosome that would be produced by TTFs. Loss of telomeres associated with *tel1 mec1* strains or the high levels of spontaneous DNA lesions associated with this genotype could also affect the rate of chromosome non-disjunction.

To examine the relationship between telomere length and the increased levels of aneuploidy and chromosome rearrangements in *tel1 mec1* diploid cells, we introduced a plasmid (pVL1107-*URA3)* encoding a Cdc13p-Est2p fusion protein (Evans and Lundblad, 1999) that allows telomere elongation independently of Tel1p and Mec1p (Tsukamoto *et al*., 2001). This plasmid restored wild-type length telomeres to the *tel1 mec1* diploid (Fig. 3.5A) and substantially reduced the level of TTFs (Fig. 3.5B). The *tel1 mec1* strains with wild-type length telomeres had the same frequency of aneuploidy as the *tel1 mec1* strains with the short telomeres (Table 3.1). In contrast, only 1 of 12 *tel1 mec1* diploids with wild-type length telomeres had a chromosome alteration compared to 10 of 20 *tel1 mec1* strains with short telomeres (Table 3.2).

These results demonstrate two important points. First, the high frequencies of aneuploidy and chromosome rearrangements are caused by two different types of mechanisms. Second, in *tel1 mec1* diploids, as in haploids, it is likely that many chromosome rearrangements are initiated by telomere fusions. This conclusion is somewhat surprising since TTFs are a type of NHEJ, a recombination pathway that is suppressed in *MAT***a**/*MAT*α diploids.

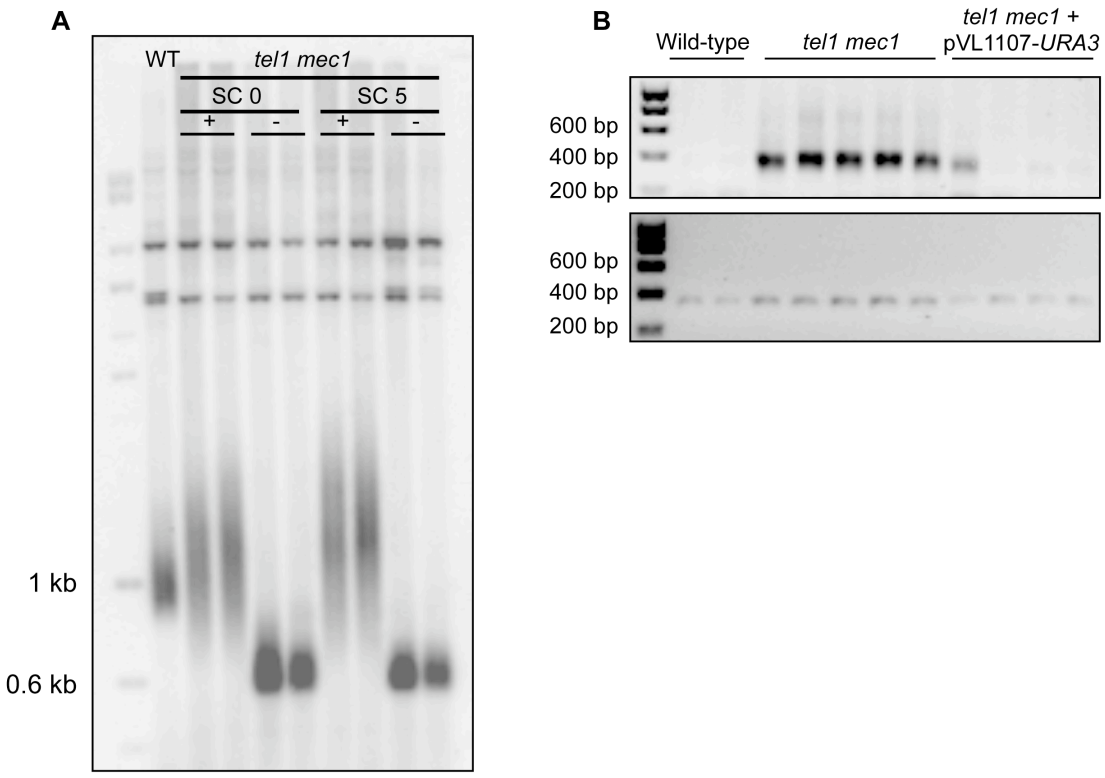

Figure 3.5 Analysis of telomere length and telomere-telomere fusions (TTFs) in *tel1 mec1* strains with and without pVL1107-*URA3*, a plasmid encoding a Cdc13p-Est2p fusion protein.

(A) Telomere lengths were determined by Southern analysis. Genomic DNA was isolated from two *tel1 mec1* diploids with a control plasmid (JLMy1301 and JLMy1311) or with the pVL1107-*URA3* plasmid (JLMy1262 and JLMy1271) immediately after transformation (SC 0) or after five rounds of subculturing (SC 5). The genomic DNA was treated with *Pst*I and the separated fragments were hybridized to the probe prepared by amplification of the plasmid pYT14 (which contains yeast telomeric sequences) with the primers Y′ F and Y′ R (Table 2.3). The lanes marked "+" contain DNA isolated from strains with pVL1107-*URA3* and the lanes marked "-" contain DNA from strains with the control plasmid. Restriction fragments containing the terminal poly $G_{1\text{-}3}T$ tract are fuzzy because of the heterogeneity of the length of the tracts in different cells and on different chromosomes; the 5.4 and 6.7 kb fragments that hybridize to the probe represent tandemly arrayed sub-telomeric repeats of two different sizes. The telomeric *Pst*I fragment is about 1 kb in wild-type cells (strain MS71) and in *tel1 mec1* diploids with pVL1107-*URA3* plasmid, and about 650 bp in *tel1 mec1* cells lacking the plasmid. Thus, as expected (Tsukamoto *et al.*, 2001), the Cdc13p-Est2p fusion protein restores telomeres to wild-type length in the *tel1 mec1* mutant. (B) PCR analysis was used to detect telomere–telomere fusions (TTFs) according to our published method (Mieczkowski *et al.*, 2003). PCR was performed using one primer derived from sub-telomeric repeat X and one from sub-telomeric repeat Y′ and the resulting products were examined by gel electrohoresis (upper part of (B)). A PCR product was evident in all five *tel1 mec1* diploids lacking a plasmid, but none were detected in the two wild-type strains or in three of the four *tel1 mec1* diploids bearing pVL1107-*URA3*. The same genomic samples analyzed for TTFs were also used as substrates with a control set of primers (APT1 F and APT1 R, Table 2.3) that amplified DNA from the single-copy *APT1* locus (bottom part of (B)).

3.2.5 Investigation of the relationship between the elevated levels of aneuploidy in *tel1 mec1* diploids and the spindle assembly checkpoint (SAC)

As discussed in Section 3.1, one large class of genes involved in chromosome disjunction in both yeast and mammalian cells is that involved in the spindle assembly checkpoint (SAC). In addition, in response to DNA damage, Tel1p and Mec1p activate the SAC. We investigated the relationship between Tel1p, Mec1p, and the SAC in two ways. First, we examined the aneuploidy associated with mutations in the known SAC genes *BUB1* and *MAD2* using microarrays. Second, we investigated whether *tel1 mec1* strains were arrested by the microtubule-destabilizing drug benomyl. These experiments (described below) indicate that *tel1 mec1* strains have a functional SAC.

We first examined aneuploidy in diploids with the *bub1-Δ* mutation. Since haploids with this mutation had high levels of aneuploidy (data not shown), we constructed the homozygous diploids by disrupting the remaining wild-type *BUB1* allele in a heterozygous diploid (Table 2.2), and examining the resulting independent transformants without subculturing. 8 of 8 *bub1-Δ* diploids examined by microarrays were trisomic and/or monosomic for one or more chromosomes (Appendix B). Interestingly, 16 of the 25 trisomic chromosomes observed were chromosomes II, VIII, and X (Table 3.3); these three chromosomes plus chromosome XII were the most commonly observed trisomes in the *tel1 mec1* diploid. We have preliminary evidence (Chapter 4) that DSBs within the ribosomal DNA are more frequent in *tel1 mec1* strains than in *bub1-Δ* strains. Strains monosomic for chromosomes III, IX, XI, and XVI were observed in the *bub1-Δ* strains whereas only monosomy for chromosomes I and VI were seen in the *tel1 mec1* diploids.

Table 3.3 Number of trisomic/tetrasomic and monosomic (in parentheses) chromosomes in strains with mutations in the SAC genes and/or DNA damage checkpoint genes.

Chromosome number	*bub1-Δ* diploids (SC 0)	*bub1-ΔK* diploids (SC 5)[3]	*tel1 mec1 bub1-ΔK* diploids (SC 5)[3]	*mad2* diploids (SC 5)
I	1	1	8	1 (1)
II	3	5	9	0
III	2 (1)	4	2	0
IV	0	0	1	0
V	3	1	4	0
VI	0	2	0	0
VII	0	0	0	0
VIII	8	8	11	2
IX	0 (1)	0	1 (1)	0
X	5	5	11	0
XI	0 (2)	0 (2)	1	1
XII	0	0	4	0
XIII	0	1	1	0
XIV	1 (1)	2	1	0
XV	0	0	0	0
XVI	2	6	7	0
Total # trisomic (monosomic) chromosomes[1]	25 (5)	35 (2)	61 (1)	4 (1)
Total # chromosomes analyzed[2]	128	192	192	128
Aneuploid/euploid chromosomes	30/98	37/155	62/130	5/123

[1]Aneuploidy was examined using microarrays. Strains with the null mutation of *BUB1* (*bub1-Δ*) had very high frequencies of aneuploidy without subculturing (indicated as SC 0). Strains of the other three genotypes were subcultured five times (SC 5). The numbers outside parentheses represent the number of strains in which trisomy (or, rarely, tetrasomy) was observed for a given chromosome; the numbers inside parentheses represent the number of times we observed monosomy.
[2]The total number of chromosomes was calculated by multiplying the number of independent strains examined by 16, the number of homologues in *S. cerevisiae*.
[3]The genotypes of *bub1-ΔK* and *tel1 mec1 bub1-ΔK* were not free of aneuploidy at SC 0; the data shown depicts all genetic alterations at SC 5 regardless of whether they existed at SC 0 or not. The complete spectra of aneuploidy for these strains at SC 0 and SC 5 are shown in Appendix B.

Since the pattern of trisomy in the *bub1-Δ* diploid was similar to that observed in the *tel1 mec1* diploid, we extended our analysis to examine diploids with the *bub1-ΔK* allele.

bub1-ΔK lacks the C-terminal kinase domain of Bub1p from amino acid 609, but maintains the N-terminal kinetochore localization domain and the Mad1p and Bub3p binding domains (Fernius and Hardwick, 2007). This deletion of the kinase domain of Bub1p results in a strain that has a functional kinetochore-occupancy SAC, but a defective tension-sensing SAC (Fernius and Hardwick, 2007). After approximately 100 cell divisions, 12 of 12 independent isolates were trisomic and/or monosomic for multiple chromosomes (Appendix B). Both the frequencies of aneuploidy and the types of chromosomes that become trisomic are similar to the observations with the *tel1 mec1* diploids except that the *bub1-ΔK* strains have higher frequencies of trisomy for chromosome XVI and lower levels of trisomy for chromosome XII (Tables 3.1 and 3.3).

Unlike the diploids with mutations in the *BUB1* gene, subcultured *mad2* diploids had much lower frequencies of aneuploidy (Table 3.3). Since *mad2* diploids lack all SAC function, these observations argue that aneuploidy in *tel1 mec1* and *bub1* diploids reflect a defect in chromosome segregation that is, at least in part, independent of the SAC. We also examined aneuploidy in triple mutant *tel1 mec1 bub1-ΔK* diploids. The frequency of aneuploidy exceeded the frequencies observed in *tel1 mec1* and *bub1-ΔK* strains. These results will be analyzed further in Section 3.3.

We also examined the effect of the *tel1 mec1* and *bub1* mutations on the frequency of loss of a *URA3* centromere-containing plasmid (pRS316; Sikorski and Hieter, 1989). Diploid strains of various genotypes containing the plasmid were grown on rich solid medium and then replica-plated to medium lacking uracil. The frequencies of Ura^+/Ura^- sectored colonies (frequencies in parentheses; total number of colonies scored in brackets) were: wild-type (0.04 [491]), *tel1 mec1* (0.50 [275]), *bub1-ΔK* (0.33 [396]), and *tel1 mec1 bub1-ΔK* (0.81 [79]). These results suggest that the triple mutant strain has a higher level of plasmid loss than either the *tel1 mec1* or *bub1-ΔK* strains.

Since yeast strains with a defective SAC are sensitive to the microtubule-destabilizing drug benomyl (Hoyt *et al.*, 1991; Li and Murray, 1991), we also investigated the benomyl-sensitivity of the *tel1 mec1* strain. As shown in Figure 3.6A, the *tel1 mec1* strain grew poorly on all plates, including the plate lacking benomyl. The same strain with the pVL1107-*URA3* plasmid, which restores wild-type length telomeres to the *tel1 mec1* strain, had better growth on all plates and did not exhibit obvious sensitivity to benomyl, in contrast to the sensitivity of *bub1* and *mad2* strains.

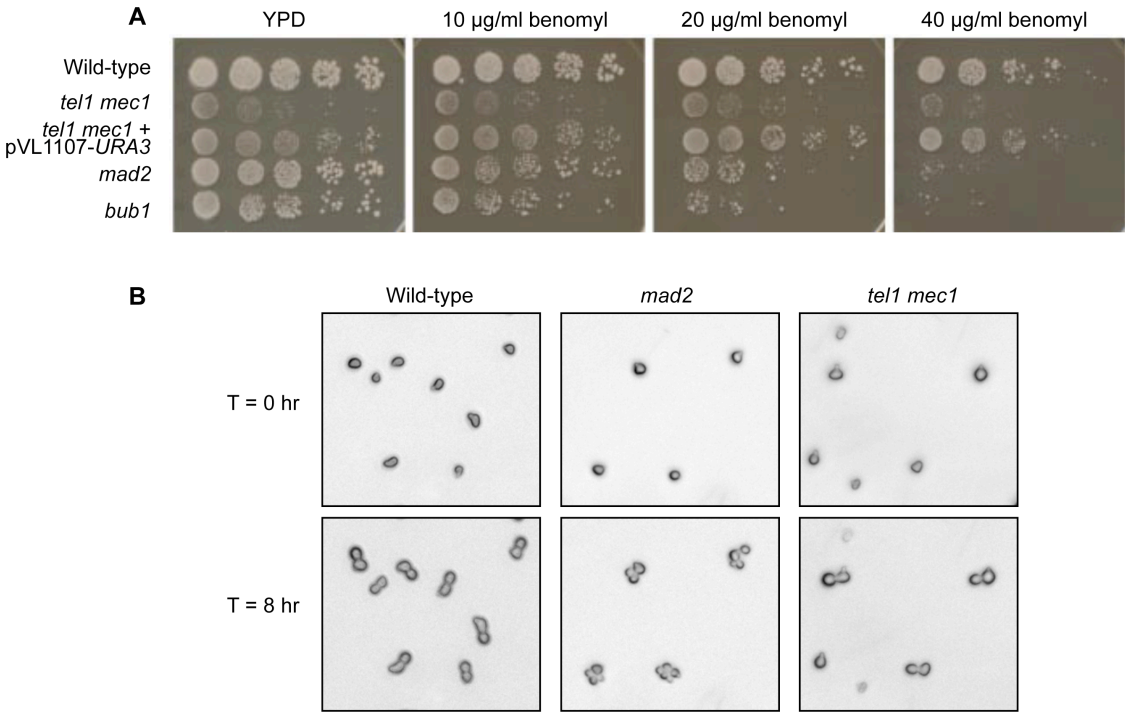

Figure 3.6 *tel1 mec1* cells have a functional spindle assembly checkpoint (SAC) in response to the microtubule-destabilizing drug benomyl.

(A) Ten-fold serial dilutions of cells from diploid wild-type (JLMy101), *tel1 mec1* (JLMy80-Trp$^-$), *tel1 mec1* + pVL1107-*URA3* (JLMy1262-Trp$^-$), *mad2* (JLMy366), and *bub1-Δ* (JLMy156) strains were spotted onto solid medium containing various amounts of benomyl. (B) Haploid wild-type (JLMy62-7c), *tel1 mec1* (JLMy62-18c-Trp$^-$), and *mad2* (JLMy309) strains were arrested in alpha factor, sonicated, and released onto plates containing 70 µg/ml benomyl. The cell cycle progression of individual cells was followed 8 hours. Representative pictures show that while *mad2* cells fail to arrest at G2/M following exposure to benomyl, wild-type and *tel1 mec1* strains demonstrate a robust cell cycle arrest. By microscopic examination, we determined that the small protuberances seen in the wild-type and *tel1 mec1* cells represent "shmoos" (cell shapes produced by long incubation of cells in alpha pheromone) rather than buds.

We also tested whether *tel1 mec1* strains arrest the cell cycle in response to benomyl by examining individual cells in the presence of the drug (Hoyt *et al.*, 1991; Li and Murray, 1991). We treated haploid *MAT***a** wild-type, *tel1 mec1*, and *mad2* strains with alpha factor for approximately 3 hours to arrest the cells in G1. We then removed alpha factor and plated the cells on rich growth medium containing benomyl (70 μg/ml) or lacking benomyl. We photographed cells that were unbudded (>80% after alpha factor treatment), and re-examined the same cells after 8 hours at room temperature. In the absence of benomyl, about 80% of the wild-type and *mad2* cells budded more than once. In the presence of benomyl, 97% of the wild-type cells arrested as doublets, as expected for cells with a functional SAC (Fig. 3.6B, Table 3.4). In contrast, most (78%) of the *mad2* cells continued to divide. Less than half of the *tel1 mec1* cells produced a bud in the presence or absence of benomyl, as expected since *tel1 mec1* cultures contain many cells incapable of division (Ritchie *et al.*, 1999). Of those cells producing a bud, however, most (97%) arrested as doublets in the presence of benomyl. Because *tel1 mec1* mutants grow more slowly than the wild-type, we continued the incubation period in benomyl for an additional 4 hours; the cells remained arrested as doublets. Thus, *tel1 mec1* strains have a functional SAC.

Table 3.4 Analysis of the abilities of wild-type, *mad2*, and *tel1 mec1* strains to arrest the cell cycle in response to benomyl.

Genotype	Condition of growth[1]	# single cells examined	# viable cells	# and frequency (parentheses) of viable single cells that produce doublets	# and frequency (parentheses) of microcolonies
Wild-type	- benomyl	200	170	12 (0.07)	158 (0.93)
Wild-type	+ benomyl	200	173	168 (0.97)	5 (0.03)
mad2	- benomyl	200	167	25 (0.15)	142 (0.85)
mad2	+ benomyl	200	170	37 (0.22)	133 (0.78)
tel1 mec1	- benomyl	268	82	31 (0.38)	51 (0.62)
tel1 mec1	+ benomyl	358	154	149 (0.97)	5 (0.03)

[1]Cells synchronized in G1 (unbudded cells) were incubated on rich-growth solid medium in the absence (- benomyl) or presence (+ benomyl) of the microtubule-destabilizing drug. After 8 hours of incubation, the same cells were scored as inviable (cells that remained unbudded) or viable (cells that produced at least one bud). The viable cells were scored as doublets (mother and bud of approximately the same size), or microcolonies (more than two cells).

3.3 Discussion

As discussed in Section 3.1, CIN tumors have very elevated rates of chromosome rearrangements and aneuploidy. Our observations of diploid *tel1 mec1* strains show that both of these phenotypes can be produced by a single genotype. The main conclusions from our study are: 1) the elevated frequencies of chromosome rearrangements and aneuploidy in *tel1 mec1* strains reflect two different mechanisms, since elongation of telomeres suppresses the frequency of chromosome rearrangements and has little effect on the frequency of aneuploidy, 2) the patterns of aneuploidy in the *tel1 mec1* and *bub1* strains are similar, and 3) the aneuploidy in *tel1 mec1* strains is not a consequence of a defective SAC.

3.3.1 Chromosome rearrangements

As in our previous study in a *tel1 mec-21* haploid strain (Vernon *et al.*, 2008), most of the chromosome rearrangements in the *tel1 mec1* diploid were a consequence of homologous recombination between Ty elements. The single chromosome rearrangement resulting from NHEJ (Fig. 3.3) was in a strain that had become hemizygous for mating type, presumably resulting in derepression of the NHEJ pathway. In haploid strains in which deletions/chromosome rearrangements were selected in a region of chromosome V lacking repetitive elements, most chromosome alterations reflected NHEJ events (Craven *et al.*, 2002; Myung *et al.*, 2001b) whereas deletions/rearrangements for markers located distal to a repeated gene often involved homologous recombination (Putnam *et al.*, 2009a).

The frequency of chromosome rearrangements was substantially reduced in *tel1 mec1* strains that expressed the Cdc13p-Est2p fusion protein which elongates telomeres to wild-type lengths; these strains also have fewer telomere-telomere fusions than strains without the Cdc13p-Est2p fusion protein (Fig. 3.5B). One simple interpretation of

this result is that most chromosome rearrangements in *tel1 mec1* strains are initiated as a consequence of breakage of dicentric chromosomes resulting from telomere fusions. DSB formation in a Ty element could be repaired by recombination with an ectopic Ty element, leading to chromosome rearrangements (Vernon *et al.*, 2008). An alternative model is that chromosomes in the *tel1 mec1* background are degraded from the ends until a Ty element is rendered single-stranded and recombinogenic (Hackett and Greider, 2003). This model predicts that one of the Ty elements involved in the recombination event will be close to the telomere. Since many of our chromosome rearrangements involve Ty elements that are distant from the telomere (for example, Fig. 3.1B), we favor the model that the initiating lesion for most rearrangements reflects breakage of a dicentric.

3.3.2 Frequencies of aneuploidy in *tel1 mec1* and in spindle assembly checkpoint (SAC)-deficient strains

Strains with both *tel1* and *mec1* mutations had significantly elevated frequencies of aneuploidy relative to either single mutant strain, although the *mec1* strain also had a high frequency of aneuploidy, as expected from previous studies (Craven *et al.*, 2002; Klein, 2001). We interpret this result as indicating that Tel1p and Mec1p have functionally redundant roles in chromosome disjunction similar to their functionally redundant roles in DNA damage checkpoints and telomere length regulation. Since there is considerable heterogeneity in the growth rates of various aneuploidy strains and since many *tel1 mec1* cells fail to give rise to viable colonies, it is difficult to calculate an accurate rate of chromosome non-disjunction from the frequency data. As a crude estimate, we calculate that the probability of detecting aneuploidy in 100 cell divisions, if the rate of non-disjunction per cell division is 10^{-3}, to be 1- $(0.999)^{100}$ or about 0.1; if the rate of non-disjunction is 10^{-2}, then the probability of detecting aneuploidy in 100

divisions is $1 - (0.99)^{100}$ or about 0.7. Thus, the rate of non-disjunction per chromosome per cell division is about 10^{-2} to 10^{-3} for the most frequently lost chromosomes.

The frequency of non-disjunction was also very high in the *bub1-Δ* and *bub1-ΔK* strains, but not in the *mad2* strain. Warren *et al.* (2002) previously observed that *bub1* mutants had about 10-fold higher chromosome loss rates than *mad2* strains and suggested that Bub1p, but not Mad2p, had a role in chromosome segregation in the absence of induced spindle damage. A variety of experiments have indicated that Bub1p is important in establishing the correct inner and outer kinetochore structure (reviewed by Williams *et al.*, 2007), and cells with low levels or no Bub1p have defective associations between the kinetochore and microtubules, decreased levels of chromosomes that are bioriented at the spindle, and decreased sister chromatid cohesion at the centromere (Logarinho and Bousbaa, 2008). Thus, the loss of Bub1p, unlike the loss of Mad2p, results in defects in the mechanics of chromosome segregation in addition to defects in the SAC, resulting in very high levels of aneuploidy.

3.3.3 Non-random recovery of trisomic chromosomes in *tel1 mec1* and in spindle assembly checkpoint (SAC)-deficient strains

There is a preference for the recovery of chromosomes II, VIII, X and XII as trisomes in the *tel1 mec1* strain (Table 3.1). If we perform a Chi-square goodness of fit test for these same four chromosomes in the *bub1-Δ* and *bub1-ΔK* strains, there is a very significant ($p<0.001$) non-randomness in their recovery (Table 3.3). One difference in the pattern of trisomies in the three strains is that chromosome XII was often trisomic in the *tel1 mec1* strains and was not trisomic in the *bub1* strains.

There are three plausible explanations for the preferential recovery of certain chromosomes as trisomes. First, certain chromosomes, when present in three copies in a diploid, may greatly reduce cell growth rates. This explanation is unlikely for two reasons: 1) in nine strains with trisomic chromosomes resulting from gamma irradiation

of diploids, a broad spectrum of trisomies were observed (I, V, VIII, IX, XI, XII, XIII) that did not include chromosomes II or X (Argueso *et al.*, 2008) and 2) Torres *et al.* (2007) observed that all yeast chromosomes, except chromosome VI, were recoverable as disomes in haploids. Second, the presence of certain trisomic chromosomes may alleviate some of the negative effects of *tel1 mec1* and/or *bub1* mutations. For example, we previously showed that chromosome VIII disomy in *tel1 mec1-21* haploids was suppressed by *DNA2*, a gene located on VIII (Vernon *et al.*, 2008), although, in a single preliminary experiment, we did not see suppression of trisomy by *DNA2* in the *tel1 mec1* diploid (data not shown). A third possibility is that the defect in chromosome segregation observed in the *tel1 mec1* and *bub1* strains affects some chromosomes more than others. We suggest that the non-random recovery of trisomes is likely to reflect the two latter explanations, possibly arguing a similarity in the mechanistic chromosome disjunction defects in the *tel1 mec1* and *bub1* strains.

3.3.4 Cellular roles of Tel1p and Mec1p in regulating aneuploidy

Our analysis demonstrates that Tel1p and Mec1p have an important role in chromosome segregation in addition to their previously demonstrated roles in DNA repair and telomere length regulation. Elevated rates of chromosome loss have been observed in mutants affecting kinetochores, microtubules, the spindle pole body, sister chromatid cohesion, DNA replication/repair, and the SAC. Our results rule out an involvement of Tel1p and Mec1p in the SAC, although we cannot define what other role these proteins have in chromosome segregation.

One possibility is that Tel1p and Mec1p affect chromosome segregation in the same pathways affected by Bub1p that are related to kinetochore function (Fig. 3.7). One argument in favor of this possibility is the similar patterns of trisomies observed in *tel1 mec1* and *bub1* strains. An argument against this possibility is that the chromosome segregation defect of the triple mutant *tel1 mec1 bub1-ΔK* strain is more extreme than the

defects of the *tel1 mec1* or *bub1-ΔK* strains. Although this result could be interpreted as indicating that Tel1p/Mec1p and Bub1p affect different chromosome disjunction mechanisms, it is also possible that the Tel1p/Mec1p effects are partially redundant with those of Bub1p, acting in the same pathway (similar to the functional redundancy of Tel1p and Mec1p in regulating telomere length).

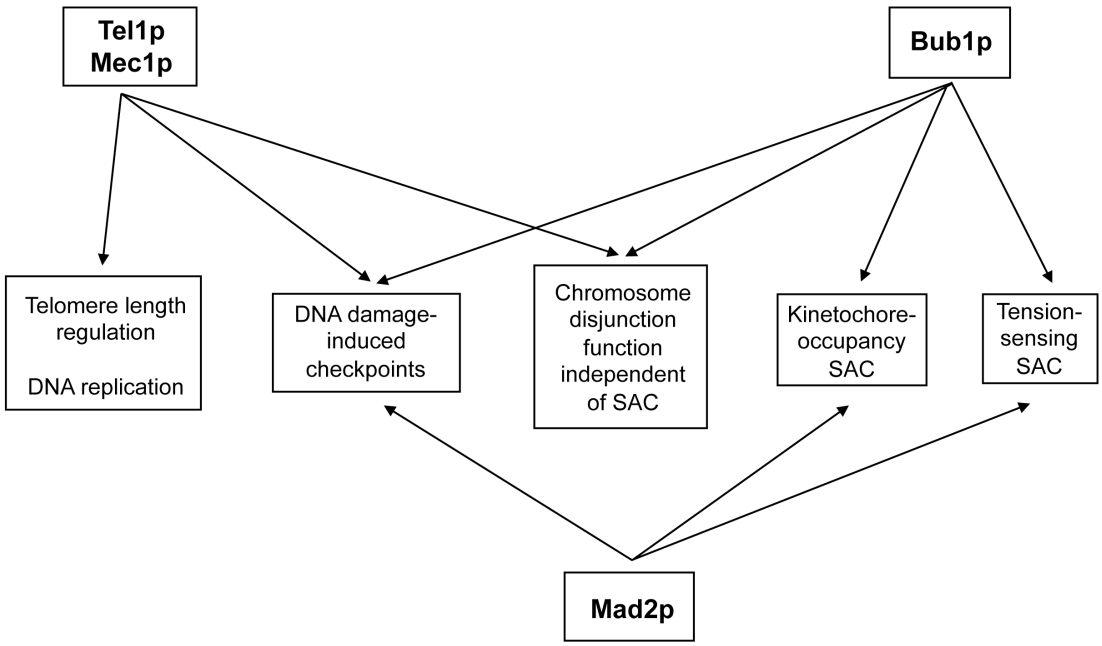

Figure 3.7 Pathways involving Tel1p, Mec1p and SAC proteins.

The indicated associations of proteins and pathways are based on information described in the text. Kim and Burke (2008) showed a role of the Bub1p and Mad2p proteins in the DNA-damage induced checkpoint.

A second model is that a high level of DSBs in *tel1 mec1* strains or perturbations of DNA replication result in aneuploidy. In support of this model, temperature-sensitive *mec1* strains, which likely do not have short telomeres, accumulate DSBs at the restrictive temperature (Cha and Kleckner, 2002), and repaired DSBs interfere with proper chromosome segregation (Kaye *et al.*, 2004). In addition, *mec1* strains, exposed to

hydroxyurea, have high levels of aberrant segregation (Feng *et al.*, 2009). Although it is possible that DSBs or replication disturbances are relevant to the aneuploidy, our observations that *tel1 mec1* strains have very high rates of plasmid loss is more consistent with a problem with the kinetochores in *tel1 mec1* strains. Finally, we point out that direct investigations of kinetochore function are very difficult in *tel1 mec1* strains because this genotype results in a high rate of non-viable cells and heterogeneity in growth rates among the viable cells (Ritchie *et al.*, 1999).

4. Double-strand breaks (DSBs) within the repeated ribosomal DNA in *Saccharomyces cerevisiae* generate quasi-stable broken chromosomes in cells lacking Tel1p and Mec1p

4.1 Introduction

The accurate transfer of genetic information from generation to generation is crucial for organismal survival. Any factor that compromises genome integrity, whether it be exogenous sources of DNA damage (for example, bases damaged by ultraviolet light) or endogenous defects in cellular repair pathways (for example, DSBs at stalled replication forks), can result in critical alterations to the genomic template if the DNA damage is left uncorrected as the cell traverses into the next cycle. Because of the importance of maintaining a stable genome throughout each cell cycle, multiple signaling pathways have evolved to prevent DNA replication errors, correct damaged DNA bases, and halt the cell cycle while the repair processes are ongoing.

In the budding yeast *Saccharomyces cerevisiae*, two central players in many of these processes are known as Tel1p and Mec1p. Tel1p and Mec1p function at the top of a signaling cascade that responds to DNA damage, replication fork stalling and collapse, severe telomere attrition, and other DNA perturbations (Elledge, 1996). The DNA damage is initially detected by DNA-binding proteins such as those in the MRX complex (Mre11p, Rad50p, and Xrs2p) and 9-1-1 complex (Rad17, Ddc1, and Mec3) and these proteins subsequently activate Tel1p and Mec1p. Tel1p is activated in response to double-stranded DNA breaks (DSBs) and Mec1p by long stretches of RPA-coated single-stranded DNA (Zhou and Elledge, 2000). Following their activation, Tel1p and Mec1p phosphorylate downstream effectors to activate transcriptional responses, begin the repair process, and delay the cell cycle to ensure sufficient time for repair.

Tel1p and Mec1p are structurally similar PI3-like kinases with overlapping specificities. For example, in response to DNA damage, Rad53p is phosphorylated. In *mec1* strains, Rad53p phosphorylation is reduced; however, phosphorylation is eliminated in *tel1 mec1* strains (Clerici *et al.*, 2004). The *TEL1* gene was first identified as a gene affecting telomere length regulation (Greenwell *et al.*, 1995; Lustig and Petes, 1986). In contrast, *mec1* mutants were first characterized as strains that were sensitive to DNA damaging agents (Kato and Ogawa, 1994). Mec1p and Tel1p show partial functional redundancy in a number of assays including sensitivity to DNA damaging agents (Morrow *et al.*, 1995) and telomere length regulation (Mieczkowski *et al.*, 2003; Ritchie *et al.*, 1999).

When mutated individually, *TEL1* and *MEC1* cause slightly or moderately elevated rates of mutations and other genome alterations, but the lack of both *TEL1* and *MEC1* results in synergistically elevated rates of deletions and chromosome rearrangements (Craven *et al.*, 2002; Myung *et al.*, 2001b). Haploid yeast strains deficient in both proteins (*tel1 mec1-21* strains) have very high frequencies of chromosome III rearrangements, as well as disomy for chromosome VIII (Vernon *et al.*, 2008). I showed that diploid *tel1 mec1* strains have very high levels of trisomy and monosomy in addition to elevated levels of chromosome rearrangements (Chapter 3). Thus, Tel1p and Mec1p, in addition to their roles in the DNA damage response, are required for the accurate segregation of chromosomes during the normal cell cycle. As discussed in Chapter 3, the role of Tel1p and Mec1p in chromosome segregation is not related to their telomere functions, but is likely to reflect an interaction of these proteins with the kinetochore.

In addition to functions that Tel1p and Mec1p share, Mec1p has a unique role in preventing the collapse of stalled replication forks in response to DNA damaging agents, particularly in hard-to-replicate regions of DNA (Cha and Kleckner, 2002; Raveendranathan *et al.*, 2006). One region of the genome that is likely to have problems

in replication is the ribosomal DNA (rDNA) array on chromosome XII (Petes, 1979). This region consists of 100-150 copies of the genes encoding ribosomal RNA, each approximately 9.1 kb in length (Figs. 4.1A and 4.1B). The rRNA gene cluster has a high frequency of mitotic recombination (Andersen *et al.*, 2008; Casper *et al.*, 2008; Szostak and Wu, 1980), even in wild-type strains, indicating a high frequency of recombinogenic DNA lesions. Elevated levels of mitotic recombination in the rRNA gene cluster are observed in strains lacking the helicases Rrm3p or Dna2p (Ivessa *et al.*, 2000; Weitao *et al.*, 2003), and in strains with low levels of DNA polymerase alpha (Casper *et al.*, 2008).

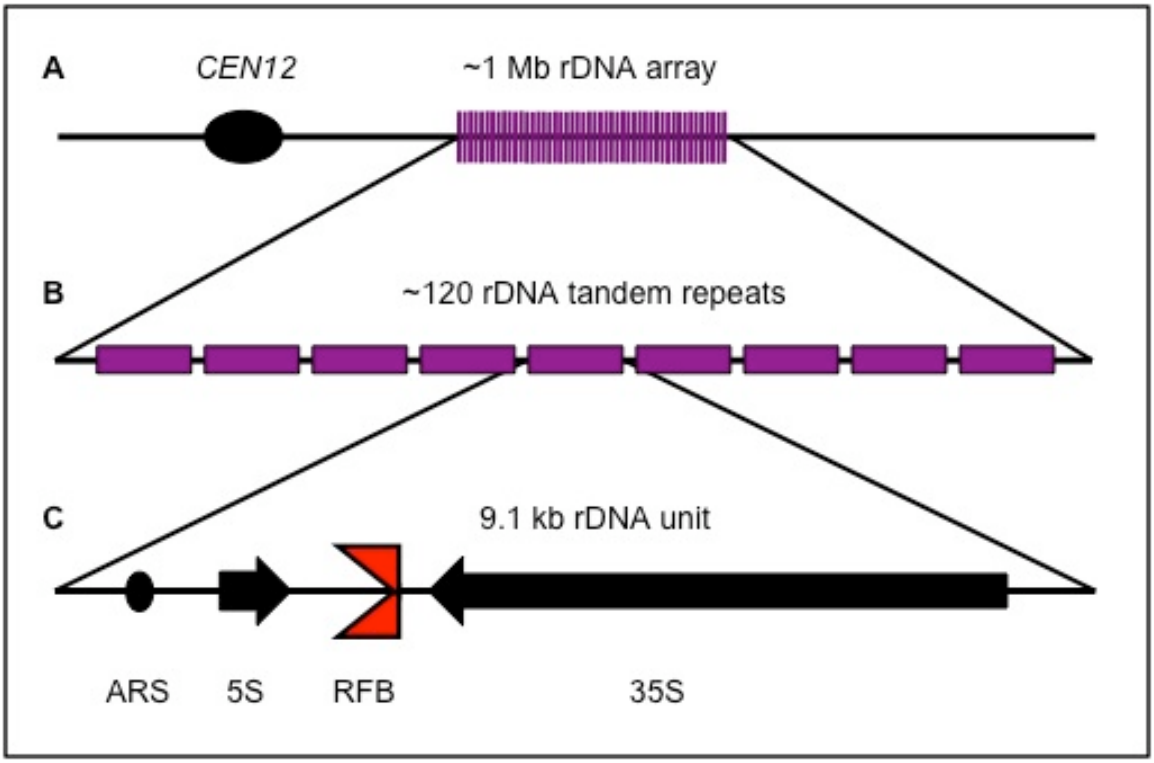

Figure 4.1 Organization of the rDNA array on chromosome XII.

(A) All rDNA genes in *Saccharomyces cerevisiae* are located in a single array on chromosome XII. (B) The rDNA array consists of approximately 120 units that each contain the 35S and 5S rRNA genes as well as an origin of replication (ARS) and a replication fork blocking site (RFB). The orientation of the arrows in (C) shows the direction of transcription.

As shown in Figure 4.1C, each 9.1 kb rRNA gene encodes a 35S rRNA (processed to yield the 18S, 28S, and 5.8S transcripts) and a 5S rRNA transcribed from the opposite strand (Petes, 1979). A replication origin (ARS element) is located between the 5′ ends of the two primary transcripts in every repeat (Skryabin *et al.*, 1984), but only about 20% of rDNA repeats contain active origins of replication (Brewer and Fangman, 1988; Linskens and Huberman, 1988; Pasero *et al.*, 2002; Saffer and Miller, 1986). Additionally, there is a polar replication fork barrier (RFB) located between the 3′ ends of the primary transcripts (Brewer and Fangman, 1988; Linskens and Huberman, 1988). This barrier prevents DNA polymerase from colliding with the transcription machinery involved in 35S transcription. The RFB binds Fob1p and this binding is required to block replication forks moving in the direction opposite transcription of the 35S transcript (Kobayashi, 2003). In strains with the *dna2-2* mutation, which have elevated rates of DSBs in the rRNA gene cluster, these DSBs are suppressed by mutations in *fob1* (Weitao *et al.*, 2003). Although the *fob1* mutation substantially decreased mitotic recombination in wild-type cells, the elevated exchanges observed in strains with low levels of DNA polymerase were Fob1p-independent (Casper *et al.*, 2008). Thus, there are at least two classes of recombinogenic lesions in the rRNA gene cluster, those that are Fob1p-dependent and those that are Fob1p-independent.

DSBs are repaired through two primary mechanisms: homologous recombination (HR) and non-homologous end joining (NHEJ; Shrivastav *et al.*, 2008). In the yeast *Saccharomyces cerevisiae*, homologous recombination is the primary repair pathway. The repair of DSBs by homologous recombination is error-free; no bases are deleted or added in the course of the repair event. There are a number of different pathways of HR (Paques and Haber, 1999) as shown in Figure 1.2. The repair of DSBs can be associated with reciprocal crossing over or unassociated with exchange of flanking markers. In these classes of repair events, a small region of one chromosome is

non-reciprocally transferred to another (gene conversion). Most conversion events reflect local heteroduplex formation between the interacting DNA molecules, followed by repair of mismatches within the heteroduplex (Paques and Haber, 1999). There is also a pathway of homologous recombination in which a broken chromosome end invades a homologous chromosome. This invasion forms a replication fork that results in the copying of the homologous chromosome from the point of invasion until the end of the chromosome (Fig. 1.2). These events are called "break-induced replication" (BIR). BIR events require a number of essential replication proteins (Llorente *et al.*, 2008).

In this chapter, I show that diploid *tel1 mec1* cells often have an amplification of sequences that extends from the left telomere of chromosome XII into the rRNA gene cluster on the right arm. This amplification is a consequence of the formation of a quasi-stable chromosome fragment which I term a "schromosome." If I reintroduce a plasmid containing *MEC1* into a strain containing a schromosome, that strain becomes trisomic for chromosome XII. I interpret this finding as indicating that the end of the schromosome terminating in rRNA genes is capable of a BIR event involving the rRNA gene cluster on an intact copy of XII. Below, I describe the characterization of the schromosome and my analysis of the genetic requirements for its formation and persistence.

4.2 Results

4.2.1 The initial genetic alteration in *tel1 mec1* diploids is a break on chromosome XII within the rDNA repeats

Diploid yeast strains homozygous for deletions of *TEL1*, *MEC1*, and *SML1* (to suppress the lethality of *mec1*) were constructed; hereafter this genotype will be referred to as *tel1 mec1*. In addition, these strains contained a *MEC1*-expressing plasmid (pSAD3-3b/*MEC1*) to limit genome instability while the mutant strain was being generated; these isogenic diploids were JLMy80, JLMy81, JLMy82, and JLMy83. To begin the

experiments, I streaked these strains on rich growth medium (YPD) and isolated derivatives that had lost the *MEC1*-expressing plasmid. The resulting plasmid-deficient strains (indicated with the letters ΔP following the strain name) were immediately examined by microarray and contour-clamped homogeneous electric field (CHEF) analysis. Whole-genome microarray analysis indicated an amplification of the sequences between the left telomere and the tandem rDNA repeats on chromosome XII (JLMy82-ΔP represented in Fig. 4.2A). This duplicated region included the centromere of chromosome XII. The simplest interpretation of the microarray analysis is that JLMy82-ΔP contains a chromosome XII derivative with a break in the rDNA. In the microarrays that I used, the rRNA gene cluster is represented by only two elements. Although the microarray indicates that the rRNA genes are amplified, we cannot determine whether the amplification reflects the schromosome or changes in the number of repeats on the two other normal copies of chromosome XII.

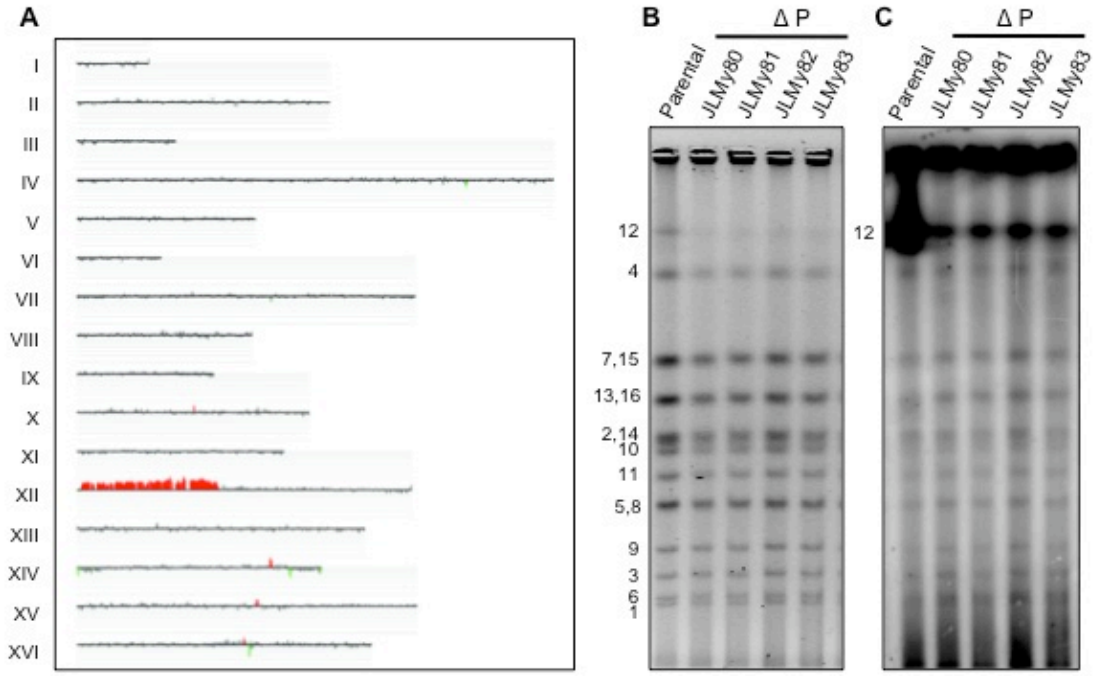

Figure 4.2 *tel1 mec1* diploid strains contain an amplification of chromosome XII between the left telomere and the rDNA repeats.

(A) Genomic microarray analysis indicates that part of chromosome XII is amplified in the representative *tel1 mec1* diploid strain JLMy82-ΔP. (B) DNA was isolated from a parental *tel1 mec1* diploid containing the pSAD3-3b/*MEC1* plasmid (lane 1) and from four derivatives lacking the plasmid (lanes 2-5) and these samples were examined by CHEF gel analysis. Ethidium-bromide staining of the gel revealed no novel chromosomes in the strains lacking the plasmid.
(C) Southern blotting analysis using an rRNA gene hybridization probe confirmed that less full-length chromosome XII enters the gel in strains without the plasmid (lanes 2-5) than in the progenitor strain with the plasmid (lane 1).

Four *tel1 mec1* diploids lacking the plasmid were examined. All four had the schromosome and the breakpoints of the amplified region were the same within the resolution of the microarray. For three of the strains, no other chromosome alterations were detected. In the strain JLMy81-ΔP, however, I found that chromosome X was trisomic. In summary, prior to subculturing, the first genetic alteration that occurs in diploid *tel1 mec1* strains is the formation of a broken chromosome XII derivative. All four strains also had two unbroken copies of chromosome XII.

The distance between the left telomere of chromosome XII and the beginning of the rRNA gene cluster is about 450 kb. Since there are about 120 rRNA genes in the cluster (Petes, 1979), the cluster is about 1080 kb, and it is about 610 kb from the end of the cluster to the right telomere (based on the DNA sequencing coordinates in the Saccharomyces Genome Database). Thus, the predicted size of the schromosome is between 450 kb and 1530 kb, depending on the position of the DSB in the cluster. By CHEF gel analysis, no novel chromosome band in this size range was apparent in the ethidium-bromide stained gel (Fig. 4.2B). Furthermore, the band representing the normal-sized copy of chromosome XII was much fainter in the *tel1 mec1* derivatives lacking the pSAD3-3b/*MEC1* plasmid (lanes 2-4 compared to lane 1). I also performed Southern analysis of the separated chromosomal DNA molecules using an rRNA gene hybridization probe (Casper *et al.*, 2008). No chromosome fragment representing the schromosome was detectable (Fig. 4.2C). In addition, the amount of hybridization to the normal-sized chromosome XII was reduced and the amount of hybridization present in the wells in lanes 2-5 was high. These observations are consistent with a number of possibilities. First, the DNA molecule representing the schromosome may have a morphology (branched or circular DNA molecule) that prevents it from leaving the well of the gel. Alternatively, the schromosome has an electrophoretic mobility that is identical to the normal-sized chromosome XII. These alternatives will be discussed further below.

4.2.2 Formation of the schromosome in the diploid requires deletions of both *TEL1* and *MEC1*

To determine if the chromosome XII fragment was a result of a deficiency of both *TEL1* and *MEC1*, I examined wild-type and single mutant diploid strains immediately after loss of the pSAD3-3b/*MEC1* plasmid. In all three *mec1* strains analyzed (JLMy111-ΔP, JLMy112-ΔP, and JLMy113-ΔP), there were no genomic alterations detectable by

microarrays. Similarly, *tel1* diploids (JLMy102-ΔP and JLMy104-ΔP) and wild-type diploids (JLMy102-ΔP and JLMy101-ΔP) that lost the plasmid did not have a schromosome. Together, these data show that loss of both Tel1p and Mec1p is required for the formation of the schromosome.

4.2.3 Removing the replication-fork-blocking protein Fob1p reduces the frequency of schromosome formation and/or elevates the rate at which the schromosome is repaired

The tandem array of rRNA genes on chromosome XII has a high rate of recombination and DSBs even in wild-type yeast strains (Casper *et al.*, 2008). Some of these breaks are associated with stalled replication forks at the replication fork block (RFB) located within each 9.1 kb repeat (Brewer and Fangman, 1988). Fob1p is required for replication fork stalling at the RFB (Kobayashi and Horiuchi, 1996), and a deletion of *FOB1* substantially reduces mitotic recombination within the rDNA (Casper *et al.*, 2008; Defossez *et al.*, 1999; Johzuka and Horiuchi, 2002; Kobayashi *et al.*, 1998).

I investigated whether Fob1p was required for the formation of the schromosome. We constructed four independent, but isogenic, *fob1 tel1 mec1* strains (JLMy229, JLMy230, JLMy233, and JLMy237); these strain contained pSAD3-3b/*MEC1*. Following loss of the plasmid from each of these four strains, I examined them by microarrays. None of the four contained the schromosome. Instead, all four strains were trisomic for chromosome XII; no other ploidy changes or chromosome rearrangements were detected in these strains.

This result has two plausible interpretations. First, it is possible that the DSB that initiates formation of the schromosome requires a replication fork that is stalled by a Fob1p-dependent mechanism. Since the *fob1 tel1 mec1* strains very rapidly become trisomic for chromosome XII, we also need to postulate a very high rate of chromosome non-disjunction for XII and/or a strong selection for strains that have an extra copy of chromosome XII. A second possibility is that the *fob1 tel1 mec1* strains form a

schromosome at the same rate as *tel1 mec1* strains but the broken chromosome is rapidly repaired leading to trisomy. In support of this possibility, the rRNA genes are oriented on chromosome XII such that the BIR-associated replication fork would be blocked by the Fob1p-bound RFB sites. Thus, loss of Fob1p would presumably make the BIR event more efficient. Although I cannot currently distinguish between these two possibilities, the second interpretation is a more parsimonious explanation of the data.

4.2.4 Overexpression of *SRL2* does not suppress formation of the schromosome

As discussed above, *tel1 mec1* diploids without the *MEC1*-containing plasmid usually have two normal copies of chromosome XII in addition to the schromosome rather than one normal copy of chromosome XII and the schromosome. One interpretation of this result is that there may be selective pressure for acquiring a schromosome. More specifically, *tel1 mec1* strains with three copies of the sequences between the left telomere and the rRNA gene cluster may grow better than strains with only two copies of these sequences. Alternatively, strains with only one copy of the sequences on the right arm of XII distal to the rRNA gene cluster may be at a competitive disadvantage. I should point out that *tel1 mec1* strains grow very slowly and, therefore, selection for a duplicated gene that alleviates their growth problems seems plausible.

I scanned the schromosome for genes that could potentially alleviate the growth defect of *tel1 mec1* strains. One candidate gene, *SRL2*, is located about 293 kb from the left telomere of XII. This gene, when overexpressed, suppresses the lethality of *rad53* and *mec1* null mutations (Desany *et al.*, 1998). Consequently, I tested whether amplification of *SRL2* in a *tel1 mec1* diploid strain would reduce the tendency of these strains to acquire and maintain the schromosome.

The *SRL2* gene was cloned under its native promoter on the centromeric plasmid pRS316-*SRL2* (Chapter 2). This plasmid was transformed into *tel1 mec1* diploid strains JLMy80 and JLMy81 to create the strains JLMy350 and JLMy354, respectively. I also cloned *SRL2* on a multi-copy plasmid pRS426 to generate pRS426-*SRL2* (Chapter 2). The plasmid pRS426-*SRL2* was transformed into the *tel1 mec1* diploids JLMy81 and JLMy82 to generate the strains JLMy356 and JLMy360, respectively. All four of the diploids with the *SRL2*-containing plasmids were cured of the complementing pSAD3-3b/*MEC1* plasmid, and examined by microarray analysis. All four of these diploids contained the schromosome. I conclude, therefore, that acquisition of an extra copy of *SRL2* is not the primary reason for generation and maintenance of the schromosome.

4.2.5 The schromosome persists over many generations in *tel1 mec1* diploids, but is repaired upon reintroduction of a wild-type copy of *MEC1*

As described above, the schromosome was formed soon after loss of the plasmid-borne *MEC1* gene from the *tel1 mec1* strains. I next examined whether the schromosome could persist after subculturing. Strains with the schromosome (JLMy80-ΔP-1 and JLMy80-ΔP-2) were analyzed after five subculturings (approximately 100 generations) and ten subculturings (approximately 200 generations); both strains retained the schromosome (Table 4.1). In addition, I subcultured two other similar strains (JLMy80-ΔP-3 and JLMy80-ΔP-5) for 200 generations. One retained the schromosome and one did not. As expected from my previous studies of subcultured *tel1 mec1* diploids (Chapter 3), additional trisomies and chromosome rearrangements were also observed in the subcultured strains (Table 4.1). Microarray analysis of JLMy82-ΔP-2 following 200 generations is shown in Fig. 4.3A. In summary, in cells subcultured without selection, the schromosome is maintained over many cell generations.

Table 4.1 Genetic alterations in *tel1 mec1* diploids lacking the pSAD3-3b/*MEC1* plasmid after 100 or 200 generations of non-selective growth.

Strain	Genetic alterations as diagnosed by microarray
JLMy80-ΔP-1 100 generations	Schromosome; trisomy of chromosome X; deletion/duplication event on chromosome II
JLMy80-ΔP-1 200 generations	Schromosome; trisomy of chromosome X; deletion/duplication event on chromosome II
JLMy82-ΔP-2 100 generations	Schromosome; trisomy of chromosomes II and X
JLMy82-ΔP-2 200 generations	Schromosome; trisomy of chromosomes II and X
JLMy80-ΔP-3 200 generations	Schromosome; trisomy of chromosome II; terminal amplification on chromosome X
JLMy80-ΔP-5 200 generations	Monosomy of chromosomes VI and IX; trisomy of chromosome II; tandem deletion-duplication event on chromosomes III and XII

Although the schromosome is maintained in the *tel1 mec1* diploid in the absence of the pSAD3-3b/*MEC1* plasmid, I found that, when the plasmid was reintroduced, the resulting transformants lost the schromosome and acquired trisomy for chromosome XII. I transformed pSAD3-3b/*MEC1* into JLMy80-ΔP and JLMy82-ΔP. Without subculturing these strains were examined by microarrays. Both strains lost the schromosome and were trisomic for chromosome XII; the microarray for JLMy82-ΔP+P is shown in Fig. 4.3B.

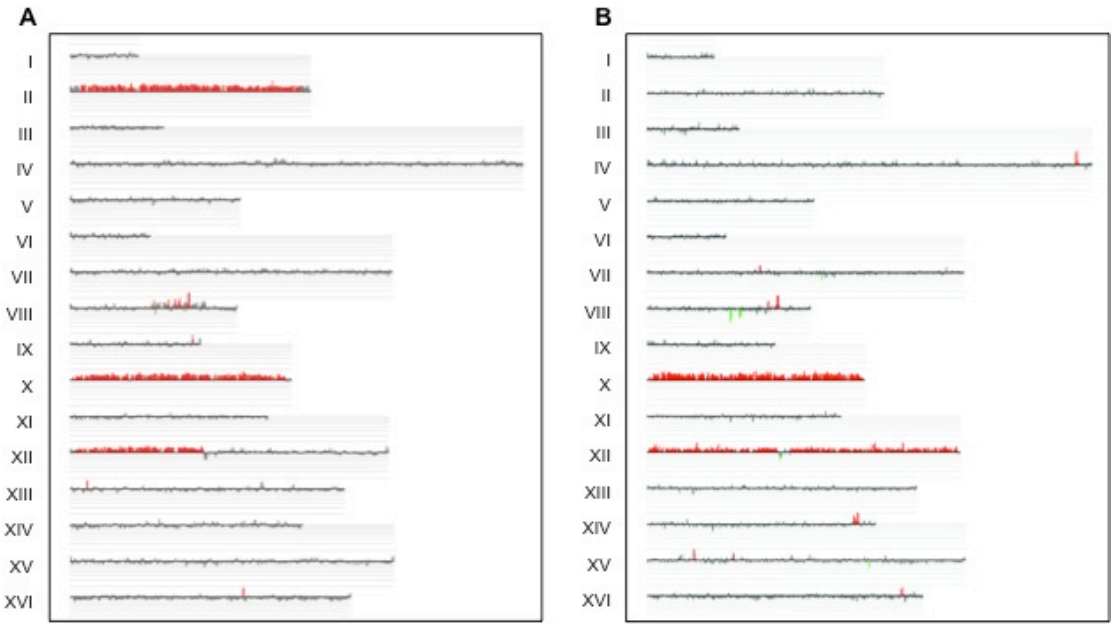

Figure 4.3 Analysis of the effect of *MEC1* on the stability of the schromosome in *tel1 mec1* diploid strains.

(A) The schromosome persists for at least 200 generations of growth in strain JLMy82-ΔP-2. (B) Reintroducing the plasmid-borne *MEC1* into the *tel1 mec1* strain JLMy82-ΔP (JLMy82-ΔP+P) results in trisomy of chromosome XII.

My interpretation of these experiments is that *tel1 mec1* diploids without the plasmid-borne *MEC1* gene have a broken chromosome, and their ability to repair this break by homologous recombination is limited. Re-introduction of the *MEC1* gene allows the cell to repair the schromosome by BIR using one of the intact chromosome XIIs as a template, resulting in trisomy. These results suggest that *MEC1* is required for some types of BIR events, possibly those that require that the replication fork proceed through very long (Mb) chromosome regions. It should also be pointed out that BIR is likely to be favored as the homologous recombination pathway of choice because other types of homologous recombination (gene conversion or crossovers) require the availability of both broken ends (Deem *et al.*, 2008). Since the chromosome fragment presumably formed at the same time as the schromosome lacks a centromere, it would be expected to be lost soon after its formation.

4.2.6 Formation and repair of the schromosome is not a consequence of the short telomeres in *tel1 mec1* strains

In *tel1 mec1* diploid strains, chromosome rearrangements are a result of telomere dysfunction (Chapter 3). As described in the Chapter 1, *tel1* strains have short but stable (50 bp) telomeres, while *mec1* strains have telomeres that are only slightly shorter than wild-type. However, *tel1 mec1* strains have extremely short telomeres, and many of the cells with this genotype senesce in a manner similar to that observed in strains lacking telomerase (Ritchie *et al.*, 1999). Those derivatives that survive this crisis elongate their telomeres by a recombination-dependent mechanism (Ritchie *et al.*, 1999). In addition, *tel1 mec1* strains have a high frequency of telomere-telomere fusions, as diagnosed by PCR analysis (Chapter 3; Mieczkowski *et al.*, 2003) and very high frequencies of chromosome rearrangements (Chapter 3). Expression of a plasmid that expresses the Cdc13p-Est2p fusion protein (pVL1107-*URA3*; Evans and Lundblad, 1999) elongates the telomeres of *tel1 mec1* cells to wild-type length (Tsukamoto *et al.*, 2001). This plasmid also reduces the frequency of telomere-telomere fusions and the frequency of chromosome rearrangements in *tel1 mec1* diploids (Chapter 3). Our interpretation of these results is that most of the chromosome rearrangements that occur in *tel1 mec1* diploids are initiated by telomere-telomere fusions. Fusions between telomeres of different chromosomes would generate a dicentric chromosome that would be broken during mitosis. The repair of these broken chromosomes would generate translocations and other types of chromosome rearrangements (deletions and duplications). In order to determine whether the DSBs that give rise to the schromosome were initiated by telomere-telomere fusions, I investigated whether the Cdc13p-Est2p fusion protein could suppress schromosome formation.

I introduced the pVL1107-*URA3* plasmid into *tel1 mec1* diploids JLMy80 and JLMy82 to create strains JLMy1262 and JLMy1271, respectively. The complementing pSAD3-3b/*MEC1* plasmid was then cured from the strains, and the resulting derivatives

(JLMy1262-ΔP and JLYMy1271-ΔP) were examined using microarrays. The restoration of proper telomere length to the *tel1 mec1* diploids did not prevent formation of the schromosome in either strain analyzed (JLMy1271-ΔP pictured in Fig. 4.4A). This result demonstrates that the DSBs leading to formation of the schromosome are not a consequence of telomere dysfunction and subsequent telomere-telomere fusions. Furthermore, reintroducing pSAD3-3b/*MEC1* results in trisomy for chromosome XII (JLMy1271-ΔP+P, Fig. 4.4B), similar to the *tel1 mec1* strains without the pVL1107-*URA3* plasmid. Both JLMy1262-ΔP and JLMy1271-ΔP also became trisomic for chromosome VIII after reintroduction of the plasmid-borne *MEC1*.

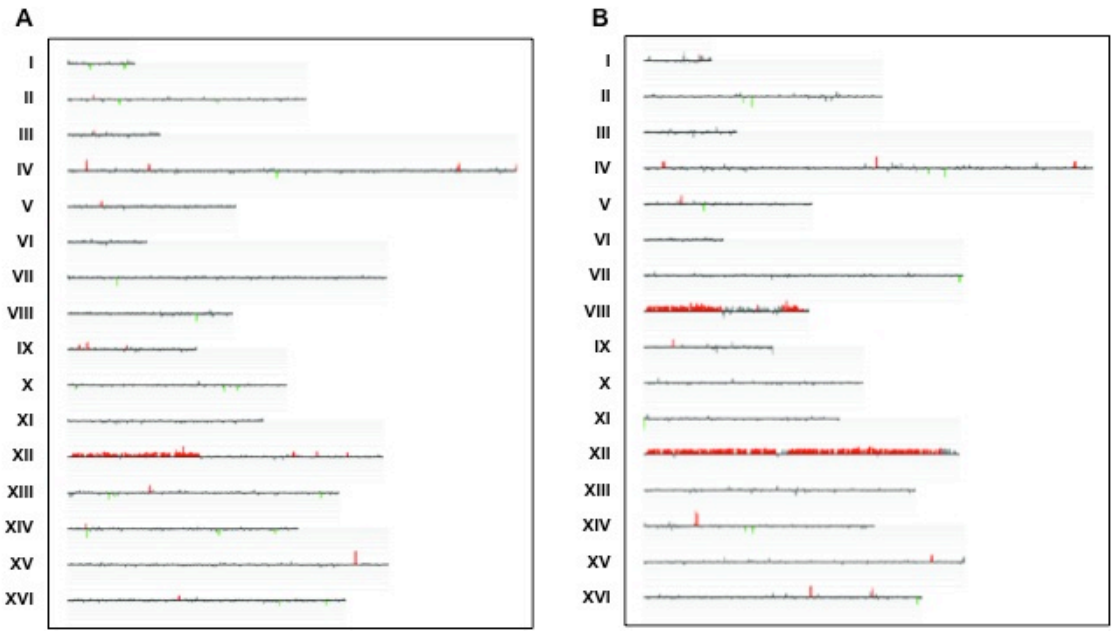

Figure 4.4 Restoring wild-type length telomeres to *tel1 mec1* strains does not affect the formation or repair of the schromosome.

(A) Transformation of the pVL1107-*URA3* plasmid (containing the fusion *CDC13-EST2* fusion gene) into *tel1 mec1* strains restores wild-type telomere lengths (Chapter 3) but does not prevent the generation of the schromosome. Microarray analysis of DNA isolated from the diploid strain JLMy1271-ΔP (*tel1 mec1* + pVL1107-*URA3*) is shown as a representative example. (B) Re-introducing the plasmid pSAD3-3b/*MEC1* into JLMy1271-ΔP (JLMy1271-ΔP+P) results in trisomy for chromosome XII.

4.2.7 The schromosome is formed in haploid *tel1 mec1* strains

In the experiments described thus far in this chapter, we examined the schromosome in diploid *tel1 mec1* strains. The schromosome is also observed in haploid strains. I isolated *tel1 mec1* haploid strains containing the pSAD3-3b/*MEC1* plasmid as spores derived from JLMy62. Derivatives that lost the *MEC1*-containing plasmid were subcultured for 100 cell generations and then pSAD3-3b/*MEC1* was re-introduced. Of the nine *tel1 mec1* haploids examined with microarrays, two had the schromosome (JLMy62-6b-4b-ΔP+P shown in Fig. 4.5A). Of the remaining seven strains, two had other chromosome XII rearrangements, two were disomic for chromosome XII, and three had

no chromosome XII alterations. As described in Section 4.2.5, I observed the schromosome in diploid strains prior to introduction of the *MEC1*-containing plasmid but, following re-introduction of the plasmid, I observed trisomy of chromosome XII instead of the schromosome. I have not yet examined *tel1 mec1* haploids that do not contain the *MEC1* plasmid by microarrays.

In contrast to the schromosome-containing diploid strains (without pSAD3-3b/*MEC1*) in which no novel chromosome could be detected by CHEF electrophoresis (Fig. 4.2), I detected a novel chromosome of about 1250 kb in the *tel1 mec1* haploid strain JLMy62-6b-4c-ΔP+P (Fig. 4.5B). This fragment hybridized to an rDNA probe (Fig. 4.5C), but not to an *ASP3* probe (Fig. 4.5D); the *ASP3* genes are located immediately centromere-distal to the rRNA gene cluster (Johnston *et al.*, 1997). As expected, the normal chromosome XII hybridizes to both of these probes (Figs. 4.5C and 4.5D). The band which represents the schromosome is diffuse, suggesting that the schromosome is heterogeneous in length within the cell population.

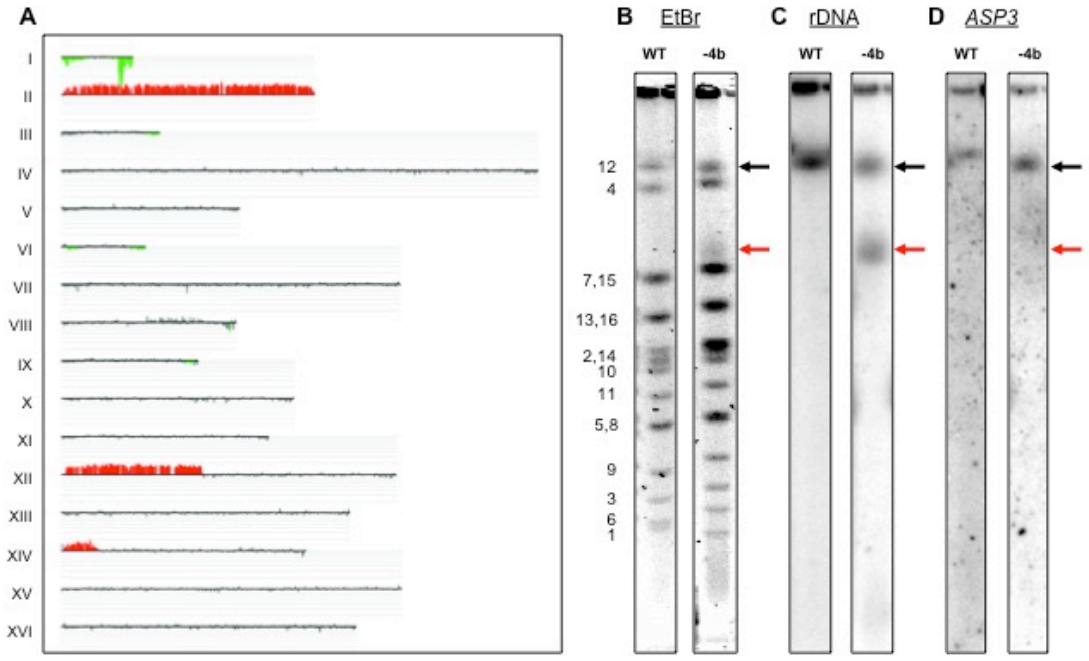

Figure 4.5 The schromosome is found in haploid *tel1 mec1* strains.

(A) Microarray analysis indicates that haploid *tel1 mec1* strain JLMy62-6b-4b-ΔP+P contains a schromosome, as well as other genetic alterations. JLMy62-6b-4b-ΔP+P is a haploid strain that was cured of the complementing *MEC1* plasmid, grown for 100 generations, and retransformed with pSAD3-3b/*MEC1* to limit further genetic instability during analysis. (B) Separation of chromosomes in strain JLMy62-6b-4b-ΔP+P with a CHEF gel followed by staining with ethidium bromide indicates the appearance of a novel band at approximately 1250 kb (indicated by the red arrow; the black arrow depicts the normal chromosome XII band). The novel band is not present in the wild-type (WT) control strain MS71 in the first lane. (C) Southern blotting with an rDNA probe labels both the normal chromosome XII band and the novel band at 1250 kb. (D) An *ASP3* probe (located immediately centromere-distal to the rRNA gene cluster) does not hybridize to the novel band, but does hybridize to the normal chromosome XII.

In the microarray analysis shown in Fig. 4.5A, it is clear that a portion of chromosome XIV is duplicated. I performed a band analysis of the schromosome and found that the duplicated segment of XIV was attached to the schromosome. I have not yet determine whether this segment is attached to the left end (the left telomere) or the right end (rRNA gene cluster) of the schromosome, although the instability of the schromosome described in Section 4.2.8 suggests that the chromosome XIV segment is attached to the left end.

4.2.8 The schromosome loses rRNA genes during subculturing in *tel1 mec1* haploid strains

To determine if the schromosome is stable in the haploid strain with the plasmid upon further subculturing, I subcultured JLMy62-6b-4b-ΔP+P for another 200 generations and analyzed samples collected every 20 generations on a CHEF gel. Remarkably, the diffuse band representing the broken chromosome XII fragment migrated more slowly as the strain was subcultured, but the amount of hybridization to an rDNA-specific probe decreased over time relative to the normal chromosome XII (Fig. 4.6A). In addition, microarray analysis indicated that the schromosome, which was present in most cells before further subculturing (Fig. 4.6B, left panel) was eventually lost (Fig. 4.6B, center and right panels).

My interpretation of these observations is that the schromosome end is not "capped" by telomeric repeats or fused to other chromosomal sequences. Thus, this end is degraded upon subculturing, resulting in loss of rRNA genes. Although one might expect that shorter chromosomes would have faster electrophoretic mobility in CHEF gels, it has been recently shown that chromosomes with large single-stranded "tails" run more slowly in CHEF gels (Westmoreland *et al.*, 2009). If my interpretation is correct, it is likely that the chromosome XIV segment is fused to the left telomere of chromosome XII rather than to the rRNA gene repeats. This possibility will be investigated in experiments outlined in Chapter 5.

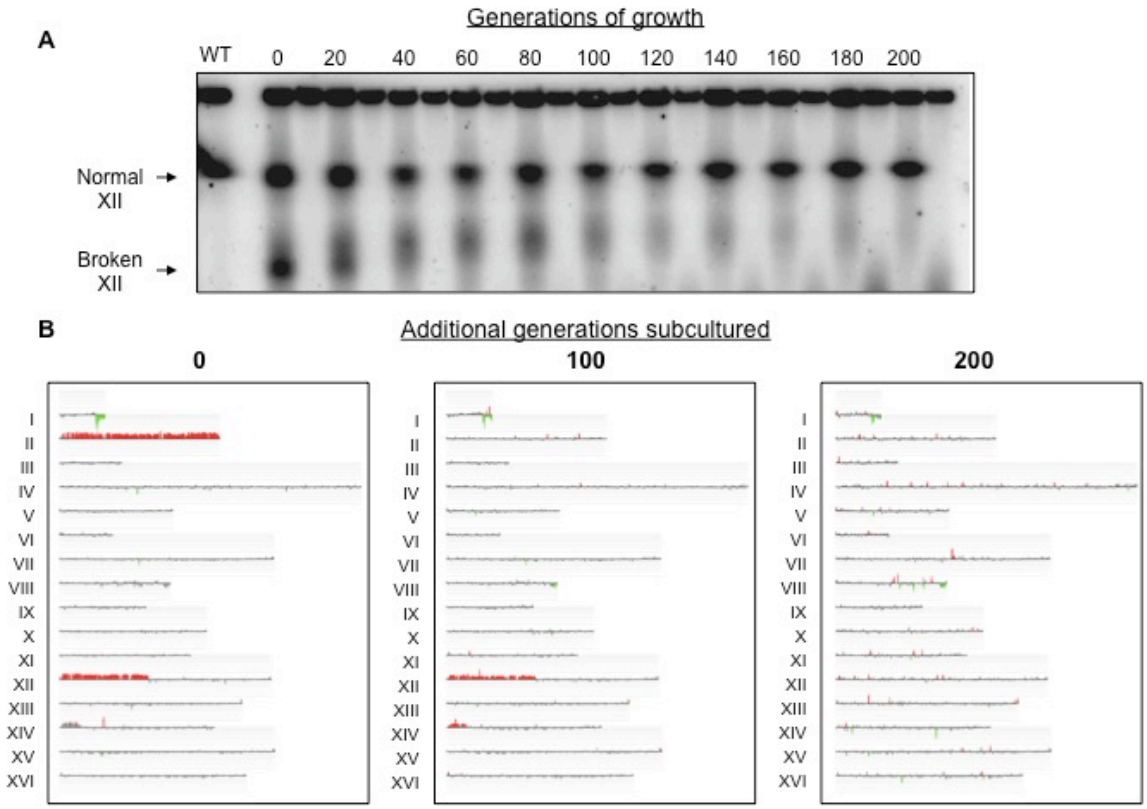

Figure 4.6 The broken chromosome XII fragment in *tel1 mec1* strain JLMy62-6b-4b disappears over time.

(A) Initially, I examined the strain JLMy62-6b-4b-ΔP+P after 100 generations of subculturing (Fig. 4.5). I subsequently subcultured the strain for an additional 200 generations, followed by CHEF gel analysis. This CHEF gel was probed with radiolabeled rDNA to label the full-length (normal) and broken chromosome XII. (B) Microarray analysis indicates the gradual disappearance of the chromosome XII fragment. JLMy62-6b-4b-ΔP+P was analyzed after no additional outgrowth (left panel and Fig. 4.5A), after 100 additional generations (center panel), and after 200 additional generations (right panel).

4.3 Discussion

Above, I present evidence that diploid *tel1 mec1* strains have an amplification of chromosome XII sequences that extends from the left telomere to the rRNA gene tandem array. This amplification persists for at least 200 cell generations in the absence of selection. By CHEF gel analysis, no novel chromosome of the size expected for the amplified segment was detected in the diploids. When *MEC1* is reintroduced into these strains, the diploids become trisomic for XII. In haploids, we observed a novel

chromosome of the size expected for the amplified segment in two of nine strains subcultured in the absence of the *MEC1*-containing plasmid, followed by reintroduction of the plasmid. As expected, this novel chromosome (the schromosome) hybridized to an rDNA probe, but did not hybridize to a probe located centromere-distal to the rRNA gene cluster. Upon subculturing the haploid strain with the schromosome, I observed that the schromosome migrated more slowly in the gel, but hybridized less intensely to the rDNA-specific probe. The result is consistent with degradation of the schromosome by a mechanism that produces single-stranded "tails." Below, I will discuss these observations in more detail and outline some of the unanswered questions.

4.3.1 Genetic requirements for the formation of the schromosome in diploid *tel1 mec1* strains

I was able to dissect some of the genetic requirements for the formation of the break on chromosome XII in the diploid *tel1 mec1* strains. Deletions of both *TEL1* and *MEC1* are required to generate the schromosome, as neither single *tel1* nor *mec1* mutant alone acquired the broken chromosome fragment. However, schromosome formation is not associated with short telomeres. This indicates that the breaks in the rDNA on chromosome XII are not the result of telomere-telomere fusions and subsequent breakage of dicentric chromosomes within the rDNA. Interestingly, most other chromosome rearrangements in *tel1 mec1* diploid strains result from telomere dysfunction (Chapter 3). Thus, the schromosome represents a novel class of aberrant chromosome structure in *tel1 mec1* cells.

As discussed in the Introduction, strains with a null mutation of *MEC1* accumulate DSBs at "hard-to-replicate" regions of chromosome III (Cha and Kleckner, 2002). Thus, one interpretation of our results is that the *tel1 mec1* strains have difficulty in replicating the rRNA gene cluster and stalled replication forks lead to DSBs. Wild-type cells have a high level of DSBs within the rDNA and loss of the Fob1p reduces the

frequency of these breaks. I showed that loss of Fob1p in the *tel1 mec1* diploids eliminates the schromosome, consistent with the possibility that the *tel1 mec1* strains have a specific problem in replicating rDNA in which Fob1p is bound to the RFB site. An alternative possibility (discussed below) is that the absence of Fob1p permits more efficient repair of the schromosome fragment, thus preventing its detection. Finally, functions of Fob1p independent of DSB formation or repair could contribute to the formation of the schromosome. For example, the action of Cdc14p and condensin are required for proper separation of chromosome XII sister chromatids during mitosis (D'Amours *et al.*, 2004). Fob1p is known to regulate the release of Cdc14p from the nucleolus as part of the FEAR (Cdc14p Early Anaphase Release) pathway governing mitotic exit. Fob1p negatively regulates Cdc14p and a lack of Fob1p causes premature Cdc14p release (Machin *et al.*, 2006), thus facilitating premature mitotic exit. It is possible that the break within the rDNA is not formed when *FOB1* is deleted because rDNA disjunction and mitotic exit are facilitated by the early release of Cdc14p. Of course, it is possible that both the formation and repair of the schromosome are affected by loss of Fob1p.

4.3.2 Mechanisms responsible for repair of the schromosome

Reintroduction of *MEC1* into *tel1 mec1* strains containing the schromosome results in trisomy for chromosome XII. I interpret this result as reflecting the rapid repair of the schromosome by homologous recombination to generate trisomy. It is likely that this repair reflects BIR (Fig. 1.2). In BIR events, a DNA end that has been resected to generate a single-stranded tail invades a region of sequence homology on another chromosome, establishing a unidirectional replication fork. This fork copies the homologous chromosome to the end (Llorente *et al.*, 2008). By this model, the schromosome is prepared to initiate a BIR event because it is not capped with telomeric repeats.

Since I do not observe trisomy for chromosome XII in the *tel1 mec1* diploids, I suggest that Mec1p is required for the BIR event that generates trisomy. The event that generates chromosome XII trisomy requires the replication of 600-1000 kb of DNA. As *MEC1* is known to be required for efficient DNA replication in difficult-to-replicate regions on chromosome III (Cha and Kleckner, 2002), it is plausible that *MEC1* is also required for efficient replication of the rDNA.

As previously mentioned, it is possible that the Fob1p is not required to create DSBs that lead to schromosome formation, but instead inhibits efficient BIR-dependent repair of the schromosome. In all *fob1 tel1 mec1* strains tested, chromosome XII is trisomic instead of possessing a schromosome. Fob1p physically binds the polar RFB site (Kobayashi, 2003) and prevents replication forks from colliding with the transcription machinery that produces the 35S transcript (Takeuchi *et al.*, 2003). The orientation of the RFB is such that the replication fork associated with BIR would encounter a RFB in every rDNA repeat (Fig. 4.1). Thus, I would expect that stalling at the RFB, dependent on Fob1p (Kobayashi and Horiuchi, 1996), would hinder BIR and limit repair of the schromosome. By this model, DSBs in the rDNA are created through a Fob1p-independent mechanism in *fob1 tel1 mec1* strains but are repaired by BIR even in the absence of Mec1p, generating the observed trisomy of chromosome XII. Previously, Casper *et al.* (2008) showed that the elevated rate of instability of the rRNA gene cluster caused by low levels of DNA polymerase alpha was independent of Fob1p. While we cannot at this time determine whether Fob1p affects the formation or repair of the schromosome (or both the formation and repair), I will describe experiments in Chapter 5 that can distinguish these possibilities.

4.3.3 Differences in the schromosome between haploid and diploid *tel1 mec1* cells

Using DNA microarrays, I discovered that the schromosome persists in both haploid and diploid *tel1 mec1* cells through at least 100 generations. However, in diploid cells, the schromosome is rapidly repaired upon reintroduction of *MEC1* to generate trisomy, while in haploid cells, the schromosome persists upon reintroduction of *MEC1* but is eventually lost over time. One difference in haploid and diploid cells is the efficiency of homologous recombination. Some types of homologous recombination are more efficient in strains expressing both *MAT***a** and *MAT*α information (Paques and Haber, 1999). In addition, NHEJ is downregulated in diploids (Kegel *et al.*, 2001), favoring repair by HR. This more efficient repair by HR in diploids over haploids is consistent with the rapid generation of chromosome XII trisomy upon reintroduction of *MEC1* in the diploids versus the persistence of the schromosome in the haploid strains.

In addition, the difference in the efficiencies of HR in diploids and haploids might explain the observations that the schromosome is detectable by CHEF gels in the haploid but not the diploid. It is possible that, in the diploid, the schromosome is constantly attempting HR, but cannot accomplish the task in the absence of Mec1p. The formation of branched structures associated with abortive attempts to perform BIR may be one reason that I fail to detect the schromosome in the *tel1 mec1* diploids. If this type of intermediate is downregulated in the haploid, the resulting branched structures are not formed and the schromosome is detectable. It is also possible that in diploid, but not haploid, *tel1 mec1* strains, the rDNA-containing end of the schromosome does a strand invasion into its own rDNA sequences, forming a loop. Again, such molecules would not be detectable in the CHEF gel, since they would not escape the well of the gel. An alternative explanation for the failure to detect the schromosome in diploid *tel1 mec1* cells is that the broken chromosome in the *tel1 mec1* diploids is resected to variable lengths in the cell populations, resulting in a diffuse undetectable smear in the CHEF gel

analysis. This possibility could be tested by constructing *tel1 mec1* strains that are missing proteins involved in nuclease-processing of broken ends such as Exo1p.

An alternative explanation for our failure to see the schromosome in the diploid cell could be that replication of the rRNA gene tandem array of the schromosome is very slow and, consequently, most of the schromosomes are branched DNA molecules that cannot migrate into the CHEF gel. One rationale for why the schromosome is replicated slowly relative to the intact chromosome XII is that the rRNA genes of the normal chromosome can be replicated by internal replication origins, and replication forks initiated centromere-distal and centromere-proximal to the cluster. The schromosome will lack replication forks located centromere-distal to the cluster.

4.3.4 Structural characterization of the schromosome terminus in haploid and diploid *tel1 mec1* strains

The schromosome exists as a stable fragment in diploid *tel1 mec1* cells but is immediately repaired to trisomy upon reintroduction of *MEC1*. This suggests that the rDNA end of the fragment is "uncapped" and primed to initiate DNA synthesis to repair the fragment. If the fragment were capped with a telomere, the chromosome would be stable, but unlikely to be capable of a BIR event after *MEC1* reintroduction. Furthermore, telomere capping is very inefficient in *tel1 mec1* strains (Myung *et al.*, 2001b), rendering this possibility unlikely. As described above, it is more likely that the end is somewhat protected from degradation in the diploid by pairing interactions with the rDNA of the intact chromosome XII or by formation of an intrachromosomal loop.

In the haploids, it is likely that the schromosome is uncapped and is being degraded over time to generate an extensive 3' DNA overhang. It has been shown that an increase in single-stranded DNA results in slower migration of DNA molecules in a CHEF gel (Westmoreland *et al.*, 2009). We detected slower migration of the chromosome XII fragment in the CHEF gel of *tel1 mec1* haploid strains as the strains were

subcultured. In addition, this alteration in the rate of electrophoretic migration was accompanied by a diminution and broadening of the rDNA signal. These results suggest that the end of the schromosome within the rDNA is uncapped by telomeric repeats, although this conclusion requires additional experimental support.

4.3.5 Basis for selection of the schromosome in *tel1 mec1* strains

It is not surprising that I only detect the left portion of the broken chromosome XII in the microarray analysis. Chromosome fragments containing centromeres are much more stable than acentric chromosome fragments (Spencer *et al.*, 1990). It is surprising, however, that *tel1 mec1* strains always contain an amplification of the left region of chromosome XII, indicating the presence of two normal copies of chromosome XII rather than having one normal chromosome in addition to the schromosome. This result can be explained by several models. First, it is possible that triplication of certain chromosome XII sequences helps alleviate the slow growth phenotype of *tel1 mec1* strains or, alternatively, that one copy of chromosome XII sequences centromere-distal to the rRNA genes accentuates the growth defect. I ruled out the possibility that an extra copy of *SRL2* is responsible for the effect. However, this result does not rule out the possibility that other genes present on chromosome XII, singly or in combination, would affect the slow growth phenotype of the *tel1 mec1* strains. It is possible that the relevant genes are the rRNA genes. The rRNA gene cluster is highly unstable in *tel1 mec1* strains and often contracts over time (Chapter 3). It is possible that the schromosome confers a growth advantage by increasing the total number of rDNA repeats. Alternatively, it is possible that the mechanism by which the schromosome is formed results in a schromosome and two normal copies of chromosome XII. This possibility will be discussed in Section 4.3.7.

4.3.6 Unanswered questions concerning the schromosome

Although there are plausible explanations for many of our observations concerning the schromosome, many of these explanations need further experimental support. Perhaps the most critical question in our understanding of the schromosome is why we fail to detect it by CHEF gel analysis in the diploid. If this failure is a consequence of a secondary DNA structure, what is the nature of that structure? If the schromosome lacks a telomere cap on the rDNA-containing end, how is the end protected from rapid nuclease degradation? Does our failure to detect the schromosome in *fob1 tel1 mec1* strains reflect a role of Fob1p in the formation of the schromosome or in its repair? Why can we detect a schromosome by CHEF gels in haploid, but not diploid, *tel1 mec1* strains? Experiments designed to further characterize the nature of the schromosome will be discussed in Chapter 5.

4.3.7 Conclusions

Our preferred model to explain the formation and repair of the schromosome is shown in Figure 4.7. Figure 4.7A depicts two chromosome XII homologues prior to replication. During S phase (Fig. 4.7B), one chromosome is replicated efficiently, but the other chromosome encounters problems replicating the rDNA, which results in replication fork stalling and a break on one of the two sister chromatids within the rDNA. This DSB may be Fob1p-dependent. The acentric broken chromosome is lost (Fig. 4.7C), but the centromere-containing schromosome is missegregated along with its full-length sister chromatid during mitosis (Fig. 4.7D), generating one daughter cell with one full-length copy of chromosome XII and another daughter cell with two full-length copies of chromosome XII and the schromosome. Finally, repair of the schromosome by BIR to generate trisomy requires *MEC1* and diploidy. Fob1p may be a negative regulator of the BIR event (Fig. 4.7E).

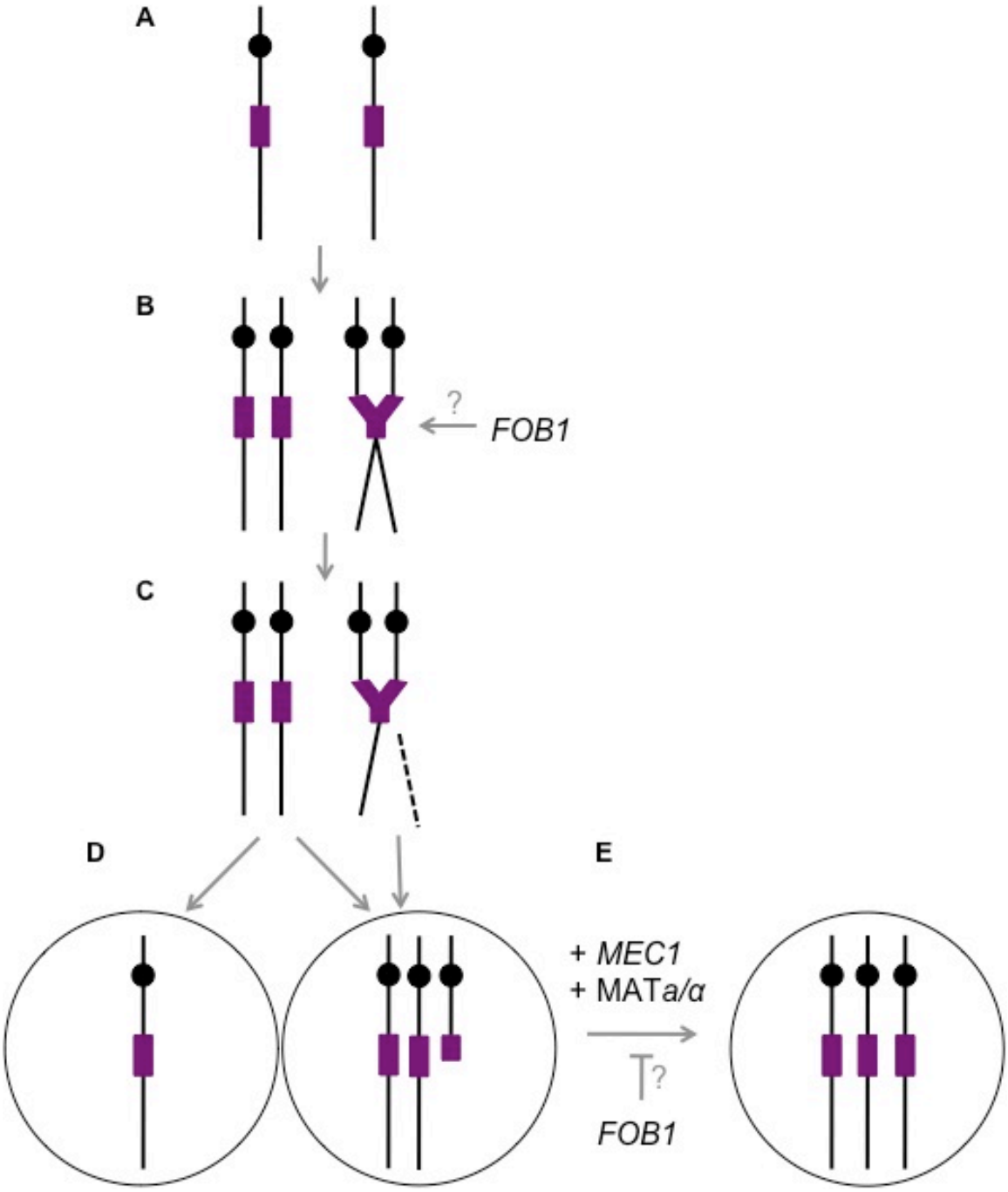

Figure 4.7 A model for the formation and repair of the schromosome.

The non-rDNA and rDNA sequences are shown in black and purple, respectively. The centromere is represented as a circle. (A-E) These steps are explained in the text.

There is an alternative model that is based on a completely different view of the schromosome. If the replication of the rRNA gene cluster is very delayed in *tel1 mec1* diploids and if the replication of chromosome XII sequences distal to the rDNA is also delayed, the sequences from the left telomere of XII to the cluster would appear amplified relative to the sequences located centromere-distal to the cluster. Such a branched molecule would also be trapped in the wells of the CHEF gel. We do not favor this model for several reasons. First, since the right arm of chromosome XII distal to the rDNA genes contains multiple replication origins, there is no obvious reason why this region of the chromosome should not be duplicated. Second, by CHEF gel analysis, we have physical evidence in haploid *tel1 mec1* strains of a schromosome.

In conclusion, from these genetic and molecular analyses, we conclude that the schromosome exists in diploid *tel1 mec1* strains and the formation and/or repair of the schromosome requires Fob1p. Efficient repair of the schromosome requires Mec1p and diploidy. The schromosome is likely to exist as an uncapped chromosome fragment. Formation of the schromosome does not require short telomeres. Further characterizing the molecular nature of the chromosome fragment and the genetic requirements for its formation will help clarify how Tel1p and Mec1p regulate the generation and repair of DNA lesions.

5. Discussion and Future Directions

In this dissertation, I have demonstrated that a single genetic background can give rise to elevated rates of changes in both chromosome number and chromosome structure. I have found that *tel1 mec1* diploids are extremely genetically unstable; 100% of *tel1 mec1* diploids grown for 100 generations had chromosomal aberrations including aneuploidy and chromosome rearrangements. These two types of chromosome alterations result from independent mechanisms, as restoring telomere function to *tel1 mec1* strains prevents chromosome rearrangements but does not affect aneuploidy. *tel1 mec1* cells demonstrate an aneuploidy profile similar to that of the spindle assembly checkpoint (SAC) mutant *bub1*. However, *tel1 mec1* strains arrest the cell cycle in response to benomyl, indicating a functional SAC. Finally, *tel1 mec1* strains support the persistence of a chromosome fragment that arises as the first genetic anomaly in *tel1 mec1* diploid yeast strains.

In this chapter, I will first discuss the important conclusions from my thesis work concerning the function of Tel1p and Mec1p in maintaining genome stability. I will then outline experiments to address questions raised by my research. Finally, I will discuss the broader implications of my thesis research results in the context of better understanding the causes of human disease.

5.1 Tel1p and Mec1p are required for maintaining numerical stability of chromosomes

5.1.1 Diploid *tel1 mec1* strains have higher rates of aneuploidy than haploid strains

Both haploid and diploid *tel1 mec1* strains developed aneuploidy following 100 generations of growth (Chapter 3). As expected, whole chromosome loss (monosomy) was only found in the diploid yeast strains, as haploid strains cannot tolerate loss of

whole chromosomes, all of which contain essential genes. The rate of entire chromosome duplication was also significantly higher in the diploid yeast strains (trisomy) than in the haploids (disomy). It is likely that yeast cells tolerate a 1.5-fold difference in gene dosage (2 copies to 3 copies in diploids) better than they tolerate a two-fold difference in gene dosage (1 copy to 2 copies in haploids). Alternatively, chromosome segregation may be inherently less accurate in diploids than in haploids. However, diploid cells are more radiation-resistant than haploid cells (Fasullo and Dave, 1994; Heude and Fabre, 1993) and demonstrate increased microtubule stability (Steinberg-Neifach and Eshel, 2002). These factors would seem to lead to more accurate chromosome disjunction in diploids than in haploids, the opposite of what I observed in *tel1 mec1* cells.

5.1.2 Diploid cells that lack Tel1p and Mec1p show a non-random aneuploidy distribution

Two striking aneuploidy biases were apparent in the *tel1 mec1* diploids: a bias towards trisomy of chromosomes II, VIII, X, and XII, and a bias towards monosomy of chromosomes I and VI. There are two major factors that could drive the biased aneuploidy that develops during the growth of *tel1 mec1* strains. One possibility is that there is something structurally different about chromosomes II, VIII, X, and XII that predisposes them to missegregation in the *tel1 mec1* genetic background. For example, differences in the timing of attachment of kinetochores to microtubules or the strength of the kinetochore-microtubule attachment could bias some chromosomes towards missegregation. Our experimental data argue that local centromere structure is not causing biased missegregation, as replacing 1 kb of DNA surrounding the centromere of chromosome II with that of chromosome XIV does not prevent chromosome II from becoming trisomic at a high frequency (Appendix B). However, centromeric chromatin covers a distance of approximately 20 kb surrounding the centromere (He *et al.*, 2000), so

it is possible that longer-range chromatin structure may influence kinetochore-microtubule dynamics. Other structural properties may exist which may bias the missegregation. However, I was unable to correlate the high rate of aneuploidy of *tel1 mec1* strains with the length of chromosome, the amount of condensin binding (Wang *et al.*, 2005), the number of ribosomal protein genes per chromosome, the timing of replication, or the distance from the closest *ARS* to the *CEN* of each chromosome.

Another reason for biased aneuploidy is that extra copies of certain chromosomes help the growth of *tel1 mec1* strains. For example, chromosomes frequently found trisomic in *tel1 mec1* strains may possess one or more genes that provide a growth advantage to the *tel1 mec1* diploids. Previously, Vernon *et al.* (2008) showed that haploid strains with the hypomorphic *mec1-21* allele frequently became disomic for chromosome VIII. The essential gene *DNA2* (encoding a DNA replication-associated helicase) is located on chromosome VIII, and introducing an additional plasmid-based copy of *DNA2* into *tel1 mec1-21* strains suppresses the tendency of the haploid strain to become disomic. However, we were not able to completely suppress the trisomy of chromosome VIII in diploid *tel1 mec1* strains by introducing a plasmid-borne copy of *DNA2*. Chromosome VIII became trisomic or tetrasomic in two out of four *tel1 mec1 + DNA2* strains (Appendix B). This contradictory result could be due to differences in the strain background, the *mec1* allele or in the ploidy of the cell. The experiments of Vernon *et al.* were done with a W303-derived haploid with a hypomorphic allele, whereas I used a MS71-derived diploid strain with a *mec1* null allele. There are two possibly relevant issues. First, Vernon *et al.* observed that the plasmid-borne *DNA2* gene suppressed disomy of chromosome VIII in 5 of 6 *mec1-21* strains, but in only one of two *tel1 mec1-21* strains. Second, adding an extra copy of *DNA2* on a centromeric plasmid in a haploid strain increases its expression by two-fold, but such a plasmid increases the level of the Dna2p by only 1.5-fold in a diploid strain.

Thus, my experiments do not rule out the possibility that the observed trisomy in the *tel1 mec1* diploids is related to the dosage of *DNA2*.

An alternative explanation for the non-random pattern of aneuploidy is that chromosomes II, VIII, X, and XII are the only chromosomes that can be tolerated in three copies in diploids. This explanation is very unlikely for multiple reasons. First, several studies have shown that every chromosome, with the exception of chromosome VI, can be recovered as disomes in haploids (Campbell *et al.*, 1981; Torres *et al.*, 2007). Chromosome-specific growth rates were observed, and, in general, strains that are disomic for the larger chromosomes grow more slowly than those that are disomic for the smaller chromosomes (Torres *et al.*, 2007). There is no relationship between chromosome size and the aneuploidy pattern observed in my data. In particular, chromosome XII is the largest yeast chromosome. Another argument that the pattern of aneuploidy in my experiments is not related to the inability of cells to tolerate trisomy for other chromosomes is that we have observed aneuploidy for other chromosomes in the same genetic background in other experiments. When diploid yeast strains are irradiated with gamma irradiation, derivatives that were trisomic for chromosomes I, V, VIII, IX, XI, XII, or XIII were observed (Argueso *et al.*, 2008).

It is likely that chromosome XII trisomy is a consequence of a mechanistically distinct pathway from trisomy for chromosomes II, VIII, and X for several reasons. First, as discussed in Chapter 4, I observed a chromosome XII fragment (the schromosome) in *tel1 mec1* diploids without the *MEC1* plasmid, and these strains became trisomic for XII when the *MEC1* plasmid was re-introduced. No such fragments were observed for the other three chromosomes. Second, I found that chromosome XII, but not other chromosomes, had difficulty entering the CHEF gels in *tel1 mec1* diploids. DNA molecules with branches (replication forks or recombination structures) have difficulties entering CHEF gels. Unlike chromosome XII, chromosomes II, VIII, and X had no

obvious difficulty entering the CHEF gel. Finally, chromosomes II, VIII, and X are commonly found trisomic in *bub1* strains while chromosome XII is not. This result suggests that *bub1* cells and *tel1 mec1* strains may have a common mechanism or selective pressure affecting chromosomes II, VIII, and X, but chromosome XII trisomy reflects a second mechanism specific to *tel1 mec1* diploids.

Chromosomes I and VI, and no other chromosomes, are frequently monosomic in *tel1 mec1* strains. These chromosomes are the smallest and, therefore, it is likely that their monosomy is better tolerated because they carry fewer genes. Evidence supporting this hypothesis comes from a study of 16 diploid yeast strains that were selected to be monosomic for specific chromosomes (Reid *et al.*, 2008). When these strains were sporulated and examined by tetrad analysis, only the two strains that were selected to be monosomic for chromosomes I and VI had the expected 2 live:2 dead spore segregation pattern. In the other diploids, the tetrads had four viable spores, indicating that the monosomic chromosome had spontaneously duplicated to return the strain to euploidy. This result, coupled with my observations, suggests that diploid cells cannot easily tolerate monosomy of chromosomes other than I and VI.

5.1.3 Aneuploidy profiles of *tel1 mec1*, *bub1*, and *mad2* diploids

Many spindle assembly checkpoint (SAC) mutants, including *bub1*, have elevated levels of aneuploidy (Warren *et al.*, 2002). It is also known that a functional SAC is required for complete cell cycle arrest in response to DNA damage, indicating that part of the DNA damage response pathway is channeled through SAC components such as Mad2p (Kim and Burke, 2008). I hypothesized that Tel1p and Mec1p may play a role in initiating or maintaining the spindle assembly checkpoint in addition to their canonical roles in the DNA repair and replication checkpoints. To test this hypothesis, I first monitored the aneuploidy profiles of *bub1* diploids. I found that *bub1* strains were highly aneuploid, and like the *tel1 mec1* strains, had a similar bias for trisomy of chromosomes

VIII and X. The rate of chromosome missegregation is higher for *bub1* strains than for *tel1 mec1* strains, as I detected high levels of aneuploidy in *bub1* strains prior to subculturing.

Because *bub1* has functions outside of the SAC (Williams *et al*., 2007), I then tested the aneuploidy profiles of diploids lacking the SAC-specific gene *MAD2*. Unlike *bub1* strains, *mad2* strains had very low rates of aneuploidy. The likely explanation for this difference is that not only do *bub1* strains have a dysfunctional SAC, they have severe defects with chromosome biorientation as well. This suggestion is supported by evidence that yeast cells correctly biorient chromosomes more often than not in the absence of cellular insults (Indjeian and Murray, 2007). Thus, strains without a functional SAC (such as *mad2*) but no defect in biorientation, would correctly align and disjoin their chromosomes the majority of the time. The occasionally misaligned chromosomes would escape the SAC and show up as rare aneuploidies. However, strains such as *bub1* that possess a defect in chromosome biorientation as well as the SAC would often misalign chromosomes and then fail to detect or fix the errors, leading to extremely high rates of aneuploidy. Since the *bub1* strains have structurally abnormal kinetochores (Boyarchuk *et al*., 2007), the more extreme segregation problems of *bub1* compared to *mad2* might be related to this defect rather than the biorientation problem. I also examined the aneuploidy profile of *bub1-ΔK*, an allele of *BUB1* that lacks the kinase domain. The *bub1-ΔK* strains have an intact kinetochore-occupancy SAC but possess defects in chromosome biorientation and tension-dependent SAC signaling. This analysis would test the hypothesis that defects in chromosome biorientation and/or tension-dependent SAC signaling cause high rates of aneuploidy outside of the canonical kinetochore-occupancy SAC. Interestingly, *bub1-ΔK* mutants had similar rates of aneuploidy as the *tel1 mec1* strains, with a similar bias towards trisomy of chromosomes II, VIII, and X. The *bub1-ΔK* strains were also frequently trisomic for

chromosomes III and XVI. To test if *tel1 mec1* and *bub1-ΔK* function in similar genome-stabilizing pathways, I created *bub1-ΔK tel1 mec1* diploids. The triple mutant diploid had a level of aneuploidy that was approximately additive with the levels observed in the *tel1 mec1* and *bub1-ΔK* strains. This result indicates that the *tel1 mec1* and *bub1-ΔK* mutations either affect separate pathways governing chromosome disjunction, or possess partially redundant roles in the same cellular pathway. I cannot differentiate between these two possibilities at this time.

5.1.4 *tel1 mec1* strains have an intact spindle assembly checkpoint (SAC)

The high rate of aneuploidy observed in the *tel1 mec1* strains suggested the possibility that these strains lacked a functional SAC. Sensitivity to the microtubule-destabilizing agent benomyl is one phenotype associated with SAC-defective strains (Hoyt *et al.*, 1991; Li and Murray, 1991). I found that *tel1 mec1* strains did not show sensitivity to benomyl in growth assays. In addition, in the presence of benomyl, most of the *tel1 mec1* strains arrested the cell cycle as doublets (G2/M border). Thus, Tel1p and Mec1p do not participate in checkpoint signaling in response to unattached kinetochores caused by microtubule depolymerization.

It is formally possible that *tel1 mec1* strains have a functional kinetochore-occupancy checkpoint (the checkpoint assayed by benomyl sensitivity), but are defective in the tension-sensing component of the SAC. Since *tel1 mec1* strains have higher levels of aneuploidy than *mad2* strains, which lack both the kinetochore-occupancy and the tension-sensing components of the SAC, this possibility is unlikely. Instead, I believe that the severe aneuploidy in *tel1 mec1* mutant diploids is due to defects in kinetochore structure or function such that proper biorientation of the duplicated chromatids is rarely achieved. The SAC either does not recognize this misorientation or is overwhelmed by the number of misaligned chromosomes, and the cell eventually

divides despite the lack of proper biorientation. Although this explanation of the high level of non-disjunction in the *tel1 mec1* strains is my favored hypothesis, I cannot rule out other explanations including defects in the completion of DNA replication, sister chromatid cohesion, or other cell cycle processes. These alternatives will be discussed below.

5.1.5 Other mechanisms that could contribute to aneuploidy in *tel1 mec1* strains

In this thesis, I have demonstrated that *tel1 mec1* strains possess an intact SAC and thus do not accumulate aneuploidy through a failure to detect misaligned chromosomes. Additionally, telomere defects do not underlie chromosome non-disjunction in *tel1 mec1* strains. *tel1 mec1* diploid strains that have normal or supra-normal telomere lengths through introduction of the pVL1107-*URA3* (Cdc13p-Est2p) plasmid still have high rates of aneuploidy, although the rate of chromosome rearrangements is reduced (Chapter 3). Additional investigations using the *tel1 mec1* strain with the pVL1107-*URA3* plasmid should help illuminate the pathways involved in failure to ensure proper chromosome segregation. Below, I briefly describe a few of the cellular processes that could contribute to the aneuploidy of *tel1 mec1* strains.

5.1.5.1 Role of Tel1p and Mec1p in the phosphorylation of histone H2A

As described in Chapter 1, histone H2A is phosphorylated by Mec1p and Tel1p on serine 129 (S129) in response to DNA damage (Downs *et al.*, 2000). The phosphorylated H2A (γH2A) spreads over at least 50 kb on both sides of the DSB (Shroff *et al.*, 2004). Interestingly, Bub1p also phosphorylates the H2A "tail", but on a different residue, serine 122 (S122; Kawashima *et al.*, 2010). Mutations in H2A that abolish either phosphorylation site sensitize the cells to DNA damaging agents, and mutations that abolish both sites result in more extreme sensitivity than those associated with either single mutant (Harvey *et al.*, 2005; Moore *et al.*, 2007; Wyatt *et al.*, 2003). Mutating S122

to alanine (S122A) impairs the localization of Sgo1p to the centromere. Sgo1p is a target of Bub1p that is required for centromeric cohesion in meiosis and chromosome biorientation in meiosis and mitosis (Fernius and Hardwick, 2007; Kiburz *et al.*, 2005). Thus, one hypothesis for the similar aneuploidy profiles of *tel1 mec1* and *bub1* strains is that both genotypes fail to properly phosphorylate histone H2A. If phosphorylation at S122 by Bub1p and S129 by Tel1p and Mec1p are partially functionally redundant, mutations in either of these pathways could produce chromosome missegregation and similar aneuploidy profiles. In mammals, the homologous protein H2AX is similarly phosphorylated in response to DNA damage to create γH2AX (Rogakou *et al.*, 1998). Underscoring its importance in maintaining genome stability, a deficiency of H2AX in mice leads to genetic alterations such as chromosome translocations (Celeste *et al.*, 2002).

5.1.5.2 Impaired kinetochore or microtubule function

Like Bub1p, Tel1p and Mec1p may also regulate proper kinetochore or microtubule function. In addition to histone H2A described above, there are many other potential candidates for phosphorylation by Tel1p and/or Mec1p that could affect chromosome disjunction. Mutants that disrupt the inner kinetochore complex CBF3 (*ncd10*, *ctf13*, and *cep3*) have a defective SAC (Gardner *et al.*, 2001). Thus, *tel1 mec1* strains must possess an intact inner kinetochore structure, as they have a functional SAC. However, some of the non-essential kinetochore proteins, such as *CSE4*, *MIF2*, *CBF1*, *MCM21*, *CTF19*, *SLK19*, *MCK1*, and *KAR3*, are not required for the SAC, and defective regulation of one or more of these proteins in *tel1 mec1* strains could result in chromosome missegregation. For example, Cbf1p is a phosphorylation target of Tel1p and Mec1p (Smolka *et al.*, 2007). Preliminary experiments in the Petes laboratory have demonstrated that *cbf1* diploids do not have high rates of aneuploidy (Yi Yin, unpublished results). However, there may be other kinetochore or microtubule targets of Tel1p and Mec1p that are important for genome stability.

5.1.5.3 Defective sister chromatid cohesion

As described in the Chapter 1, strains with defective cohesion often have high rates of chromosome loss (Michaelis *et al.*, 1997). Additionally, Tel1p and Mec1p are required for damage-induced cohesion surrounding a DSB and genome-wide (Strom *et al.*, 2007; Unal *et al.*, 2007). It is possible that Tel1p and Mec1p also regulate cohesion in the absence of endogenous damage. Cohesion cleavage that is not temporally coordinated in anaphase can facilitate premature sister chromatid separation and chromosome non-disjunction. In their roles as DNA damage checkpoint genes, in the presence of DNA damage, Tel1p and Mec1p stabilize Pds1p, an anaphase inhibitor of SC separation (Cohen-Fix and Koshland, 1997). It is possible that that Tel1p and Mec1p promote the stability of Pds1p even in the absence of DNA damage. In the absence of Tel1p and Mec1p, Pds1p is down-regulated, allowing the premature activation of separase and leading to premature loss of sister chromatid cohesion.

5.1.5.4 Tetraploidization followed by chromosome loss

In human cells, tetraploidization followed by rapid chromosome loss can lead to very high rates of aneuploidy (Shi and King, 2005). If the diploid *tel1 mec1* cells efficiently formed tetraploids, I would expect a high rate of aneuploidy, since polyploid yeast strains rapidly lose chromosomes (Mayer and Aguilera, 1990). This mechanism, however, is not the likely cause of aneuploidy in the *tel1 mec1* diploids because of the kinetics of accumulation of trisomic chromosomes. During the first twenty generations of growth, most *tel1 mec1* strains are aneuploid for only one or two chromosomes. By 100 generations of growth, the cells are aneuploid for about 2.5 chromosomes. This pattern is not what would be predicted if tetraploidization initiated the process.

5.1.5.5 Aneuploidy generated by extra spindle pole bodies

Another genetic alteration that could lead to elevated levels of aneuploidy is extra spindle pole bodies (SPBs). SPBs are the yeast equivalent of the mammalian

centrosome. Cancer cells often possess supernumerary centrosomes that can form multipolar spindles and cause many chromosomes to pass through a multipolar intermediate during mitosis (Cimini, 2008; Fukasawa *et al.*, 1996; Ganem *et al.*, 2009). In humans, the DNA damage response induces centrosome amplification in a *Chk1*-dependent manner (Bourke *et al.*, 2007; Fukasawa *et al.*, 1996). In yeast, deleting all four B-type cyclin genes in yeast can cause supernumerary SPBs and can result in unequal DNA segregation (Haase *et al.*, 2001). If Tel1p and Mec1p are required for regulating the number of SPBs, then cells lacking these proteins might have elevated levels of aneuploidy.

5.1.5.6 Aneuploidy induced by chromosome re-replication

In yeast strains with mutations in a number of components of the pre-replicative complex (for example, certain *orc6* alleles), re-replication of chromosome sequences occurs. In *Saccharomyces cerevisiae* the extent of re-replication is restrained by a Mec1p-dependent checkpoint (Archambault *et al.*, 2005). Although this study was carried out in strains containing mutations that promoted re-replication, it is possible that the Mec1p also constrains re-replication in a wild-type cell. Re-replication could lead to aneuploidy. In addition, re-replication induces DSBs (Green and Li, 2005), a phenotype associated with *tel1 mec1* cells.

5.1.5.7 Summary of the possible explanations of the aneuploidy

In summary, I cannot definitely rule out a variety of mechanisms that could be responsible for the aneuploidy of the tel1 mec1 diploids. However, I favor the model in which the function of the kinetochore is affected by phosphorylation of H2A by Tel1p and Mec1p, since this model rationalizes the similarity of the effects of the *bub1* mutation and the *tel1 mec1* mutations. Although an effect of Tel1p and Mec1p on sister chromatid cohesion is also a plausible model, preliminary experiments done in collaboration with Jennifer Gerton (Stowers Institute) did not indicate a strong cohesion defect, at least for

regions of the chromosome that are far from the centromere. Experiments to investigate the causes of the aneuploidy will be described below.

5.2 Chromosome alterations in *tel1 mec1* diploids

In diploid *tel1 mec1* strains, as in haploids of the same genotype (Vernon *et al.*, 2008), we observed high levels of chromosome rearrangements, deletions, duplications and translocations. The alterations were observed after a limited amount of sub-culturing in the absence of selection. Below, I will discuss the mechanisms responsible for generating these alterations and my analysis of a novel chromosome alteration that appears to reflect a DSB within the rRNA gene cluster.

5.2.1 The relationship between telomere defects and chromosome rearrangements in *tel1 mec1* strains

It is clear from my study that the telomere length defect of *tel1 mec1* strains is almost entirely responsible for the high level of chromosome rearrangements. The introduction of a fusion protein in which a telomere-binding protein (Cdc13p) is fused to a telomerase protein (Est2p) into *tel1 mec1* cells restores wild-type telomere length and significantly reduces the frequency of chromosome rearrangements (Chapter 3). The very short telomeres of the *tel1 mec1* strains behave as though they lack a telomere "cap", the structure that prevents telomeres being used as a substrate for DNA repair. Consequently, both haploid (Mieczkowski *et al.*, 2003) and diploid (Chapter 3) *tel1 mec1* cells have high rates of telomere-telomere fusions (TTFs). The high rate of chromosome rearrangements in *tel1 mec1* strains is likely due to cascades of instability arising from breakage-fusion-bridge cycles that originate from these TTFs (Sabatier *et al.*, 2005). TTFs create dicentric chromosomes that can break during anaphase to generate broken ends that then interact with broken ends derived from other chromosomes or that can fuse with shortened telomeres.

These breakage-fusion-bridge cycles can explain the tripartite chromosome found in strain JLMy80-5L (described in Chapter 3). This chromosome was composed of a fusion of an internal segment of chromosome XII to the telomere of chromosome II, followed by the fusion of a terminal fragment of chromosome III to one end of the II-XII fusion (Fig. 3.3). Such a chromosome could be generated by a break in the centromere-distal region of chromosome XII that fused with the eroded telomere of chromosome II. The resulting dicentric chromosome could be broken in anaphase to create the centromere-proximal break on chromosome XII. This broken end could then join through NHEJ with the broken chromosome III. Because the other end of chromosome III contains a telomere, this fusion would end the cascading instability. This tripartite rearranged chromosome is unusual in that all other chromosome rearrangements observed in the *tel1 mec1* diploid (described below) occur by homologous recombination rather than NHEJ. The explanation for this observation is that NHEJ is suppressed in diploids that express both *MAT***a** and *MAT*α information (Kegel *et al.*, 2001). In the strain JLMy80-5L with the tripartite chromosome, one copy of chromosome III was deleted for the mating type locus, activating the NHEJ pathway. Finally, I note that the TTFs, which occur efficiently in the diploids, are a type of NHEJ. This type of NHEJ must be regulated differently than the NHEJ events that occur between non-telomeric repeats.

While the lack of TTFs and chromosome rearrangements are correlated with longer telomere lengths in *tel1 mec1* + pVL1107-*URA3* strains, it is possible that the lengthened telomeres *per se* is not what prevents chromosome rearrangements. It is possible that the Cdc13p-Est2p fusion protein acts as a telomere cap preventing TTFs in the *tel1 mec1* strains. Patients with mutated ATM also have dysfunctional telomeres (accelerated telomere shortening and the presence of telomere-telomere fusions) despite possessing normal telomerase activity (Metcalfe *et al.*, 1996).

5.2.2 Chromosome rearrangements in *tel1 mec1* strains involving homologous recombination (HR) between repetitive Ty elements

Most of the genome rearrangements in *tel1 mec1* diploids occurred between repetitive Ty elements using homologous recombination (HR; Chapter 3). As discussed previously, this result is in contrast to observations of deletion-associated chromosome rearrangements in haploid *tel1 mec1* strains in which the chromosome rearrangements occur through NHEJ (Craven *et al.*, 2002; Myung *et al.*, 2001b). Although NHEJ is repressed in diploid cells, this difference is not the primary reason for the different types of chromosome rearrangements, since unselected chromosome rearrangements in haploid *tel1 mec1* strains also primarily reflect homologous recombination between Ty elements (Vernon *et al.*, 2008). The main difference is that the deletion analysis of Myung *et al.* (2001b) and Craven *et al.* (2002) selected for events on chromosome V in a region that had no repetitive elements and, therefore, homologous recombination would not generate the required deletion. In a follow-up study of deletion-associated rearrangements, Putnam *et. al* (2009a) introduced a repetitive sequence at the relevant position on chromosome V and observed chromosome rearrangements that involved homologous recombination between repeats in *tel1 mec1* strains.

The Ty-Ty mediated chromosome rearrangements are likely to reflect a chromosome with a DSB within one Ty that is repaired by a BIR event involving a Ty on a different chromosome. There are two mechanisms by which a chromosome with a DSB in a Ty could be produced. First, as described above, a TTF could produce a dicentric chromosome, and breakage of that chromosome could occur within a Ty element, producing a recombinogenic end. The broken end could alternatively be processed by exonucleases to expose the Ty homology. A second possibility is that nucleolytic degradation of the uncapped telomeres of the *tel1 mec1* strain could produce the recombinogenic end. From the patterns of marker loss in strains lacking telomerase, Hackett and Greider (2003) argued in favor of this mechanism. If such a mechanism was

responsible for the chromosome rearrangements in my study, one would expect that most of the chromosome rearrangements would involve Ty elements that were close to the telomere. Since many of my rearrangements do not involve this class of Ty elements, I favor the first explanation.

In addition to my research, numerous other studies have identified Ty elements as being important in generating chromosome rearrangements (Argueso *et al.*, 2008; Lemoine *et al.*, 2005; Putnam *et al.*, 2005; Vernon *et al.*, 2008). Although DSBs were generated by independent mechanisms in each of these studies, all resulted in the same genetic product: deletions, duplications or translocations involving homologous recombination between ectopic repeats. X-ray irradiation presumably creates DSBs (Argueso *et al.*, 2008), low DNA polymerase α generates DSBs as a consequence of processing secondary structures in DNA at the replication forks (Lemoine *et al.*, 2005), and the Ty-mediated rearrangements in my study are a result of TTFs formation and the subsequent breakage of dicentric chromosomes. Despite these differences, chromosome rearrangements occur primarily through Ty-dependent HR. Many chromosome rearrangements, such as those indicated by a deletion on one chromosome and an amplification on another chromosome within the same microarray, can be attributed to BIR events (Argueso *et al.*, 2008; Lemoine *et al.*, 2005). Other rearrangements, such as a microarray showing two chromosomes with terminal amplifications or two chromosomes with terminal deletions, are likely to represent other HR events such as single-strand annealing, synthesis-dependent strand annealing, or half-crossovers.

5.2.3 Chromosome XII fragments generated in *tel1 mec1* strains

The first chromosome aberration observed in *tel1 mec1* diploids after loss of the *MEC1*-containing plasmid is an amplification of sequences on chromosome XII between the left telomere and tandem array of rRNA genes on the right arm of XII. We have termed this amplified sequence a "schromosome" (Chapter 4). Although I have

observed persistence of this amplified segment for 200 cell generations by microarray analysis, I have been unable to detect this fragment in diploid *tel1 mec1* strains by CHEF gel analysis. It is possible that the fragment is frequently engaged in recombination and is, therefore, unable to enter the gel or that the processing of the fragment makes it difficult to visualize as a discrete entity by gel electrophoresis. When *MEC1* is reintroduced into diploid *tel1 mec1* cells containing the schromosome, the strain becomes trisomic for XII. This result suggests that the schromosome lacks a telomere cap and is, consequently, prone to recombination.

The rRNA gene cluster consists of 100-150 tandem 9.1 kb genes, each encoding four species of ribosomal RNA (Petes, 1979). The rRNA gene cluster has a high rate of mitotic recombination even in wild-type strains (Andersen *et al.*, 2008; Casper *et al.*, 2008; Szostak and Wu, 1980), suggesting that DSBs are common in the rDNA under normal cellular conditions. In addition, strains with low levels of the DNA helicases Rrm3p and Dna2p have greatly elevated levels of rDNA recombination (Ivessa *et al.*, 2000; Weitao *et al.*, 2003).

One explanation for the elevated rates of DSBs in the *tel1 mec1* strains is that they have an elevated frequency of DSBs at the Fob1p-dependent replication fork block. To prevent replication forks from colliding with the transcription machinery, there is a polar replication fork barrier (RFB) within each repeat that allows replication to proceed in only one direction (Brewer and Fangman, 1988; Linskens and Huberman, 1988). The RFB functions through binding of the protein Fob1p, which is necessary to enforce the replication block in one direction while allowing the fork from the other direction to pass through (Kobayashi, 2003). Yeast strains lacking *FOB1* have decreased levels of mitotic recombination, indicating that Fob1p increases the rate of recombinogenic lesions within the rDNA (Casper *et al.*, 2008; Defossez *et al.*, 1999; Johzuka and Horiuchi, 2002; Kobayashi *et al.*, 1998; Kobayashi *et al.*, 2004). However, the elevated mitotic

recombination within the rDNA array observed in strains with low levels of DNA polymerase are Fob1p-independent (Casper *et al.*, 2008). Thus, DSBs within the rDNA arise through both Fob1p-dependent and Fob1p-independent mechanisms. In a *tel1 mec1* background, the schromosome is not formed in *fob1 tel1 mec1* strains (Chapter 4). One interpretation of this result is that Fob1p is required to generate DSBs within the rDNA through its fork-stalling action. Alternatively, it is possible that the schromosome is constitutively formed in *tel1 mec1* strains, but Fob1p prevents efficient repair of the schromosome by BIR. By this model, loss of Fob1p would facilitate repair of the schromosome, preventing its detection.

Another mechanism to explain formation of schromosomes in *tel1 mec1* cells is that the hyper-activation of rDNA replication origins in *tel1 mec1* cells elevates the frequency of DSBs. Although each rDNA repeat contains an ARS element, only 20% of rDNA origins are activated in any given S phase (Brewer and Fangman, 1988; Linskens and Huberman, 1988; Pasero *et al.*, 2002; Saffer and Miller, 1986). Tel1p and Mec1p are known to restrain the firing of replication origins in response to DNA damage (Santocanale and Diffley, 1998). By extension, it is possible that Tel1p and Mec1p are also required to restrain origin firing within the rDNA in the absence of DNA damage. Thus, *tel1 mec1* strains may possess many more active origins than wild-type cells, leading to increased numbers of stalled replication forks at the RFB sites.

5.2.4 The role of Mec1p in break-induced replication (BIR)

Repair of DSBs through break-induced replication (BIR) can occur using allelic or non-allelic sequences (Llorente *et al.*, 2008). In non-allelic BIR events, a chromosomal fragment with a break in one repeated gene invades the same type of repeat on a non-homologous chromosome. The strand invasion sets up a replication fork that copies the other chromosome to the end, resulting in a translocation. In an allelic BIR event, the broken chromosome invades a homologous chromosome. The ensuring replication

results in loss of heterozygosity (LOH) centromere distal to the invading end. My results suggest that Mec1p is involved in at least some types of BIR events. As discussed above, I find that the schromosome in *tel1 mec1* strains is maintained as a chromosome fragment until the introduction of Mec1p. Following the introduction of Mec1p, I observe trisomy for chromosome XII. This result argues that the BIR event required to generate trisomy cannot be completed in a *mec1* strain. It should be emphasized that the amount of DNA synthesis required to generate trisomy for chromosome XII is substantial. The rRNA gene cluster is about 1 Mb in size and the distance between the centromere-distal end of the cluster and the right telomere of XII is about 600 kb. Since the rate of DNA fork movement in yeast is about 3 kb per minute (Petes and Williamson, 1975), it would take about 200-500 minutes to complete the BIR event even in a wild-type strain; this estimate is a minimum because it does not include the amount of time that the replication forks are stalled at the RFB.

5.3 Future Directions

Although my thesis research could be extended in many directions, I will restrict my discussion to two general types of experiments: further characterization of the roles of Tel1p and Mec1p in regulating chromosome disjunction and further analysis of the schromosome. Many of my proposed experiments to analyze aneuploidy involve whole-genome microarray analysis, which is a very effective tool to analyze genome instability events (Lemoine *et al.*, 2005). Prior to the advent of microarrays, researchers had to rely on events involving one or two specific genetic markers to gain information about genome instability events. Microarray analysis allows the detection of all large-scale (> 5 kb) genetic changes within the entire genome. This non-selective approach, of course, is only useful if there is a high frequency of genetic alterations. Higher-resolution methods, such as high-throughput DNA sequencing, will allow detection of smaller

changes and mutations, while methods such as CHEF gels and multiplex PCR are useful in detecting gross changes in chromosome structure or number.

It is very difficult to perform certain microscopic studies (for example, monitoring sister chromatid cohesion) of *tel1 mec1* strains because many of the cells are inviable (Chapter 3; Ritchie *et al.*, 1999). However, *tel1 mec1* diploids with the pVL1107-*URA3* plasmid (encoding the Cdc13p-Est2p fusion protein) have much better viability than cells without the plasmid, and yet still have very high rates of aneuploidy. Such strains could be used to examine chromosome and kinetochore structure on a molecular level with immunofluorescence microscopy, as well as other cell biological techniques.

5.3.1 Investigating the role of histone H2A in aneuploidy

I still have not identified the mechanism responsible for generating the extremely high rate of aneuploidy in *tel1 mec1* strains. One intriguing possibility is that *tel1 mec1* strains and *bub1* strains have similar problems with chromosome disjunction as a result of defects in phosphorylating a common substrate, histone H2A. As discussed above, Kawashima *et al.* (2010) showed that phosphorylation of S122 of H2A is Bub1p-dependent, and S122A mutants of H2A fail to localize Sgo1p to the kinetochore. Tel1p and Mec1p, in response to DNA damage, phosphorylate S129 of H2A (Downs *et al.*, 2000). To determine whether these events are mechanistically related, I will examine the frequency of aneuploidy and the patterns of the aneuploid chromosomes in yeast strains containing mutations of S122 and/or S129. For these studies, I will use yeast strains with chromosomal deletions of the two genes encoding H2A (*H2A1* and *H2A2*), with the mutated copies of H2A supplied on a plasmid (Harvey *et al.*, 2005). Initially, I will examine three strains, those with the S129A mutation, the S122A mutation, and the double mutation S129A and S122A. Based on the results of Kawashima *et al.* (2010), I expect that the S122A mutation will have an elevated level of aneuploidy. If phosphorylation of S129 is specific to the DNA damage response, I will not observe

elevated aneuploidy in the S129A strain and the double mutant strain will have the same level of instability as the S122A strain. Alternatively, it is possible that the role of H2A at the kinetochore is affected by phosphorylation of both serines. In that circumstance, I expect that the double mutant will have the highest level of aneuploidy.

Another important experiment is to investigate the properties of the strains containing the histone alterations in strains with the *bub1* and/or *tel1 mec1* mutations. For example, if the S129A H2A variant has the same level of aneuploidy in wild-type and in *tel1 mec1* strains, it would argue that the aneuploidy phenotype of *tel1 mec1* is mediated through its ability to phosphorylate S129. Similar epistasis studies could be performed with S122A and the *bub1* mutation. Although I will not discuss all variations, these types of experiments can test the hypothesis that the similar aneuploidy phenotypes of *bub1* and *tel1 mec1* are mediated through phosphorylation of H2A at nearby sites.

5.3.2 Examining kinetochore, microtubule, and spindle pole body (SPB) defects in *tel1 mec1* strains

As discussed above, diploids of the *tel1 mec1* genotype are poor candidates for most microscopic studies. Many of the cells in cultures of this strain fail to divide and many have abnormal morphologies. In contrast, strains with the *tel1 mec1* genotype that contain the Cdc13p-Est2p fusion protein divide at a faster rate and have more normal morphologies. In this type of strain, it may be possible to examine some properties of the kinetochore, microtubule, and SPB. Fluorescently tagging any kinetochore-specific protein, such as Ncd10p, and monitoring localization of the protein could be used to investigate the integrity of the kinetochore and the positioning of kinetochores at different times during the cell cycle. Alternatively, it is possible that *tel1 mec1* strains have defective microtubules. Many microtubule mutants are cold sensitive (Schatz *et al.*, 1988); I have noticed that *tel1 mec1* strains are also cold sensitive. I could fluorescently

label Tub1p (Straight *et al.*, 1997) in *tel1 mec1* strains to determine if the spindle is normal in cycling cells. A third possibility is that *tel1 mec1* strains have supernumerary SPBs, leading to unequal DNA segregation. A straightforward experiment to test this possibility would be to fluorescently tag the SPB protein Spc42 and monitor the number of SPBs in cells undergoing mitosis.

5.3.3 Experiments to characterize the structure of the schromosome

I also plan to further characterize the structure of the schromosome and the genetic requirements for its formation. One puzzle is that the schromosome can be detected in CHEF gels in DNA isolated from haploid *tel1 mec1* strains, but not in diploid *tel1 mec1* strains. It is possible that the ribosomal DNA from diploid strains has a branched morphology that keeps the DNA from entering the CHEF gel; such branches could arise as a consequence of recombination or stalled replication forks. I will examine this issue several ways. First, I will look for aberrant structures using two-dimensional gel electrophoresis, followed by Southern blotting with an rDNA probe (Weitao *et al.*, 2003). Second, I will determine if recombination is responsible for my failure to detect the schromosome in diploid cells by deleting *RAD52* in the *tel1 mec1* background, and examining DNA isolated from the resulting triple mutant strain with CHEF gels. Although strains with the triple mutation are likely to grow very slowly, by using strains that have the Cdc13p-Est2p fusion protein (encoded by the plasmid pVL1107-*URA3*), I hope to alleviate some of the growth problems.

It is also possible that the rate of DNA fork movement in the rDNA is very slow in *tel1 mec1* strains, and the resulting branched DNA molecules prevent XII from entering the CHEF gel. To address this issue, I will try two approaches. First, I will simply incubate the strain for longer growth periods to be sure that the cells are fully in stationary phase. Second, before harvesting the cells, I will incubate them in nocodazole for 6 hours to allow completion of DNA replication. Following these treatments, I will

examine DNA isolated from the cells by CHEF gels to determine whether the schromosome can be visualized.

It appears that the schromosome exists in *tel1 mec1* diploid strains as a fragment that is stable but uncapped with telomeric sequences because it can be rapidly repaired to generate chromosome XII trisomy upon reintroduction of *MEC1*. In the haploid strain, I do not know if the schromosome has a telomere cap. I observed, however, that subculturing of cells containing the schromosome resulted in slower electrophoretic mobility of the schromosome. This result could indicate that the schromosome is gaining repeats within the rRNA gene cluster. Alternatively, it is more likely that the schromosome is being processed to generate long single-stranded "tails" since such processing has been shown to result in reduced electrophoretic mobility in CHEF gels (Westmoreland *et al.*, 2009). As the haploid strain is subcultured, the microarray analysis indicates that the schromosome starts to become lost in the cell population.

To confirm the conclusion that the schromosome has long single-stranded extensions, I could do two types of experiments. First, using strand-specific probes for the ribosomal DNA and "dot blots" (Parenteau and Wellinger, 1999), I could determine whether undenatured genomic DNA isolated from schromosome-containing strains hybridized to one probe, but not the other. Second, I could construct strains that are deficient in exonucleases (such as Exo1p) that process broken ends. In such strains, the schromosome should maintain a more homogeneous pattern of migration in the CHEF gels.

One other interesting question is why the *tel1 mec1* strains retain the schromosome. It is possible that the retention is a consequence of selection for rRNA genes. To test this possibility, I will construct a *tel1 mec1* strain in which rRNA synthesis is regulated from an rDNA-containing plasmid (Wai *et al.*, 2000). If such a strain does

not contain a schromosome, I will conclude that the selective force for retention of the schromosome is the extra copies of rRNA genes.

5.3.4 Experiments to characterize genetic requirements for the formation and repair of the schromosome

As described above, the rDNA is a common site of DSBs even in wild-type strains. Breaks within the rDNA have been attributed to Fob1p-dependent replication fork collapse at the RFB (Weitao *et al.*, 2003). The binding of Fob1p blocks replication forks from one direction but allows replication fork passage from the opposite direction. I found that *fob1 tel1 mec1* strains did not have a schromosome, although such strains were trisomic for chromosome XII (Chapter 4). This result could be explained in two ways: 1) Fob1p is necessary for formation of the schromosome or 2) elimination of Fob1p allows efficient repair of the schromosome, preventing its detection. I can differentiate between these possibilities by monitoring the number of breaks within the rDNA in *fob1 tel1 mec1* strains versus *tel1 mec1* strains.

DSBs at the RFB can be detected by Southern analysis using *Bgl*II digests and an rDNA-specific probe (Casper *et al.*, 2008). I will examine DNA isolated from wild-type, *tel1 mec1*, and *fob1 tel1 mec1* strains. If DSBs at the RFB site are relevant in formation of the schromosome, I expect to see more breaks at this position in the *tel1 mec1* strain than in the wild-type, and this elevated rate of breakage will be eliminated in the triple mutant strain.

I have suggested that the schromosome in the *tel1 mec1* diploid is repaired to generate trisomy for chromosome XII upon introduction of a plasmid containing the wild-type *MEC1* gene. One common mechanism by which DSBs are repaired is through break-induced replication (BIR). A BIR event involves one broken chromosome end invading a region of homology on another chromosome. A unidirectional replication fork is set up that copies the invaded chromosome through to the telomere. Morrow *et*

al. (1997) showed that BIR events rarely extend through the centromere. Thus, it usually the centromere-containing chromosome fragment that initiates a productive BIR event. BIR events result in loss-of-heterozygosity (LOH) of all markers centromere-distal to the DSB on the recipient chromosome, while the donor template remains unchanged (Llorente *et al.*, 2008).

Pol32p is required for the majority of BIR events in yeast cells as part of the Polδ replication complex (Lydeard *et al.*, 2007). To test whether repair of the chromosome XII fragment upon reintroduction of *MEC1* is dependent on BIR, I deleted *POL32* in isogenic *tel1 mec1* diploid yeast strains. I will subsequently monitor the repair of the schromosome in this strain. While I cannot yet make a conclusion regarding schromosome formation, I have preliminary evidence that the *pol32 tel1 mec1* strains have higher rates of chromosome loss than *tel1 mec1* strains. This result indicates that proper replication function is imperative to maintain genome stability. Thus, DNA breaks formed by stalled replication forks or by breakage of dicentric chromosomes may need to be repaired in a replication-dependent mechanism such as BIR. The Malkova lab has recently reported that *POL32* deficiency results in elevated rates of chromosome loss as well as inefficient BIR (Deem *et al.*, 2008).

5.4 Roles of ATM (Tel1p) and ATR (Mec1p) in maintaining genome stability

Because DNA damage repair pathways are highly conserved between yeast and humans, studying the function of Tel1p and Mec1p in maintaining genome stability in yeast has important implications in understanding the roles of ATM and ATR in human health and disease. Below, I discuss the evidence that mutations in *Atm* and *Atr* are relevant to carcinogenesis and mechanisms by which these genes may act to stabilize the genome.

5.4.1 Evidence that mutations in *Atm* and *Atr* promote oncogenesis

Many genes involved in genome stability pathways have been implicated in cancer. There are a number of studies correlating mutations in *Atm* or *Atr* with cancer. As discussed in Section 1.1.3, individuals with heterozygous mutations in *Atm* have an increased risk of breast cancer. In addition, T-cell prolymphocytic leukemias and non-Hodgkin's lymphomas homozygous for mutations in *Atm* have been observed in several studies (Meyn, 1999; Stilgenbauer *et al.*, 1997; Vorechovsky *et al.*, 1997). Another study found that *Atm* expression was decreased in 8/20 tumors (Stankovic *et al.*, 1999). Furthermore, the breast cancer susceptibility protein BRCA1 is a target of phosphorylation by ATM and ATR (Cortez *et al.*, 1999; Gatei *et al.*, 2000; Xu *et al.*, 2001), and mice that lack ATM targets H2AX or 53BP1 are susceptible to oncogenesis (Kastan and Bartek, 2004). MRE11-deficient mice show an increase in chromosome breaks and telomere-telomere fusions, but do not develop lymphomas like ATM-deficient mice (Theunissen *et al.*, 2003; Xu *et al.*, 1996). In addition, mice lacking MRE11 and p53 exhibit decreased tumor latency relative to mice lacking only p53; this result suggests that a checkpoint deficiency is required in addition to chromosome instability to facilitate tumorigenesis. Interestingly, deleting the homologous recombination protein RAD52 in *Atm*-/- mice reduces the incidence of lymphomas, suggesting that homologous repair of DSBs plays a role in tumorigenesis (Treuner *et al.*, 2004). One study found that a repression of *Atr* or *Chk1* in combination with mismatch repair deficiency could induce chromosome instability (Jardim *et al.*, 2009). Neither MMR nor *Atr*/*Chk1* deficiency alone could promote chromosome instability.

5.4.2 Mechanisms by which mutations in *Atm* and *Atr* promote oncogenesis

Based on my observations concerning the functions of Tel1p and Mec1p, and those of many other yeast and mammalian labs, there are multiple mechanisms by

which mutations or down-regulation of the activities of ATM and ATR could promote oncogenesis including: 1) loss of DNA damage and DNA replication checkpoints, 2) high rates of aneuploidy resulting in dysregulation of genes involved in regulating cell growth, and 3) increased rates of DSBs, particularly at "fragile" chromosome sites. These mechanisms are discussed further below.

One barrier to malignant transformation is an intact DNA damage response that prevents cells with damaged DNA from replicating until the DNA damage is repaired; in addition, these mechanisms can channel cells with irreparable DNA damage into apoptosis (Bartkova *et al.*, 2005; Gorgoulis *et al.*, 2005). Mutations in genes involved in the DNA damage checkpoint (*Atm* and *Atr*), the apoptotic pathway (*Tp53*), or the spindle assembly checkpoint pathway (*Bub1*) can have elevated rates of DNA damage. This damage would be expected to cause an elevated rate of mutation in tumor suppressor genes. In addition, repair of broken chromosomes by NHEJ may result in the activation of cellular oncogenes.

Cells derived from solid tumors are often highly aneuploid, and this high degree of aneuploidy has been correlated with genetic instability (Duesberg *et al.*, 1998). Although the exact mechanisms by which aneuploidy promotes the development of cancer cells is not known, it is likely that aneuploid cells dysregulate gene expression, resulting in either reduction in the efficiency of various tumor suppressor pathways (for example, the DNA damage checkpoint pathways) or increased activity of growth-promoting pathways. The aneuploidy of cancer cells may eventually be a target for therapy. Because aneuploid cells demonstrate a stress response due to the additional proteins being translated, inhibiting the proteasome or chaperone systems could preferentially kill aneuploid cells (Williams and Amon, 2009).

A third mechanism by which mutations in *Atm* or *Atr* could predispose cells to cancer is by affecting chromosome fragile sites. Fragile sites are regions of mammalian

chromosomes that break when cells are treated with aphidicolin, a DNA polymerase inhibitor. These same sites are also hotspots for chromosome rearrangements in tumor cells (Arlt *et al.*, 2003). Fragile sites are associated with replication fork pausing and the stability of fragile sites is greatly reduced in human cells lacking ATR (Casper *et al.*, 2002). Similarly, in yeast, Raveendranathan *et al.* (2006) showed that some replication origins are not replicated efficiently in *mec1* mutants, resulting in DSBs. As fragile sites are frequently found at the breakpoint of chromosome rearrangements in tumor cells, understanding the mechanism by which Mec1p/ATR prevents chromosome breaks at these sites will be important for developing future anti-cancer therapies.

5.5 Concluding remarks

It has long been postulated that aneuploidy is a driving force of carcinogenesis (Boveri, 1914). A high degree of aneuploidy is strongly correlated with genetic instability in human cancer cells (Duesberg *et al.*, 1998). For this reason, it is imperative that the mechanisms that generate aneuploidy be elucidated. A major rationale of my study is that some of the features of the aneuploidy observed in human cells can be modeled in yeast.

I found that *tel1 mec1* diploid yeast cells have extremely high frequencies of aneuploidy and chromosome rearrangements; this phenotype mimics the genetic instability of metastatic tumor cells. The aneuploid phenotype is much more evident in diploid strains than in haploid strains, arguing that diploids (which are rarely analyzed in yeast studies of genome stability) may represent a better model for examining genome stability than haploids. I showed that restoring wild-type telomere length to *tel1 mec1* strains reduced the frequency of chromosome rearrangements without affecting the aneuploidy. Thus, the effects of Tel1p and Mec1p on chromosome number and structure can be separated. One very interesting experiment would be to examine

the expression level of the human homologues of Tel1p and Mec1p (ATM and ATR) in metastatic tumors.

Appendix A

Description of chromosome alterations in subcultured *tel1 mec1* diploid strains

Below is a detailed description of the chromosome aberrations identified in the *tel1 mec1* diploid yeast strains following approximately 100 generations of growth. Changes in chromosome number and structure were characterized with CHEF analysis, Southern blotting, CGH microarrays, "band microarrays" (hybridization of isolated chromosomes to microarrays), and PCR techniques. Except where noted, hybridization probes were generated by amplifying genomic DNA of wild-type yeast strains using pairs of PCR primers described in Table 2.3.

JLMy80-1s: Genomic microarray analysis indicated that JLMy80-1s is monosomic for chromosome I and trisomic for chromosomes X, XII, and XVI. Separation of the yeast chromosomes with CHEF electrophoresis showed two novel bands located at approximately 1070 kb (directly above chromosomes XIII/XVI) and 1300 kb. A band microarray performed with the 1070 kb chromosome following its excision from the CHEF gel indicated that the novel chromosome does not represent a translocation, but simply the addition of extra copies of the sub-telomeric Y' element to XVI. By band array analysis, the novel chromosome of 1300 kb hybridized only to chromosome XII sequences. The genomic microarray showed a significant decrease in hybridization to the ribosomal RNA (rRNA) genes that are located on XII. Since chromosome XII in the wild-type strain is about 2 Mb, we calculated that about 80 rRNA gene repeats were deleted in the 1300 kb chromosome. For all Southern analysis involving rRNA genes, we used the plasmid pY1rG12, which contains one complete copy of the 9 kb repeat (Petes *et al.*, 1978). Chromosomes V and VIII were both slightly altered in size relative to the comparable chromosomes in the wild-type strain. These altered chromosomes were not examined by band arrays.

JLMy80-2s: Genomic microarray analysis demonstrated that JLMy80-2s is trisomic for chromosomes II and XII. Chromosome X is likely tetrasomic as indicated by a signal in the microarray analysis that is approximately twice that observed with chromosomes II and XII. No novel chromosome bands were apparent according to CHEF analysis, and Southern analysis with a probe for the ribosomal DNA did not reveal an altered XII.

JLMy80-3L: Genomic microarray analysis showed that JLMy80-3L is trisomic for chromosomes II and VIII. Most of chromosome I was deleted except for a 64 kb region at the right end. The breakpoint of this deletion is at the Crick-oriented *YARCTy1-1* located at SGD coordinates 160239-166163. Microarray analysis showed a partial amplification of chromosome X that includes the left arm, extends through the centromere, and ends about 540 kb from the left telomere; there is a Crick-oriented Ty element at this position that is not annotated in SGD (Argueso *et al.*, 2008). Additionally, there is a terminal amplification on the right arm of chromosome XII with a breakpoint about 220 kb from the left telomere. There is a Crick-oriented Ty element at this position that is not annotated in SGD (Gabriel *et al.*, 2006).

CHEF gel separation of chromosomes showed two novel chromosomes, one slightly larger than chromosome II (about 850 kb) and a second slightly smaller than chromosome XII (about 1.8 Mb). Southern analysis of JLMy80-3L showed that the novel band at 850 kb hybridized to the *PDR3* probe from chromosome II (located at SGD coordinates 217-220 kb). This probe was generated by amplification of genomic DNA using the primers PDR3 F and PDR3 R (Table 2.3). Band microarray analysis of this chromosome showed that it had DNA derived from the right arm of chromosome I and almost all of chromosome II. There is a Ty element (*YBLWTy2-1*) near the left telomere of II (SGD coordinate about 29 kb). A break-induced replication (BIR) event between the *YARCTy1-1* Ty element on I and this Ty element on II would produce a chromosome of about 847 kb, approximately the size of 850 kb novel chromosome. By the genomic

microarray, all sequences on chromosome II, except for those centromere-distal to *YBLWTy2-1*, are represented in three copies; those distal to *YBLWTy2-1* are represented in two copies. If chromosome I was monosomic prior to the translocation and chromosome II was trisomic, the gene dosages according to the microarray are congruent. The Tys on chromosomes I and II are in the correct orientation for this arrangement.

The 1.8 Mb chromosome is also likely to reflect homologous recombination between the Ty elements on chromosomes X and XII. The precise size expected for such a translocation is difficult to predict, since the chromosome XII-derived segment of the translocation contains the rRNA gene tandem array. The size would be approximately 800 kb, plus the size of the rDNA array. By Southern analysis, probes derived from chromosome X (*YJR030C*, located between SGD coordinates 486188 and 483951; amplified using primers YJR030C F and YJR030C R) and XII (rDNA probe pY1rG12**),** hybridized to the 1.8 Mb chromosome. The most likely explanation for the formation of this translocation is that, in a strain trisomic for chromosome X, one of copies was broken near the Crick-oriented Ty. This broken chromosome engaged in a BIR event with the Crick-oriented Ty on chromosome XII. The resulting chromosome would be a monocentric chromosome of the observed size. Alternatively, in a strain trisomic for both chromosomes X and XII, double-strand breaks in the Ty elements of both chromosomes reannealed (single-strand annealing pathway or SSA) or recombined in a half-crossover event (Casper *et al.*, 2009).

JLMy80-4L: Genomic microarray analysis showed that JLMy80-4L is trisomic for chromosomes VIII and IX. There is a terminal amplification on the left arm of chromosome V that extends through the centromere and ends at Crick-oriented *YERCTy1-1* (SGD coordinates 443393-449316). Additionally, there is a deletion of most of chromosome VI, including the centromere, with a possible breakpoint about 100 kb from

the left telomere near *YFLWdelta1*. CHEF gel showed several novel chromosomes at approximate sizes 460 kb, 540 kb, and 625 kb. In addition, the sizes of both copies of chromosome XII were reduced in JMY80-4L. We found by Southern analysis (probe generated by amplification of genomic DNA with primers CUP1 F and CUP1 R, Table 2.3) that the strain had a deletion of *CUP1* repeats, suggesting that the 625 kb chromosome was likely a derivative of chromosome VIII with this deletion, carrying 5 *CUP1* repeats instead of 10. A V-VI translocation with the observed breakpoints would result in a novel chromosome of about 550 kb. This chromosome would be close to the size of one of the observed novel chromosomes. We did nothing further to confirm this conclusion or to characterize the other rearranged chromosomes. Finally, it was clear from the genomic microarray that the Y' repeats in JLMy80-4L were amplified.

JLMy80-5L: Genomic microarray analysis showed that JLMy80-5L is monosomic for chromosome VI and trisomic for chromosome II. Additionally, there was a tandem deletion/duplication event on chromosome III with the breakpoint at SGD coordinate 114081 (302 bp from *CEN3*). About 110 kb of the left arm is deleted and 201 kb of the right arm is duplicated. There was also an interstitial amplification on the right arm of XII with the centromere-proximal and –distal breakpoints at SGD coordinates 544799 and 949329, respectively. CHEF analysis of JLMy80-5L showed a novel chromosome of about 1350 kb, as well as a novel chromosome slightly larger than chromosome VIII, about 610 kb.

We examined the 1350 kb chromosome by band microarray. This analysis showed that this chromosome had all of chromosome II, the left arm of chromosome III, and the internal region of chromosome XII. Restriction digestion and Southern blotting revealed the orientation and connectivity of the chromosome fragments. The 1350 kb chromosome hybridized to probes derived from the left arm of chromosome III (*CHA1*, generated by amplification of genomic DNA with primers CHA1 F and CHA1 R), the

intrachromosomal region of chromosome XII (*NEJ1*, generated by amplification of genomic DNA with primers JLMo67 NEJ1 F and JLMo68 NEJ1 R), and the left arm of chromosome II (*PDR3*, described above). We used information derived from the band microarrays to design primers that would allow us to generate a PCR fragment that spanned the two breakpoints. The primers JLMo106 and JLMo119 (sequences in Table 2.3) spanned the II-XII junction, and the primers JLMo149 and JLMo158 detected the XII-III junction.

Sequencing across these breakpoints demonstrated that both junctions were formed through NHEJ events, since there was no repetitive DNA at either of the junctions. The end of chromosome II, with just two base pairs of telomeric DNA, was fused to the centromere-proximal breakpoint of chromosome XII. The centromere-distal portion of chromosome XII was fused to the left arm of chromosome III close to *CEN3*. By adding the lengths of the three component chromosomes, we calculated the translocation to be 1330 kb, close to the size observed by the CHEF gel. The simplest explanation for the tandem deletion-duplication event on III identified on the whole-genome microarray is that the tripartite chromosome exists in two copies in this strain. There is one unrearranged copy of II, one unrearranged copy of III, and two unrearranged copies of chromosome XII.

Performing a band array on the 610 kb novel chromosome, we found that it contained all of the DNA from chromosome VIII and no DNA from additional chromosomes. Using a probe for the tandem array of *CUP1* genes located on chromosome VIII (described above), we showed that the novel chromosome did not have an intrachromosomal expansion of the tandem array of *CUP1* repeats. It is possible, therefore, that the longer VIII was a consequence of additional Y' elements at the chromosome end(s).

JLMy81-1L: Genomic microarray analysis indicated that JLMy81-1L is trisomic for chromosome VIII. Additionally, there is an interstitial deletion on chromosome IV between two Crick-oriented Ty elements (*YDRCTy1-1* located at about SGD coordinate 650000 and *YDRCTy1-2* located at about SGD coordinate 880000). This deletion would reduce the size of IV from 1535 kb to about 1300 kb. We found a novel chromosome of this size by CHEF gel analysis. The 1300 kb chromosome hybridizes to sequences from the left (*LYS2*, generated by amplifying genomic DNA with primers LYS20 F and LYS20 R) and right (*DOT1*, generated by amplifying genomic DNA with primers DOT1 F and DOT1 R) arms of chromosome IV. This strain also had a deletion derivative of XII that was missing a substantial number of rRNA genes as well as the variant 5S and *ASP3* genes located immediately centromere-distal to the rRNA gene cluster (McMahon *et al.*, 1984).

JLMy81-2s: Genomic microarray analysis demonstrated that JLMy81-2s is trisomic for chromosomes I, II, X, and XII. No other obvious changes in gene dosage were detected. By CHEF gel analysis, we found a novel chromosome about 540 kb in size, slightly smaller than chromosome V. By Southern analysis, we found that this chromosome has an intrachromosomal deletion within the tandemly repeated *CUP1* loci on both copies of chromosome VIII.

JLMy81-3s: Genomic microarray analysis showed that JLMy81-3s is trisomic for chromosomes II, X, and XII. There was also a small terminal deletion on chromosome XIV near the right telomere with a breakpoint at approximately SGD coordinate 755 kb. By CHEF analysis, we observed the unrearranged chromosome XIV was missing, and the band at 750 kb (the size representing the unrearranged chromosome X) was more intense than in the progenitor parental strain. The simplest explanation of this result is that there was a double-stranded DNA break on chromosome XIV and that broken end was capped by telomere addition. Although most telomere addition is Tel1-dependent,

telomere capping has been observed in *tel1* mutant strains previously (Myung *et al.*, 2001b). Since the unrearranged chromosome XIV is missing in JLMy81-3s, it is likely that the DSB occurred in a strain that was monosomic for chromosome XIV and the deleted/capped chromosome was subsequently re-duplicated. Deletion of the terminal end of the right arm of both copies of chromosome XIV would support viability, as none of the lost genes are essential.

JLMy81-4s: Genomic microarray analysis showed that JLMy81-4s is monosomic for chromosome VI and trisomic for chromosomes II, V, and VIII. No other changes in gene dosage were evident. Separation of chromosomes with a CHEF gel indicated a chromosome slightly smaller than chromosomes V/VIII. We found that this chromosome was derived from chromosome VIII by an intrachromosomal deletion of two repeats within the tandem *CUP1* loci.

JLMy81-5L: Genomic microarray analysis demonstrated that JLMy81-5L is monosomic for chromosome VI and trisomic for chromosomes VIII and XII. Chromosomal XII had a large deletion, removing involving both the tandem array of 9 kb repeats and the centromere-distal *ASP3*/deviant 5S repeats (McMahon *et al.*, 1984). By CHEF gel analysis, we found a novel chromosome slightly larger than the V/VIII doublet. Southern analysis demonstrated that the novel chromosome resulted from amplification of the tandem *CUP1* loci on chromosome VIII.

JLMy82-1s: Genomic microarray analysis indicated that JLMy82-1s is monosomic for chromosome VI. In addition, this strain had a terminal deletion of the left arm of chromosome VII (located at SGD coordinate of 815 kb) coupled with a terminal amplification of the right arm of chromosome VII (located at SGD coordinate 115 kb). There is a full-length Ty element located at approximately SGD coordinate 115 kb that is unannotated in SGD (J. L. Argueso and A. Casper, personal communication). There is a pair of inverted Ty elements located at SGD coordinates 815 kb. Thus, the pattern of

deletion and amplification on VII can be explained by a DSB near the Ty on the left arm of VII and the repair of that DSB by a BIR event involving one of the Ty elements on the right arm. The predicted size of this chromosome is about 1250 kb and a novel chromosome of this size was detected in JLMy82-1s by CHEF gel analysis. To further confirm our conclusion, we performed a band array on the novel chromosome. As expected, the novel chromosome had chromosome VII sequences from SGD coordinates 115-1091 kb, with the region centromere-distal to coordinate 815 kb having a gene dosage greater that the rest of the chromosome.

In addition, the genomic microarray indicated that chromosome I had a small (12 kb) terminal deletion centromere-distal to *YAL065C*. We observed a novel chromosome shorter than the wild-type chromosome I, suggesting the possibility that this chromosome represented a simple deletion of chromosome I with a telomere cap. Microarray analysis also demonstrated extensive amplification of the Y′ sub-telomeric repeats in this strain.

JLMy82-2s: Genomic microarray analysis demonstrated that JLMy82-2s is trisomic for chromosomes II and XII. There is an amplification of the left arm of chromosome X with two different gene dosages (four gene copies from the left telomere through SGD coordinate 370 kb, then three copies from the centromere up to 455 kb). There is a Watson-oriented Ty1 element (*YJRWTy1-1*) located close to the right end breakpoint (SGD coordinate 473 kb) and an unannotated Ty element on the left arm of chromosome X close to 355 kb (Gabriel *et al.*, 2006). The most likely explanation consistent with this microarray pattern is a rearrangement in one copy of chromosome X in a precursor trisomic strain. A DSB in the *YJRWTy1-1* followed by repair of this break by a BIR event using the Ty element at position 355 kb would generate an isochromosome of about 830 kb. By CHEF gel analysis, we observed a novel chromosome of approximately this size. We also observed by gel analysis a novel chromosome of about 1300 kb. Band analysis

confirms that this chromosome is chromosome XII with a large deletion within the rDNA cluster.

JLMy82-3L: Genomic microarray analysis showed that JLMy82-3L is trisomic for chromosomes I, II, IV, and VIII. There is also an additional terminal duplication of the right arm of chromosome IV, starting at approximately SGD coordinate 980 kb, and an amplification of most of chromosome X, starting at approximately SGD coordinate 200 kb and extending through the centromere to the right telomere. There is a Crick-oriented delta element (*YJLCdelta3*), as well as a Watson-oriented Ty4 element located at SGD coordinate 200 kb on chromosome X and a Watson-oriented Ty2 element located at SGD coordinate 980 kb on chromosome IV. A recombination event between *YJLCdelta3* and one of the delta elements of *YDRWTy2-3* would result in a monocentric translocation of about 1180 kb. We did not observe a novel chromosome of this size, possibly because the expected size of the chromosome is similar to that of chromosome VIII (1090 kb).

The CHEF gel analysis showed that chromosome XII was missing from its normal position. Southern analysis with an rDNA probe indicated that there were multiple species of chromosome XII, representing multiple deletions, resulting in chromosome XII derivatives between 1.5 and 2 Mb in size. The genomic microarray analysis confirmed the deletion of rDNA repeats.

JLMy82-4L: Genomic microarray analysis indicated that JLMy82-4L is monosomic for chromosome I and trisomic for chromosome X. In this strain, in the CHEF gel, chromosome XII is missing from its normal migration position and there is a diffuse band in the size range of 1.5 to 2 Mb. As expected, the genomic microarray indicated a deletion of rRNA genes from the tandem array.

JLMy82-5L: Genomic microarray analysis showed that JLMy82-5L is monosomic for chromosome I and trisomic for chromosomes VIII, XI, and XII. Additionally, there is a tandem deletion/duplication event on chromosome IV. The interstitial deletion on

chromosome IV occurs between two Crick-oriented Ty elements (*YDRCTy1-1* at SGD coordinate 646 kb and *YDRCTy1-2* at SGD coordinate 878 kb). The amplification is from *YDRCTy1-2* to the right telomere. Most of chromosome V is also amplified, including the entire left arm, the centromere, and some of the right arm with the breakpoint at a Crick-oriented *YERCTy1-2* element (located at about SGD coordinate 500 kb). Separation of chromosomes with a CHEF gel demonstrated two novel chromosomes, one of about 1200 kb and one of 730 kb. Southern analysis demonstrated that the 1200 kb chromosome hybridizes with sequences from the left arm of chromosome V (*CAN1* probe generated by amplification of genomic DNA with primers CAN1 F and CAN1 R) and sequences from the right arm of chromosome IV (*DOT1*, described above). The 730 kb chromosome hybridizes band with sequences from the left arm of chromosome IV (*LYS20*, described above) and sequences from the right arm of chromosome V (*RAD24*, generated by amplification of genomic DNA with primers RAD24 F and RAD24 R).

The pathway for generating two novel chromosomes involves several steps. We suggest that the first step is an unequal crossover on one copy of chromosome IV between *YDRCTy1-1* and *YDRCTy1-2*. This chromosome then undergoes a reciprocal exchange with chromosome V between the hybrid *YDRCTy1-1* and *YDRCTy1-2* element on IV and *YERCTy1-2* on V. Finally, there is a non-disjunction of the 730 kb chromosome to generate a cell with two copies. There would still be one normal copy of chromosome IV and one normal copy of chromosome V in addition to the three rearranged chromosomes. These events would result in chromosomes of the observed sizes and are consistent with the microarray analysis.

JLMy83-1s: Genomic microarray analysis indicated that JLMy83-1s is monosomic for chromosome VI and trisomic for chromosomes VIII, XI, and XII. By CHEF gel analysis, we observed a chromosome slightly shorter than chromosome VIII. Southern analysis

demonstrated that this chromosome had a small deletion of repeats from the *CUP1* locus.

JLMy83-2L: Genomic microarray analysis showed that JLMy83-2L is monosomic for chromosomes I and VI, and trisomic for chromosomes II, IX, and X. CHEF gel analysis showed that both copies of chromosome XII were shorter than in the wild-type strain with estimated sizes of about 1425 kb and 1700 kb. Genomic microarray analysis confirmed a loss of ribosomal RNA genes in JLMy83-2L.

JLMy83-3L: By genomic microarray analysis, JLMy83-3L is trisomic for chromosomes I, II, VII, and X, and tetrasomic for chromosome IX. In addition to trisomy for chromosome I, there is a terminal amplification of the right arm of I, starting at *YARCTy1-1* (SGD coordinates of 166163-160239). There is a tandem deletion/duplication event on chromosome XVI, with most of the chromosome being amplified (except for the left end) up to Watson-oriented *YPLWTy1-1* (SGD coordinates 56452-62375). The region from the left telomere to *YPLWTy1-1* is deleted. CHEF gel analysis showed a novel chromosome about 960 kb in size. By band array analysis, we found that this chromosome had most of the sequence of XVI and the right end of chromosome I. This translocation likely arose as a consequence of a DSB at or near *YPLWTy1-1* on chromosome XVI followed by a BIR event utilizing the *YARCTy1-1* on chromosome I as a template. Based on the genomic microarray analysis, this novel chromosome is likely present in two copies. Thus, the JLMy83-3L strain has three unrearranged copies of chromosome I, one unrearranged copy of chromosome XVI, and two copies of the I-XVI translocation. Additionally, there is an amplification event on chromosome III, including the left arm, centromere, and DNA sequences up to FS2 (Lemoine *et al.*, 2005). This rearrangement was not characterized.

JLMy83-4s: Genomic microarray analysis showed that JLMy83-4s is monosomic for chromosome VI and trisomic for chromosomes I, II, VIII, and XII. Separation of

chromosomes with a CHEF gel indicated two novel chromosomes of about 850 kb and 1000 kb. Genomic microarray analysis indicated the Y′ elements were extensively duplicated in this strain and there was a substantial deletion of rRNA genes, but no other deletions and duplications were observed. By Southern analysis, we showed that the 1000 kb chromosome was a derivative of chromosome XII with a deletion of the rRNA genes. The 850 kb chromosome is likely to be derived from one of the smaller chromosomes by addition of sub-telomeric repeats; this possibility, however, was not checked by a band array.

JLMy83-5s: Genomic microarray analysis showed that JLMy83-5s is trisomic for chromosome X. No altered chromosomes were detected by CHEF gel analysis.

Appendix B

Chromosomes that are trisomic, monosomic, or rearranged in *tel1 mec1* diploids and other relevant strains

tel1 mec1 diploids after 100 generations of growth

	Trisomes	Monosomes	Rearrangements
JLMy80-1s	8, 10, 16	1	
JLMy80-2s	2, 10, 12		
JLMy80-3L	8		1, 2, 10, 12
JLMy80-4L	8, 9		5, 6
JLMy80-5L		6	2, 3, 12
JLMy81-1L	8		4
JLMy81-2s	1, 2, 10, 12		
JLMy81-3s	2, 10, 12		14
JLMy81-4s	2, 5, 8	6	
JLMy81-5L	8, 12	6	
JLMy82-1s		6	7
JLMy82-2s	2, 12		10
JLMy82-3L	1, 2, 4, 8		4, 10
JLMy82-4L	10	1	
JLMy82-5L	7, 11, 12	1	4, 5
JLMy83-1s	8, 11, 12	6	
JLMy83-2L	2, 9, 10	1, 6	
JLMy83-3L	1, 2, 7, 9, 10		1, 3, 16
JLMy83-4s	1, 2, 8, 12	6	
JLMy83-5s	10		

tel1 mec1 haploids after 100 generations of growth

	Disomes	Monosomes	Rearrangements
JLMy62-6b-2L	3		10
JLMy62-6b-3L			12
JLMy62-6b-4L	2		1, 12, 14
JLMy62-6b-5s			4
JLMy62-17c-2L	2, 8		12
JLMy62-17c-5L	2, 12		3, 10
JLMy62-18c-1L			12
JLMy62-18c-4s			1
JLMy62-18c-5L	12		12

Wild-type diploids after 100 generations of growth

	Trisomes	Monosomes	Rearrangements
JLMy100-1L			
JLMy100-2s			
JLMy101-1L			
JLMy101-2s			

tel1 diploids after 100 generations of growth

	Trisomes	Monosomes	Rearrangements
JLMy102-1L			
JLMy100-2s			
JLMy104-1L	1, 8		
JLMy104-2s		6	

mec1 sml1 diploids after 100 generations of growth

	Trisomes	Monosomes	Rearrangements
JLMy111-1L			
JLMy111-2L	9, 10		
JLMy111-3L	10		
JLMy113-1L	2		
JLMy113-1s		no alterations	
JLMy113-2L		no alterations	
JLMy113-2s	10, 14		
JLMy113-3L	8, 16		
JLMy113-3s			1, 12

tel1 mec1 + pVL1107-*URA3* diploids after 100 generations of growth

	Trisomes	Monosomes	Rearrangements
JLMy1262-1L	9		
JLMy1262-2s	8		
JLMy1262-3L	8, 9, 10	1	
JLMy1262-4s	1, 2, 7, 16		
JLMy1262-5L	2, 8, 12, 13		
JLMy1262-6s	2, 7, 12	3	
JLMy1271-1L	1, 7, 8, 9, 10		1, 4
JLMy1271-2L	1, 5, 8, 11, 13, 16		
JLMy1272-1L	5, 7, 8, 12		
JLMy1272-2s	2, 4, 8, 11		
JLMy1272-3L	8, 12		
JLMy1272-4s	1, 7, 9, 12, 13		

tel1 mec1 + pRS316 diploids after 100 generations of growth

	Trisomes	Monosomes	Rearrangements
JLMy1301-1L	8, 11, 12		
JLMy1301-2L	8		
JLMy1311-1L	12		2, 15, 16

mad2 diploids after 100 generations of growth

	Trisomes	Monosomes	Rearrangements
JLMy327-s			
JLMy328-L	11		
JLMy329-s		1	
JLMy330-L	8		
JLMy366-L			
JLMy367-s			
JLMy376-L			
JLMy377-s	1		

bub1-Δ diploids with no subculturing

	Trisomes	Monosomes	Rearrangements
JLMy148-19	2, 5, 8, 10, 14, 16		
JLMy148-48	5, 8, 10, 16		
JLMy148-108	8	3, 14	
JLMy148-112	2, 3, 8, 10		
JLMy148-132	8, 10	11	12
JLMy149-34	8	9	
JLMy149-45	8	11	
JLMy149-93	1, 2, 3, 5, 8, 10		

bub1-ΔK diploids before and after 100 generations of growth

	Subculture 0		Subculture 5 (100 generations)		
	Trisomes[1]	Monosomes	Trisomes[1]	Monosomes	Rearrangements
JLMy405-L	2, **8**		2, **8**, 10, 16		
JLMy406-s	**8**, 16		**8**, 13, 16		
JLMy407-L	2, **8**, 16		2, **8**, 16		
JLMy408-s	3, **8**		3, **8**, 16		
JLMy409-L	3, **8**, 10		3, 6, 8, 10		
JLMy410-s	**8**, 16		5, 6	9	
JLMy411-L	10, 16	1	3, 8, 14, 16		
JLMy412-s	**8**		10	11	
JLMy448-L	1, 2, **8**		2, 16		
JLMy449-s	2, **8**		2, **8**, 10		
JLMy450-L	2, **8**, 14, 16		1, 2, **8**, 14		
JLMy451-s	3, 10	9	3, 10		

[1]Chromosomes that were present as disomic or partially disomic in the haploids used to generate the parental diploids (subculture 0) are labeled in **bold**. The chromosomes in normal typeface arose independently during the course of subculturing. If a chromosome went from three copies at subculture 0 to four copies at subculture 5, it is counted as a new trisome for subculture 5.

bub1-ΔK tel1 mec1 diploids before and after 100 generations of growth

	Subculture 0		Subculture 5 (100 generations)		
	Trisomes[1]	Monosomes	Trisomes[1]	Monosomes	Rearrangements
JLMy413-1L	**1**, 2, **8**, 16		2, 4, 5, **8**, 10, 16		
JLMy413-2s	**1**, 2, **8**, 16		**1**, 2, 5, 8, 10, 13		12, 13
JLMy413-3L	**1**, 2, **8**, 16		**1**, 2, **8**, 10, 16		
JLMy414-1s	**1**, **8**, 16		**1**, 2, 10, 12, 16		3
JLMy414-2L	**1**, **8**, 16		**1**, 2, **8**, 10, 12, 16		
JLMy414-3s	**1**, **8**, 16		2, 8, 16		
JLMy415-1L	**1**, **3**, 5, **8**, 11, 13, 16		**1**, 2, **8**, 10, 11		
JLMy415-2s	**1**, **3**, 5, **8**, 11, 13, 16		**1**, **3**, 5, **8**, 9, 10, 12, 16		
JLMy415-3L	**1**, **3**, 5, **8**, 11, 13, 16		2, **3**, **8**, 10		
JLMy416-1s	**1**, **8**, 16		**8**, 10	9	12
JLMy416-2L	**1**, **8**, 16		**1**, 8, 10		3, 12
JLMy416-3s	**1**, **8**, 16		**1**, 2, 5, **8**, 10, 12, 14, 16		

[1]Chromosomes that were present as disomic or partially disomic in the haploids used to generate the parental diploids (subculture 0) are labeled in **bold**. The chromosomes in normal typeface arose independently during the course of subculturing. If a chromosome went from three copies at subculture 0 to four copies at subculture 5, it is counted as a new trisome for subculture 5.

tel1 mec1 diploids, subculture 0

	Trisomes	Monosomes	Rearrangements
JLMy80			12
JLMy81	10		12
JLMy82			12
JLMy83			12

fob1 tel1 mec1 diploids, subculture 0

	Trisomes	Monosomes	Rearrangements
JLMy229	12		
JLMy230	12		
JLMy233	12		
JLMy237	12		

tel1 mec1 diploids + pRS316-*SRL2* or pRS426-*SRL2*, subculture 0

	Trisomes	Monosomes	Rearrangements
JLMy350			12
JLMy354	8		12
JLMy356			12
JLMy360			12

tel1 mec1 diploids + pRS316-*DNA2* after 100 generations of growth

	Trisomes	Monosomes	Rearrangements
JLMy342-1L	8		
JLMy344-2s		6	
JLMy346-1L	2, 12, 15	1	1, 12
JLMy348-2s	3, 8		

cen2::CEN14 tel1 mec1 diploids after 100 generations of growth

	Trisomes	Monosomes	Rearrangements
JLMy294-2s	1, 2, 4, 8, 10		5
JLMy294-3L	12	6	
JLMy295-1s	1, 5, 8, 10		2, 10
JLMy295-2L	2, 3, 6, 7, 8		
JLMy296-1L	2, 9, 12	3	
JLMy296-2s	2, 7, 8		
JLMy297-1s	2, 8		
JLMy297-2L	2, 7, 9, 10, 12		
JLMy298-1L	2, 9, 10, 12		
JLMy298-2s	5, 10, 12, 16		12

chk1 diploids after 100 generations of growth

	Trisomes	Monosomes	Rearrangements
JLMy444-1L			
JLMy445-1s			
JLMy460-1L			
JLMy461-1s			4, 5

sgo1 diploids after 100 generations of growth

	Trisomes	Monosomes	Rearrangements
JLMy468-1L	1, 2, 3, 5, 10		
JLMy469-1L	1, 3, 8, 10, 16		
JLMy470-1s	1, 2, 3, 5, 10, 11, 16		

mre11 diploids after 100 generations of growth

	Trisomes[1]	Monosomes	Rearrangements
JLMy483-1L			
JLMy484-1s	**5**		
JLMy485-1L	**3**, 12	1	12
JLMy486-1s			
JLMy487-1L			
JLMy488-1s	8		
JLMy489-1L	8		2, 16
JLMy490-1s	7		12

[1]Chromosomes that were present as disomic or partially disomic in the diploids prior to subculturing are labeled in **bold**.

References

Agarwal, R., Tang, Z., Yu, H., and Cohen-Fix, O. (2003). Two distinct pathways for inhibiting Pds1 ubiquitination in response to DNA damage. J Biol Chem *278*, 45027-45033.

Ahmed, M., and Rahman, N. (2006). ATM and breast cancer susceptibility. Oncogene *25*, 5906-5911.

Ahnesorg, P., and Jackson, S.P. (2007). The non-homologous end-joining protein Nej1p is a target of the DNA damage checkpoint. DNA Repair *6*, 190-201.

Albertson, D.G., Collins, C., McCormick, F., and Gray, J.W. (2003). Chromosome aberrations in solid tumors. Nat Genet *34*, 369-376.

Andersen, M.P., Nelson, Z.W., Hetrick, E.D., and Gottschling, D.E. (2008). A genetic screen for increased loss of heterozygosity in *Saccharomyces cerevisiae*. Genetics *179*, 1179-1195.

Archambault, V., Ikui, A.E., Drapkin, B.J., and Cross, F.R. (2005). Disruption of mechanisms that prevent rereplication triggers a DNA damage response. Mol Cell Biol *25*, 6707-6721.

Argueso, J.L., Westmoreland, J., Mieczkowski, P.A., Gawel, M., Petes, T.D., and Resnick, M.A. (2008). Double-strand breaks associated with repetitive DNA can reshape the genome. Proc Natl Acad Sci U S A *105*, 11845-11850.

Arlt, M.F., Casper, A.M., and Glover, T.W. (2003). Common fragile sites. Cytogenet Genome Res *100*, 92-100.

Au, W.C., Crisp, M.J., DeLuca, S.Z., Rando, O.J., and Basrai, M.A. (2008). Altered dosage and mislocalization of histone H3 and Cse4p lead to chromosome loss in *Saccharomyces cerevisiae*. Genetics *179*, 263-275.

Bachant, J., Jessen, S.R., Kavanaugh, S.E., and Fielding, C.S. (2005). The yeast S phase checkpoint enables replicating chromosomes to bi-orient and restrain spindle extension during S phase distress. J Cell Biol *168*, 999-1012.

Baker, D.J., Chen, J., and van Deursen, J.M. (2005). The mitotic checkpoint in cancer and aging: what have mice taught us? Current Opinion in Cell Biology *17*, 583-589.

Bakkenist, C.J., and Kastan, M.B. (2003). DNA damage activates ATM through intermolecular autophosphorylation and dimer dissociation. Nature *421*, 499-506.

Barber, T.D., McManus, K., Yuen, K.W., Reis, M., Parmigiani, G., Shen, D., Barrett, I., Nouhi, Y., Spencer, F., Markowitz, S., *et al.* (2008). Chromatid cohesion defects may underlie chromosome instability in human colorectal cancers. Proc Natl Acad Sci U S A *105*, 3443-3448.

Barlow, J.H., and Rothstein, R. (2009). Rad52 recruitment is DNA replication independent and regulated by Cdc28 and the Mec1 kinase. Embo J *28*, 1121-1130.

Bartkova, J., Horejsi, Z., Koed, K., Kramer, A., Tort, F., Zieger, K., Guldberg, P., Sehested, M., Nesland, J.M., Lukas, C., *et al.* (2005). DNA damage response as a candidate anti-cancer barrier in early human tumorigenesis. Nature *434*, 864-870.

Ben-Aroya, S., Mieczkowski, P.A., Petes, T.D., and Kupiec, M. (2004). The compact chromatin structure of a Ty repeated sequence suppresses recombination hotspot activity in *Saccharomyces cerevisiae*. Mol Cell *15*, 221-231.

Bernard, P., Hardwick, K., and Javerzat, J.P. (1998). Fission yeast Bub1 is a mitotic centromere protein essential for the spindle checkpoint and the preservation of correct ploidy through mitosis. J Cell Biol *143*, 1775-1787.

Bonilla, C.Y., Melo, J.A., and Toczyski, D.P. (2008). Colocalization of sensors is sufficient to activate the DNA damage checkpoint in the absence of damage. Mol Cell *30*, 267-276.

Bourke, E., Dodson, H., Merdes, A., Cuffe, L., Zachos, G., Walker, M., Gillespie, D., and Morrison, C.G. (2007). DNA damage induces Chk1-dependent centrosome amplification. EMBO Rep *8*, 603-609.

Boveri, T. (1914). Zur Frage der Entstehung maligner Tumoren. Gustav Fischer Verlag, Jena.

Boyarchuk, Y., Salic, A., Dasso, M., and Arnaoutov, A. (2007). Bub1 is essential for assembly of the functional inner centromere. J Cell Biol *176*, 919-928.

Boyer, J.C., Umar, A., Risinger, J.I., Lipford, J.R., Kane, M., Yin, S., Barrett, J.C., Kolodner, R.D., and Kunkel, T.A. (1995). Microsatellite instability, mismatch repair deficiency, and genetic defects in human cancer cell lines. Cancer Res *55*, 6063-6070.

Brewer, B.J., and Fangman, W.L. (1988). A replication fork barrier at the 3' end of yeast ribosomal RNA genes. Cell *55*, 637-643.

Brown, E.J., and Baltimore, D. (2000). ATR disruption leads to chromosomal fragmentation and early embryonic lethality. Genes Dev *14*, 397-402.

Brush, G.S., Morrow, D.M., Hieter, P., and Kelly, T.J. (1996). The ATM homologue *MEC1* is required for phosphorylation of replication protein A in yeast. Proc Natl Acad Sci U S A *93*, 15075-15080.

Burds, A.A., Lutum, A.S., and Sorger, P.K. (2005). Generating chromosome instability through the simultaneous deletion of Mad2 and p53. Proc Natl Acad Sci U S A *102*, 11296-11301.

Cahill, D.P., Lengauer, C., Yu, J., Riggins, G.J., Willson, J.K., Markowitz, S.D., Kinzler, K.W., and Vogelstein, B. (1998). Mutations of mitotic checkpoint genes in human cancers. Nature *392*, 300-303.

Campbell, D., Doctor, J.S., Feuersanger, J.H., and Doolittle, M.M. (1981). Differential mitotic stability of yeast disomes derived from triploid meiosis. Genetics *98*, 239-255.

Carminati, J.L., and Stearns, T. (1999). Cytoskeletal dynamics in yeast. Methods Cell Biol *58*, 87-105.

Casper, A.M., Durkin, S.G., Arlt, M.F., and Glover, T.W. (2004). Chromosomal instability at common fragile sites in Seckel syndrome. Am J Hum Genet *75*, 654-660.

Casper, A.M., Greenwell, P.W., Tang, W., and Petes, T.D. (2009). Chromosome aberrations resulting from double-strand DNA breaks at a naturally occurring yeast fragile site composed of inverted ty elements are independent of Mre11p and Sae2p. Genetics *183*, 423-439, 421SI-426SI.

Casper, A.M., Mieczkowski, P.A., Gawel, M., and Petes, T.D. (2008). Low levels of DNA polymerase alpha induce mitotic and meiotic instability in the ribosomal DNA gene cluster of *Saccharomyces cerevisiae*. Plos Genetics *4*, -.

Casper, A.M., Nghiem, P., Arlt, M.F., and Glover, T.W. (2002). ATR regulates fragile site stability. Cell *111*, 779-789.

Celeste, A., Petersen, S., Romanienko, P.J., Fernandez-Capetillo, O., Chen, H.T., Sedelnikova, O.A., Reina-San-Martin, B., Coppola, V., Meffre, E., Difilippantonio, M.J., *et al.* (2002). Genomic instability in mice lacking histone H2AX. Science *296*, 922-927.

Cha, R.S., and Kleckner, N. (2002). ATR homolog Mec1 promotes fork progression, thus averting breaks in replication slow zones. Science *297*, 602-606.

Chan, C.S., and Botstein, D. (1993). Isolation and characterization of chromosome-gain and increase-in-ploidy mutants in yeast. Genetics *135*, 677-691.

Chan, C.S., and Tye, B.K. (1983). Organization of DNA sequences and replication origins at yeast telomeres. Cell *33*, 563-573.

Cheeseman, I.M., Brew, C., Wolyniak, M., Desai, A., Anderson, S., Muster, N., Yates, J.R., Huffaker, T.C., Drubin, D.G., and Barnes, G. (2001). Implication of a novel multiprotein Dam1p complex in outer kinetochore function. J Cell Biol *155*, 1137-1145.

Chen, C., and Kolodner, R.D. (1999). Gross chromosomal rearrangements in *Saccharomyces cerevisiae* replication and recombination defective mutants. Nat Genet *23*, 81-85.

Chen, S.H., Smolka, M.B., and Zhou, H. (2007). Mechanism of Dun1 activation by Rad53 phosphorylation in *Saccharomyces cerevisiae*. J Biol Chem *282*, 986-995.

Christianson, T.W., Sikorski, R.S., Dante, M., Shero, J.H., and Hieter, P. (1992). Multifunctional yeast high-copy-number shuttle vectors. Gene *110*, 119-122.

Cimini, D. (2008). Merotelic kinetochore orientation, aneuploidy, and cancer. Biochim Biophys Acta *1786*, 32-40.

Cimprich, K.A., and Cortez, D. (2008). ATR: an essential regulator of genome integrity. Nat Rev Mol Cell Biol *9*, 616-627.

Clemenson, C., and Marsolier-Kergoat, M.C. (2006). The spindle assembly checkpoint regulates the phosphorylation state of a subset of DNA checkpoint proteins in Saccharomyces cerevisiae. Mol Cell Biol *26*, 9149-9161.

Clerici, M., Baldo, V., Mantiero, D., Lottersberger, F., Lucchini, G., and Longhese, M.P. (2004). A Tel1/MRX-dependent checkpoint inhibits the metaphase-to-anaphase transition after UV irradiation in the absence of Mec1. Mol Cell Biol *24*, 10126-10144.

Cohen-Fix, O., and Koshland, D. (1997). The anaphase inhibitor of *Saccharomyces cerevisiae* Pds1p is a target of the DNA damage checkpoint pathway. Proc Natl Acad Sci U S A *94*, 14361-14366.

Collura, A., Blaisonneau, J., Baldacci, G., and Francesconi, S. (2005). The fission yeast Crb2/Chk1 pathway coordinates the DNA damage and spindle checkpoint in response to replication stress induced by topoisomerase I inhibitor. Mol Cell Biol *25*, 7889-7899.

Cortez, D., Wang, Y., Qin, J., and Elledge, S.J. (1999). Requirement of ATM-dependent phosphorylation of Brca1 in the DNA damage response to double-strand breaks. Science *286*, 1162-1166.

Craven, R.J., Greenwell, P.W., Dominska, M., and Petes, T.D. (2002). Regulation of genome stability by *TEL1* and *MEC1*, yeast homologs of the mammalian ATM and ATR genes. Genetics *161*, 493-507.

D'Amours, D., Stegmeier, F., and Amon, A. (2004). Cdc14 and condensin control the dissolution of cohesin-independent chromosome linkages at repeated DNA. Cell *117*, 455-469.

de Klein, A., Muijtjens, M., van Os, R., Verhoeven, Y., Smit, B., Carr, A.M., Lehmann, A.R., and Hoeijmakers, J.H. (2000). Targeted disruption of the cell-cycle checkpoint gene ATR leads to early embryonic lethality in mice. Curr Biol *10*, 479-482.

de Lange, T. (2002). Protection of mammalian telomeres. Oncogene *21*, 532-540.

De Wulf, P., McAinsh, A.D., and Sorger, P.K. (2003). Hierarchical assembly of the budding yeast kinetochore from multiple subcomplexes. Genes Dev *17*, 2902-2921.

Deem, A., Barker, K., Vanhulle, K., Downing, B., Vayl, A., and Malkova, A. (2008). Defective break-induced replication leads to half-crossovers in *Saccharomyces cerevisiae*. Genetics *179*, 1845-1860.

Defossez, P.A., Prusty, R., Kaeberlein, M., Lin, S.J., Ferrigno, P., Silver, P.A., Keil, R.L., and Guarente, L. (1999). Elimination of replication block protein Fob1 extends the life span of yeast mother cells. Mol Cell *3*, 447-455.

DeRisi, J.L., Iyer, V.R., and Brown, P.O. (1997). Exploring the metabolic and genetic control of gene expression on a genomic scale. Science *278*, 680-686.

Desany, B.A., Alcasabas, A.A., Bachant, J.B., and Elledge, S.J. (1998). Recovery from DNA replicational stress is the essential function of the S-phase checkpoint pathway. Genes Dev *12*, 2956-2970.

Downs, J.A., Allard, S., Jobin-Robitaille, O., Javaheri, A., Auger, A., Bouchard, N., Kron, S.J., Jackson, S.P., and Cote, J. (2004). Binding of chromatin-modifying activities to phosphorylated histone H2A at DNA damage sites. Mol Cell *16*, 979-990.

Downs, J.A., Lowndes, N.F., and Jackson, S.P. (2000). A role for *Saccharomyces cerevisiae* histone H2A in DNA repair. Nature *408*, 1001-1004.

Draviam, V.M., Xie, S., and Sorger, P.K. (2004). Chromosome segregation and genomic stability. Current Opinion in Genetics & Development *14*, 120-125.

Dudasova, Z., Dudas, A., and Chovanec, M. (2004). Non-homologous end-joining factors of *Saccharomyces cerevisiae*. FEMS Microbiol Rev *28*, 581-601.

Duesberg, P., Rausch, C., Rasnick, D., and Hehlmann, R. (1998). Genetic instability of cancer cells is proportional to their degree of aneuploidy. Proc Natl Acad Sci U S A *95*, 13692-13697.

Elledge, S.J. (1996). Cell cycle checkpoints: preventing an identity crisis. Science *274*, 1664-1672.

Emili, A. (1998). *MEC1*-dependent phosphorylation of Rad9p in response to DNA damage. Mol Cell *2*, 183-189.

Evans, S.K., and Lundblad, V. (1999). Est1 and Cdc13 as comediators of telomerase access. Science *286*, 117-120.

Fang, G., Yu, H., and Kirschner, M.W. (1998). The checkpoint protein MAD2 and the mitotic regulator CDC20 form a ternary complex with the anaphase-promoting complex to control anaphase initiation. Genes Dev *12*, 1871-1883.

Fasullo, M., and Dave, P. (1994). Mating type regulates the radiation-associated stimulation of reciprocal translocation events in *Saccharomyces cerevisiae*. Mol Gen Genet *243*, 63-70.

Feldser, D.M., Hackett, J.A., and Greider, C.W. (2003). Telomere dysfunction and the initiation of genome instability. Nat Rev Cancer *3*, 623-627.

Feng, W., Bachant, J., Collingwood, D., Raghuraman, M.K., and Brewer, B.J. (2009). Centromere replication timing determines different forms of genomic instability in *Saccharomyces cerevisiae* checkpoint mutants during replication stress. Genetics *183*, 1249-1260.

Fernius, J., and Hardwick, K.G. (2007). Bub1 kinase targets Sgo1 to ensure efficient chromosome biorientation in budding yeast mitosis. PLoS Genet *3*, e213.

Friedel, A.M., Pike, B.L., and Gasser, S.M. (2009). ATR/Mec1: coordinating fork stability and repair. Curr Opin Cell Biol *21*, 237-244.

Fritz, E., Friedl, A.A., Zwacka, R.M., Eckardt-Schupp, F., and Meyn, M.S. (2000). The yeast *TEL1* gene partially substitutes for human *ATM* in suppressing hyperrecombination, radiation-induced apoptosis and telomere shortening in A-T cells. Mol Biol Cell *11*, 2605-2616.

Fu, Y., Pastushok, L., and Xiao, W. (2008). DNA damage-induced gene expression in Saccharomyces cerevisiae. FEMS Microbiol Rev *32*, 908-926.

Fukasawa, K., Choi, T., Kuriyama, R., Rulong, S., and Vande Woude, G.F. (1996). Abnormal centrosome amplification in the absence of p53. Science *271*, 1744-1747.

Gabriel, A., Dapprich, J., Kunkel, M., Gresham, D., Pratt, S.C., and Dunham, M.J. (2006). Global mapping of transposon location. PLoS Genet *2*, e212.

Ganem, N.J., Godinho, S.A., and Pellman, D. (2009). A mechanism linking extra centrosomes to chromosomal instability. Nature *460*, 278-282.

Garber, P.M., and Rine, J. (2002). Overlapping roles of the spindle assembly and DNA damage checkpoints in the cell-cycle response to altered chromosomes *in Saccharomyces cerevisiae*. Genetics *161*, 521-534.

Gardner, R.D., Poddar, A., Yellman, C., Tavormina, P.A., Monteagudo, M.C., and Burke, D.J. (2001). The spindle checkpoint of the yeast *Saccharomyces cerevisiae* requires kinetochore function and maps to the CBF3 domain. Genetics *157*, 1493-1502.

Gasch, A.P., Huang, M., Metzner, S., Botstein, D., Elledge, S.J., and Brown, P.O. (2001). Genomic expression responses to DNA-damaging agents and the regulatory role of the yeast ATR homolog Mec1p. Mol Biol Cell *12*, 2987-3003.

Gatei, M., Scott, S.P., Filippovitch, I., Soronika, N., Lavin, M.F., Weber, B., and Khanna, K.K. (2000). Role for ATM in DNA damage-induced phosphorylation of BRCA1. Cancer Res *60*, 3299-3304.

Goldstein, A.L., and McCusker, J.H. (1999). Three new dominant drug resistance cassettes for gene disruption in *Saccharomyces cerevisiae*. Yeast *15*, 1541-1553.

Gorgoulis, V.G., Vassiliou, L.V., Karakaidos, P., Zacharatos, P., Kotsinas, A., Liloglou, T., Venere, M., Ditullio, R.A., Jr., Kastrinakis, N.G., Levy, B., *et al.* (2005). Activation of the DNA damage checkpoint and genomic instability in human precancerous lesions. Nature *434*, 907-913.

Goudsouzian, L.K., Tuzon, C.T., and Zakian, V.A. (2006). *S. cerevisiae* Tel1p and Mre11p are required for normal levels of Est1p and Est2p telomere association. Mol Cell *24*, 603-610.

Green, B.M., and Li, J.J. (2005). Loss of rereplication control in *Saccharomyces cerevisiae* results in extensive DNA damage. Mol Biol Cell *16*, 421-432.

Greenwell, P.W., Kronmal, S.L., Porter, S.E., Gassenhuber, J., Obermaier, B., and Petes, T.D. (1995). *TEL1*, a gene involved in controlling telomere length in *S. cerevisiae*, is homologous to the human Ataxia Telangiectasia gene. Cell *82*, 823-829.

Haase, S.B., Winey, M., and Reed, S.I. (2001). Multi-step control of spindle pole body duplication by cyclin-dependent kinase. Nat Cell Biol *3*, 38-42.

Hackett, J.A., and Greider, C.W. (2002). Balancing instability: dual roles for telomerase and telomere dysfunction in tumorigenesis. Oncogene *21*, 619-626.

Hackett, J.A., and Greider, C.W. (2003). End resection initiates genomic instability in the absence of telomerase. Mol Cell Biol *23*, 8450-8461.

Hanahan, D., and Weinberg, R.A. (2000). The hallmarks of cancer. Cell *100*, 57-70.

Harrison, J.C., and Haber, J.E. (2006). Surviving the breakup: the DNA damage checkpoint. Annu Rev Genet *40*, 209-235.

Harvey, A.C., Jackson, S.P., and Downs, J.A. (2005). *Saccharomyces cerevisiae* histone H2A Ser122 facilitates DNA repair. Genetics *170*, 543-553.

He, X., Asthana, S., and Sorger, P.K. (2000). Transient sister chromatid separation and elastic deformation of chromosomes during mitosis in budding yeast. Cell *101*, 763-775.

Heidinger-Pauli, J.M., Unal, E., Guacci, V., and Koshland, D. (2008). The kleisin subunit of cohesin dictates damage-induced cohesion. Mol Cell *31*, 47-56.

Heude, M., and Fabre, F. (1993). a/alpha-control of DNA repair in the yeast *Saccharomyces cerevisiae*: genetic and physiological aspects. Genetics *133*, 489-498.

Hollstein, M., Sidransky, D., Vogelstein, B., and Harris, C.C. (1991). p53 mutations in human cancers. Science *253*, 49-53.

Howlett, N.G., and Schiestl, R.H. (2004). Nucleotide excision repair deficiency causes elevated levels of chromosome gain in *Saccharomyces cerevisiae*. DNA Repair *3*, 127-134.

Hoyt, M.A., Stearns, T., and Botstein, D. (1990). Chromosome instability mutants of Saccharomyces cerevisiae that are defective in microtubule-mediated processes. Mol Cell Biol *10*, 223-234.

Hoyt, M.A., Totis, L., and Roberts, B.T. (1991). *S. cerevisiae* genes required for cell cycle arrest in response to loss of microtubule function. Cell *66*, 507-517.

Hughes, T.R., Roberts, C.J., Dai, H., Jones, A.R., Meyer, M.R., Slade, D., Burchard, J., Dow, S., Ward, T.R., Kidd, M.J., *et al.* (2000). Widespread aneuploidy revealed by DNA microarray expression profiling. Nat Genet *25*, 333-337.

Hyman, A.A., and Sorger, P.K. (1995). Structure and function of kinetochores in budding yeast. Annu Rev Cell Dev Biol *11*, 471-495.

Indjeian, V.B., and Murray, A.W. (2007). Budding yeast mitotic chromosomes have an intrinsic bias to biorient on the spindle. Curr Biol *17*, 1837-1846.

Ivanov, E.L., Sugawara, N., Fishman-Lobell, J., and Haber, J.E. (1996). Genetic requirements for the single-strand annealing pathway of double-strand break repair in *Saccharomyces cerevisiae*. Genetics *142*, 693-704.

Ivessa, A.S., Zhou, J.Q., and Zakian, V.A. (2000). The *Saccharomyces* Pif1p DNA helicase and the highly related Rrm3p have opposite effects on replication fork progression in ribosomal DNA. Cell *100*, 479-489.

Jallepalli, P.V., and Lengauer, C. (2001). Chromosome segregation and cancer: cutting through the mystery. Nat Rev Cancer *1*, 109-117.

Jardim, M.J., Wang, Q., Furumai, R., Wakeman, T., Goodman, B.K., and Wang, X.F. (2009). Reduced ATR or Chk1 expression leads to chromosome instability and chemosensitization of mismatch repair-deficient colorectal cancer cells. Molecular Biology of the Cell *20*, 3801-3809.

Jaspersen, S.L., and Winey, M. (2004). The budding yeast spindle pole body: structure, duplication, and function. Annu Rev Cell Dev Biol *20*, 1-28.

Jeggo, P.A., and Lobrich, M. (2006). Contribution of DNA repair and cell cycle checkpoint arrest to the maintenance of genomic stability. DNA Repair *5*, 1192-1198.

Johnston, M., Hillier, L., Riles, L., Albermann, K., Andre, B., Ansorge, W., Benes, V., Bruckner, M., Delius, H., Dubois, E., *et al.* (1997). The nucleotide sequence of *Saccharomyces cerevisiae* chromosome XII. Nature *387*, 87-90.

Johzuka, K., and Horiuchi, T. (2002). Replication fork block protein, Fob1, acts as an rDNA region specific recombinator in *S. cerevisiae*. Genes Cells *7*, 99-113.

Jung, D., Giallourakis, C., Mostoslavsky, R., and Alt, F.W. (2006). Mechanism and control of V(D)J recombination at the immunoglobulin heavy chain locus. Annu Rev Immunol *24*, 541-570.

Kadura, S., and Sazer, S. (2005). SAC-ing mitotic errors: how the spindle assembly checkpoint (SAC) plays defense against chromosome mis-segregation. Cell Motil Cytoskeleton *61*, 145-160.

Kastan, M.B., and Bartek, J. (2004). Cell-cycle checkpoints and cancer. Nature *432*, 316-323.

Kato, R., and Ogawa, H. (1994). An essential gene, ESR1, is required for mitotic cell growth, DNA repair and meiotic recombination in Saccharomyces cerevisiae. Nucleic Acids Res *22*, 3104-3112.

Kawashima, S.A., Yamagishi, Y., Honda, T., Ishiguro, K., and Watanabe, Y. (2010). Phosphorylation of H2A by Bub1 prevents chromosomal instability through localizing shugoshin. Science *327*, 172-177.

Kaye, J.A., Melo, J.A., Cheung, S.K., Vaze, M.B., Haber, J.E., and Toczyski, D.P. (2004). DNA breaks promote genomic instability by impeding proper chromosome segregation. Curr Biol *14*, 2096-2106.

Kegel, A., Sjostrand, J.O., and Astrom, S.U. (2001). Nej1p, a cell type-specific regulator of nonhomologous end joining in yeast. Curr Biol *11*, 1611-1617.

Kendall, S.D., Linardic, C.M., Adam, S.J., and Counter, C.M. (2005). A network of genetic events sufficient to convert normal human cells to a tumorigenic state. Cancer Res *65*, 9824-9828.

Kiburz, B.M., Reynolds, D.B., Megee, P.C., Marston, A.L., Lee, B.H., Lee, T.I., Levine, S.S., Young, R.A., and Amon, A. (2005). The core centromere and Sgo1 establish a 50-kb cohesin-protected domain around centromeres during meiosis I. Genes Dev *19*, 3017-3030.

Kim, E.M., and Burke, D.J. (2008). DNA damage activates the SAC in an ATM/ATR-dependent manner, independently of the kinetochore. PLoS Genet *4*, e1000015.

Kim, J.M., Vanguri, S., Boeke, J.D., Gabriel, A., and Voytas, D.F. (1998). Transposable elements and genome organization: a comprehensive survey of retrotransposons revealed by the complete *Saccharomyces cerevisiae* genome sequence. Genome Res *8*, 464-478.

Kim, N.W., Piatyszek, M.A., Prowse, K.R., Harley, C.B., West, M.D., Ho, P.L., Coviello, G.M., Wright, W.E., Weinrich, S.L., and Shay, J.W. (1994). Specific association of human telomerase activity with immortal cells and cancer. Science *266*, 2011-2015.

Kim, S.T., Xu, B., and Kastan, M.B. (2002). Involvement of the cohesin protein, Smc1, in Atm-dependent and independent responses to DNA damage. Genes Dev *16*, 560-570.

Kitagawa, R., and Kastan, M.B. (2005). The ATM-dependent DNA damage signaling pathway. Cold Spring Harb Symp Quant Biol *70*, 99-109.

Klein, H.L. (2001). Spontaneous chromosome loss in *Saccharomyces cerevisiae* is suppressed by DNA damage checkpoint functions. Genetics *159*, 1501-1509.

Kobayashi, T. (2003). The replication fork barrier site forms a unique structure with Fob1p and inhibits the replication fork. Mol Cell Biol *23*, 9178-9188.

Kobayashi, T., Heck, D.J., Nomura, M., and Horiuchi, T. (1998). Expansion and contraction of ribosomal DNA repeats in *Saccharomyces cerevisiae*: requirement of replication fork blocking (Fob1) protein and the role of RNA polymerase I. Genes Dev *12*, 3821-3830.

Kobayashi, T., and Horiuchi, T. (1996). A yeast gene product, Fob1 protein, required for both replication fork blocking and recombinational hotspot activities. Genes Cells *1*, 465-474.

Kojis, T.L., Schreck, R.R., Gatti, R.A., and Sparkes, R.S. (1989). Tissue specificity of chromosomal rearrangements in ataxia-telangiectasia. Hum Genet *83*, 347-352.

Kondo, T., Wakayama, T., Naiki, T., Matsumoto, K., and Sugimoto, K. (2001). Recruitment of Mec1 and Ddc1 checkpoint proteins to double-strand breaks through distinct mechanisms. Science *294*, 867-870.

Kops, G.J., Weaver, B.A., and Cleveland, D.W. (2005). On the road to cancer: aneuploidy and the mitotic checkpoint. Nat Rev Cancer *5*, 773-785.

Krogh, B.O., and Symington, L.S. (2004). Recombination proteins in yeast. Annu Rev Genet *38*, 233-271.

Lavin, M.F. (2008). Ataxia-telangiectasia: from a rare disorder to a paradigm for cell signalling and cancer. Nat Rev Mol Cell Biol *9*, 759-769.

Lechner, J., and Carbon, J. (1991). A 240 kd multisubunit protein complex, CBF3, is a major component of the budding yeast centromere. Cell *64*, 717-725.

Lee, K.H., Kim, D.W., Bae, S.H., Kim, J.A., Ryu, G.H., Kwon, Y.N., Kim, K.A., Koo, H.S., and Seo, Y.S. (2000). The endonuclease activity of the yeast Dna2 enzyme is essential in vivo. Nucleic Acids Res *28*, 2873-2881.

Lee, S.E., Paques, F., Sylvan, J., and Haber, J.E. (1999). Role of yeast SIR genes and mating type in directing DNA double-strand breaks to homologous and non-homologous repair paths. Curr Biol *9*, 767-770.

Lemoine, F.J., Degtyareva, N.P., Lobachev, K., and Petes, T.D. (2005). Chromosomal translocations in yeast induced by low levels of DNA polymerase a model for chromosome fragile sites. Cell *120*, 587-598.

Lengauer, C., Kinzler, K.W., and Vogelstein, B. (1997). Genetic instability in colorectal cancers. Nature *386*, 623-627.

Lengauer, C., Kinzler, K.W., and Vogelstein, B. (1998). Genetic instabilities in human cancers. Nature *396*, 643-649.

Levine, A.J. (1997). p53, the cellular gatekeeper for growth and division. Cell *88*, 323-331.

Lew, D.J., and Burke, D.J. (2003). The spindle assembly and spindle position checkpoints. Annu Rev Genet *37*, 251-282.

Li, R., and Murray, A.W. (1991). Feedback control of mitosis in budding yeast. Cell *66*, 519-531.

Li, X., and Nicklas, R.B. (1995). Mitotic forces control a cell-cycle checkpoint. Nature *373*, 630-632.

Liang, F., and Wang, Y. (2007). DNA damage checkpoints inhibit mitotic exit by two different mechanisms. Mol Cell Biol *27*, 5067-5078.

Linskens, M.H., Harley, C.B., West, M.D., Campisi, J., and Hayflick, L. (1995). Replicative senescence and cell death. Science *267*, 17.

Linskens, M.H., and Huberman, J.A. (1988). Organization of replication of ribosomal DNA in *Saccharomyces cerevisiae*. Mol Cell Biol *8*, 4927-4935.

Llorente, B., Smith, C.E., and Symington, L.S. (2008). Break-induced replication: what is it and what is it for? Cell Cycle *7*, 859-864.

Loeb, L.A. (1991). Mutator phenotype may be required for multistage carcinogenesis. Cancer Res *51*, 3075-3079.

Logarinho, E., and Bousbaa, H. (2008). Kinetochore-microtubule interactions "in check" by Bub1, Bub3 and BubR1: The dual task of attaching and signalling. Cell Cycle *7*, 1763-1768.

Longtine, M.S., McKenzie, A., 3rd, Demarini, D.J., Shah, N.G., Wach, A., Brachat, A., Philippsen, P., and Pringle, J.R. (1998). Additional modules for versatile and economical PCR-based gene deletion and modification in *Saccharomyces cerevisiae*. Yeast *14*, 953-961.

Lustig, A.J., and Petes, T.D. (1986). Identification of yeast mutants with altered telomere structure. Proc Natl Acad Sci U S A *83*, 1398-1402.

Lydeard, J.R., Jain, S., Yamaguchi, M., and Haber, J.E. (2007). Break-induced replication and telomerase-independent telomere maintenance require Pol32. Nature *448*, 820-823.

Machin, F., Torres-Rosell, J., De Piccoli, G., Carballo, J.A., Cha, R.S., Jarmuz, A., and Aragon, L. (2006). Transcription of ribosomal genes can cause nondisjunction. J Cell Biol *173*, 893-903.

Malkova, A., Ivanov, E.L., and Haber, J.E. (1996). Double-strand break repair in the absence of *RAD51* in yeast: a possible role for break-induced DNA replication. Proc Natl Acad Sci U S A *93*, 7131-7136.

Mallory, J.C., and Petes, T.D. (2000). Protein kinase activity of Tel1p and Mec1p, two *Saccharomyces cerevisiae* proteins related to the human ATM protein kinase. Proc Natl Acad Sci U S A *97*, 13749-13754.

Marcand, S., Pardo, B., Gratias, A., Cahun, S., and Callebaut, I. (2008). Multiple pathways inhibit NHEJ at telomeres. Genes Dev *22*, 1153-1158.

Maringele, L., and Lydall, D. (2002). EXO1-dependent single-stranded DNA at telomeres activates subsets of DNA damage and spindle checkpoint pathways in budding yeast yku70Delta mutants. Genes Dev *16*, 1919-1933.

Mayer, V.W., and Aguilera, A. (1990). High levels of chromosome instability in polyploids of *Saccharomyces cerevisiae*. Mutat Res *231*, 177-186.

McGill, C., Shafer, B., and Strathern, J. (1989). Coconversion of flanking sequences with homothallic switching. Cell *57*, 459-467.

McMahon, M.E., Stamenkovich, D., and Petes, T.D. (1984). Tandemly arranged variant 5S ribosomal RNA genes in the yeast *Saccharomyces cerevisiae*. Nucleic Acids Res *12*, 8001-8016.

Melo, J.A., Cohen, J., and Toczyski, D.P. (2001). Two checkpoint complexes are independently recruited to sites of DNA damage in vivo. Genes Dev *15*, 2809-2821.

Metcalfe, J.A., Parkhill, J., Campbell, L., Stacey, M., Biggs, P., Byrd, P.J., and Taylor, A.M. (1996). Accelerated telomere shortening in Ataxia Telangiectasia. Nat Genet *13*, 350-353.

Meyn, M.S. (1999). Ataxia-telangiectasia, cancer and the pathobiology of the ATM gene. Clin Genet *55*, 289-304.

Michaelis, C., Ciosk, R., and Nasmyth, K. (1997). Cohesins: chromosomal proteins that prevent premature separation of sister chromatids. Cell *91*, 35-45.

Mieczkowski, P.A., Mieczkowska, J.O., Dominska, M., and Petes, T.D. (2003). Genetic regulation of telomere-telomere fusions in the yeast *Saccharomyces cerevisae*. Proc Natl Acad Sci U S A *100*, 10854-10859.

Mikhailov, A., Cole, R.W., and Rieder, C.L. (2002). DNA damage during mitosis in human cells delays the metaphase/anaphase transition via the spindle-assembly checkpoint. Curr Biol *12*, 1797-1806.

Moore, J.D., Yazgan, O., Ataian, Y., and Krebs, J.E. (2007). Diverse roles for histone H2A modifications in DNA damage response pathways in yeast. Genetics *176*, 15-25.

Mordes, D.A., Nam, E.A., and Cortez, D. (2008). Dpb11 activates the Mec1-Ddc2 complex. Proc Natl Acad Sci U S A *105*, 18730-18734.

Morrison, A.J., Kim, J.A., Person, M.D., Highland, J., Xiao, J., Wehr, T.S., Hensley, S., Bao, Y., Shen, J., Collins, S.R., *et al.* (2007). Mec1/Tel1 phosphorylation of the INO80 chromatin remodeling complex influences DNA damage checkpoint responses. Cell *130*, 499-511.

Morrow, D.M., Connelly, C., and Hieter, P. (1997). "Break copy" duplication: a model for chromosome fragment formation in *Saccharomyces cerevisiae*. Genetics *147*, 371-382.

Morrow, D.M., Tagle, D.A., Shiloh, Y., Collins, F.S., and Hieter, P. (1995). *TEL1*, an *S. cerevisiae* homolog of the human gene mutated in Ataxia Telangiectasia, is functionally related to the yeast checkpoint gene *MEC1*. Cell *82*, 831-840.

Moynahan, M.E., and Jasin, M. Mitotic homologous recombination maintains genomic stability and suppresses tumorigenesis. Nat Rev Mol Cell Biol *11*, 196-207.

Musacchio, A., and Salmon, E.D. (2007). The spindle-assembly checkpoint in space and time. Nat Rev Mol Cell Biol *8*, 379-393.

Musaro, M., Ciapponi, L., Fasulo, B., Gatti, M., and Cenci, G. (2008). Unprotected *Drosophila melanogaster* telomeres activate the spindle assembly checkpoint. Nat Genet *40*, 362-366.

Myung, K., Chen, C., and Kolodner, R.D. (2001a). Multiple pathways cooperate in the suppression of genome instability in *Saccharomyces cerevisiae*. Nature *411*, 1073-1076.

Myung, K., Datta, A., and Kolodner, R.D. (2001b). Suppression of spontaneous chromosomal rearrangements by S phase checkpoint functions in *Saccharomyces cerevisiae*. Cell *104*, 397-408.

Myung, K., and Kolodner, R.D. (2002). Suppression of genome instability by redundant S-phase checkpoint pathways in *Saccharomyces cerevisiae*. Proc Natl Acad Sci U S A *99*, 4500-4507.

Myung, K., Pennaneach, V., Kats, E.S., and Kolodner, R.D. (2003). *Saccharomyces cerevisiae* chromatin-assembly factors that act during DNA replication function in the maintenance of genome stability. Proc Natl Acad Sci U S A *100*, 6640-6645.

Myung, K., Smith, S., and Kolodner, R.D. (2004). Mitotic checkpoint function in the formation of gross chromosomal rearrangements in *Saccharomyces cerevisiae*. Proc Natl Acad Sci U S A *101*, 15980-15985.

Nakada, D., Matsumoto, K., and Sugimoto, K. (2003). ATM-related Tel1 associates with double-strand breaks through an Xrs2-dependent mechanism. Genes Dev *17*, 1957-1962.

Narayanan, V., Mieczkowski, P.A., Kim, H.M., Petes, T.D., and Lobachev, K.S. (2006). The pattern of gene amplification is determined by the chromosomal location of hairpin-capped breaks. Cell *125*, 1283-1296.

Navadgi-Patil, V.M., and Burgers, P.M. (2008). Yeast DNA replication protein Dpb11 activates the Mec1/ATR checkpoint kinase. J Biol Chem *283*, 35853-35859.

Nekrasov, V.S., Smith, M.A., Peak-Chew, S., and Kilmartin, J.V. (2003). Interactions between centromere complexes in *Saccharomyces cerevisiae*. Mol Biol Cell *14*, 4931-4946.

Nowak, M.A., Komarova, N.L., Sengupta, A., Jallepalli, P.V., Shih Ie, M., Vogelstein, B., and Lengauer, C. (2002). The role of chromosomal instability in tumor initiation. Proc Natl Acad Sci U S A *99*, 16226-16231.

O'Driscoll, M., Ruiz-Perez, V.L., Woods, C.G., Jeggo, P.A., and Goodship, J.A. (2003). A splicing mutation affecting expression of Ataxia-Telangiectasia and Rad3-related protein (ATR) results in Seckel syndrome. Nat Genet *33*, 497-501.

Ortiz, J., Stemmann, O., Rank, S., and Lechner, J. (1999). A putative protein complex consisting of Ctf19, Mcm21, and Okp1 represents a missing link in the budding yeast kinetochore. Genes Dev *13*, 1140-1155.

Pandita, T.K. (2002). ATM function and telomere stability. Oncogene *21*, 611-618.

Paques, F., and Haber, J.E. (1999). Multiple pathways of recombination induced by double-strand breaks in *Saccharomyces cerevisiae*. Microbiol Mol Biol Rev *63*, 349-404.

Parenteau, J., and Wellinger, R.J. (1999). Accumulation of single-stranded DNA and destabilization of telomeric repeats in yeast mutant strains carrying a deletion of *RAD27*. Mol Cell Biol *19*, 4143-4152.

Pasero, P., Bensimon, A., and Schwob, E. (2002). Single-molecule analysis reveals clustering and epigenetic regulation of replication origins at the yeast rDNA locus. Genes Dev *16*, 2479-2484.

Petes, T.D. (1979). Yeast ribosomal DNA genes are located on chromosome XII. Proc Natl Acad Sci U S A *76*, 410-414.

Petes, T.D., Hereford, L.M., and Skryabin, K.G. (1978). Characterization of two types of yeast ribosomal DNA genes. J Bacteriol *134*, 295-305.

Petes, T.D., and Williamson, D.H. (1975). Replicating circular DNA molecules in yeast. Cell *4*, 249-253.

Petukhova, G., Stratton, S., and Sung, P. (1998). Catalysis of homologous DNA pairing by yeast Rad51 and Rad54 proteins. Nature *393*, 91-94.

Petukhova, G., Sung, P., and Klein, H. (2000). Promotion of Rad51-dependent D-loop formation by yeast recombination factor Rdh54/Tid1. Genes Dev *14*, 2206-2215.

Pinsky, B.A., Tatsutani, S.Y., Collins, K.A., and Biggins, S. (2003). An Mtw1 complex promotes kinetochore biorientation that is monitored by the Ipl1/Aurora protein kinase. Dev Cell *5*, 735-745.

Putnam, C.D., Hayes, T.K., and Kolodner, R.D. (2009a). Specific pathways prevent duplication-mediated genome rearrangements. Nature *460*, 984-989.

Putnam, C.D., Jaehnig, E.J., and Kolodner, R.D. (2009b). Perspectives on the DNA damage and replication checkpoint responses in *Saccharomyces cerevisiae*. DNA Repair *8*, 974-982.

Putnam, C.D., Pennaneach, V., and Kolodner, R.D. (2005). *Saccharomyces cerevisiae* as a model system to define the chromosomal instability phenotype. Mol Cell Biol *25*, 7226-7238.

Rajagopalan, H., Nowak, M.A., Vogelstein, B., and Lengauer, C. (2003). The significance of unstable chromosomes in colorectal cancer. Nat Rev Cancer *3*, 695-701.

Raveendranathan, M., Chattopadhyay, S., Bolon, Y.T., Haworth, J., Clarke, D.J., and Bielinsky, A.K. (2006). Genome-wide replication profiles of S-phase checkpoint mutants reveal fragile sites in yeast. Embo J *25*, 3627-3639.

Reid, R.J., Sunjevaric, I., Voth, W.P., Ciccone, S., Du, W., Olsen, A.E., Stillman, D.J., and Rothstein, R. (2008). Chromosome-scale genetic mapping using a set of 16 conditionally stable *Saccharomyces cerevisiae* chromosomes. Genetics *180*, 1799-1808.

Renwick, A., Thompson, D., Seal, S., Kelly, P., Chagtai, T., Ahmed, M., North, B., Jayatilake, H., Barfoot, R., Spanova, K., *et al.* (2006). ATM mutations that cause ataxia-telangiectasia are breast cancer susceptibility alleles. Nat Genet *38*, 873-875.

Rieder, C.L., Cole, R.W., Khodjakov, A., and Sluder, G. (1995). The checkpoint delaying anaphase in response to chromosome monoorientation is mediated by an inhibitory signal produced by unattached kinetochores. J Cell Biol *130*, 941-948.

Ritchie, K.B., Mallory, J.C., and Petes, T.D. (1999). Interactions of *TLC1* (which encodes the RNA subunit of telomerase), *TEL1*, and *MEC1* in regulating telomere length in the yeast *Saccharomyces cerevisiae*. Mol Cell Biol *19*, 6065-6075.

Rogakou, E.P., Pilch, D.R., Orr, A.H., Ivanova, V.S., and Bonner, W.M. (1998). DNA double-stranded breaks induce histone H2AX phosphorylation on serine 139. J Biol Chem *273*, 5858-5868.

Sabatier, L., Ricoul, M., Pottier, G., and Murnane, J.P. (2005). The loss of a single telomere can result in instability of multiple chromosomes in a human tumor cell line. Mol Cancer Res *3*, 139-150.

Saffer, L.D., and Miller, O.L., Jr. (1986). Electron microscopic study of *Saccharomyces cerevisiae* rDNA chromatin replication. Mol Cell Biol *6*, 1148-1157.

Sanchez, Y., Bachant, J., Wang, H., Hu, F., Liu, D., Tetzlaff, M., and Elledge, S.J. (1999). Control of the DNA damage checkpoint by Chk1 and Rad53 protein kinases through distinct mechanisms. Science *286*, 1166-1171.

Santocanale, C., and Diffley, J.F. (1998). A Mec1- and Rad53-dependent checkpoint controls late-firing origins of DNA replication. Nature *395*, 615-618.

Schatz, P.J., Solomon, F., and Botstein, D. (1988). Isolation and characterization of conditional-lethal mutations in the *TUB1* alpha-tubulin gene of the yeast *Saccharomyces cerevisiae*. Genetics *120*, 681-695.

Schiestl, R.H., and Gietz, R.D. (1989). High efficiency transformation of intact yeast cells using single stranded nucleic acids as a carrier. Curr Genet *16*, 339-346.

Schmidt, K.H., Pennaneach, V., Putnam, C.D., and Kolodner, R.D. (2006). Analysis of gross-chromosomal rearrangements in *Saccharomyces cerevisiae*. Methods Enzymol *409*, 462-476.

Schollaert, K.L., Poisson, J.M., Searle, J.S., Schwanekamp, J.A., Tomlinson, C.R., and Sanchez, Y. (2004). A role for *Saccharomyces cerevisiae* Chk1p in the response to replication blocks. Mol Biol Cell *15*, 4051-4063.

Searle, J.S., Schollaert, K.L., Wilkins, B.J., and Sanchez, Y. (2004). The DNA damage checkpoint and PKA pathways converge on APC substrates and Cdc20 to regulate mitotic progression. Nat Cell Biol *6*, 138-145.

Shi, Q., and King, R.W. (2005). Chromosome nondisjunction yields tetraploid rather than aneuploid cells in human cell lines. Nature *437*, 1038-1042.

Shigeta, T., Takagi, M., Delia, D., Chessa, L., Iwata, S., Kanke, Y., Asada, M., Eguchi, M., and Mizutani, S. (1999). Defective control of apoptosis and mitotic spindle checkpoint in heterozygous carriers of ATM mutations. Cancer Res *59*, 2602-2607.

Shih, I.M., Zhou, W., Goodman, S.N., Lengauer, C., Kinzler, K.W., and Vogelstein, B. (2001). Evidence that genetic instability occurs at an early stage of colorectal tumorigenesis. Cancer Res *61*, 818-822.

Shrivastav, M., De Haro, L.P., and Nickoloff, J.A. (2008). Regulation of DNA double-strand break repair pathway choice. Cell Res *18*, 134-147.

Shroff, R., Arbel-Eden, A., Pilch, D., Ira, G., Bonner, W.M., Petrini, J.H., Haber, J.E., and Lichten, M. (2004). Distribution and dynamics of chromatin modification induced by a defined DNA double-strand break. Curr Biol *14*, 1703-1711.

Sikorski, R.S., and Hieter, P. (1989). A system of shuttle vectors and yeast host strains designed for efficient manipulation of DNA in *Saccharomyces cerevisiae*. Genetics *122*, 19-27.

Skibbens, R.V. (2004). Chl1p, a DNA helicase-like protein in budding yeast, functions in sister-chromatid cohesion. Genetics *166*, 33-42.

Skryabin, K.G., Eldarov, M.A., Larionov, V.L., Bayev, A.A., Klootwijk, J., de Regt, V.C., Veldman, G.M., Planta, R.J., Georgiev, O.I., and Hadjiolov, A.A. (1984). Structure and function of the nontranscribed spacer regions of yeast rDNA. Nucleic Acids Res *12*, 2955-2968.

Smolka, M.B., Albuquerque, C.P., Chen, S.H., and Zhou, H. (2007). Proteome-wide identification of in vivo targets of DNA damage checkpoint kinases. Proc Natl Acad Sci U S A *104*, 10364-10369.

Spencer, F., Gerring, S.L., Connelly, C., and Hieter, P. (1990). Mitotic chromosome transmission fidelity mutants in *Saccharomyces cerevisiae*. Genetics *124*, 237-249.

Stankovic, T., Weber, P., Stewart, G., Bedenham, T., Murray, J., Byrd, P.J., Moss, P.A., and Taylor, A.M. (1999). Inactivation of ataxia telangiectasia mutated gene in B-cell chronic lymphocytic leukaemia. Lancet *353*, 26-29.

Steinberg-Neifach, O., and Eshel, D. (2002). Heterozygosity in *MAT* locus affects stability and function of microtubules in yeast. Biol Cell *94*, 147-156.

Stern, B.M., and Murray, A.W. (2001). Lack of tension at kinetochores activates the spindle checkpoint in budding yeast. Curr Biol *11*, 1462-1467.

Stilgenbauer, S., Schaffner, C., Litterst, A., Liebisch, P., Gilad, S., Bar-Shira, A., James, M.R., Lichter, P., and Dohner, H. (1997). Biallelic mutations in the *ATM* gene in T-prolymphocytic leukemia. Nat Med *3*, 1155-1159.

Storici, F., Lewis, L.K., and Resnick, M.A. (2001). In vivo site-directed mutagenesis using oligonucleotides. Nat Biotechnol *19*, 773-776.

Straight, A.F., Marshall, W.F., Sedat, J.W., and Murray, A.W. (1997). Mitosis in living budding yeast: anaphase A but no metaphase plate. Science *277*, 574-578.

Strand, M., Earley, M.C., Crouse, G.F., and Petes, T.D. (1995). Mutations in the *MSH3* gene preferentially lead to deletions within tracts of simple repetitive DNA in *Saccharomyces cerevisiae*. Proc Natl Acad Sci U S A *92*, 10418-10421.

Strom, L., Karlsson, C., Lindroos, H.B., Wedahl, S., Katou, Y., Shirahige, K., and Sjogren, C. (2007). Postreplicative formation of cohesion is required for repair and induced by a single DNA break. Science *317*, 242-245.

Strunnikov, A.V., Larionov, V.L., and Koshland, D. (1993). *SMC1*: an essential yeast gene encoding a putative head-rod-tail protein is required for nuclear division and defines a new ubiquitous protein family. J Cell Biol *123*, 1635-1648.

Sugawara, N., and Haber, J.E. (1992). Characterization of double-strand break-induced recombination: homology requirements and single-stranded DNA formation. Mol Cell Biol *12*, 563-575.

Sugimoto, I., Murakami, H., Tonami, Y., Moriyama, A., and Nakanishi, M. (2004). DNA replication checkpoint control mediated by the spindle checkpoint protein Mad2p in fission yeast. J Biol Chem *279*, 47372-47378.

Sung, P. (1997). Function of yeast Rad52 protein as a mediator between replication protein A and the Rad51 recombinase. J Biol Chem *272*, 28194-28197.

Swift, M., Reitnauer, P.J., Morrell, D., and Chase, C.L. (1987). Breast and other cancers in families with Ataxia-Telangiectasia. N Engl J Med *316*, 1289-1294.

Szostak, J.W., Orr-Weaver, T.L., Rothstein, R.J., and Stahl, F.W. (1983). The double-strand-break repair model for recombination. Cell *33*, 25-35.

Szostak, J.W., and Wu, R. (1980). Unequal crossing over in the ribosomal DNA of *Saccharomyces cerevisiae*. Nature *284*, 426-430.

Takagi, M., Delia, D., Chessa, L., Iwata, S., Shigeta, T., Kanke, Y., Goi, K., Asada, M., Eguchi, M., Kodama, C., *et al.* (1998). Defective control of apoptosis, radiosensitivity, and spindle checkpoint in Ataxia Telangiectasia. Cancer Res *58*, 4923-4929.

Takeuchi, Y., Horiuchi, T., and Kobayashi, T. (2003). Transcription-dependent recombination and the role of fork collision in yeast rDNA. Genes Dev *17*, 1497-1506.

Tanaka, T.U., Stark, M.J., and Tanaka, K. (2005). Kinetochore capture and bi-orientation on the mitotic spindle. Nat Rev Mol Cell Biol *6*, 929-942.

Teixeira da Costa, L., and Lengauer, C. (2002). Exploring and exploiting instability. Cancer Biol Ther *1*, 212-225.

Theunissen, J.W., Kaplan, M.I., Hunt, P.A., Williams, B.R., Ferguson, D.O., Alt, F.W., and Petrini, J.H. (2003). Checkpoint failure and chromosomal instability without lymphomagenesis in *Mre11*$^{(ATLD1/ATLD1)}$ mice. Mol Cell *12*, 1511-1523.

Thompson, D., Duedal, S., Kirner, J., McGuffog, L., Last, J., Reiman, A., Byrd, P., Taylor, M., and Easton, D.F. (2005). Cancer risks and mortality in heterozygous *ATM* mutation carriers. J Natl Cancer Inst *97*, 813-822.

Toh, G.W., and Lowndes, N.F. (2003). Role of the *Saccharomyces cerevisiae* Rad9 protein in sensing and responding to DNA damage. Biochem Soc Trans *31*, 242-246.

Toh, G.W., O'Shaughnessy, A.M., Jimeno, S., Dobbie, I.M., Grenon, M., Maffini, S., O'Rorke, A., and Lowndes, N.F. (2006). Histone H2A phosphorylation and H3 methylation are required for a novel Rad9 DSB repair function following checkpoint activation. DNA Repair *5*, 693-703.

Torres, E.M., Sokolsky, T., Tucker, C.M., Chan, L.Y., Boselli, M., Dunham, M.J., and Amon, A. (2007). Effects of aneuploidy on cellular physiology and cell division in haploid yeast. Science *317*, 916-924.

Treuner, K., Helton, R., and Barlow, C. (2004). Loss of Rad52 partially rescues tumorigenesis and T-cell maturation in Atm-deficient mice. Oncogene *23*, 4655-4661.

Tseng, S.F., Lin, J.J., and Teng, S.C. (2006). The telomerase-recruitment domain of the telomere binding protein Cdc13 is regulated by Mec1p/Tel1p-dependent phosphorylation. Nucleic Acids Res *34*, 6327-6336.

Tsukamoto, Y., Taggart, A.K., and Zakian, V.A. (2001). The role of the Mre11-Rad50-Xrs2 complex in telomerase- mediated lengthening of *Saccharomyces cerevisiae* telomeres. Curr Biol *11*, 1328-1335.

Unal, E., Arbel-Eden, A., Sattler, U., Shroff, R., Lichten, M., Haber, J.E., and Koshland, D. (2004). DNA damage response pathway uses histone modification to assemble a double-strand break-specific cohesin domain. Mol Cell *16*, 991-1002.

Unal, E., Heidinger-Pauli, J.M., and Koshland, D. (2007). DNA double-strand breaks trigger genome-wide sister-chromatid cohesion through Eco1 (Ctf7). Science *317*, 245-248.

Valencia, M., Bentele, M., Vaze, M.B., Herrmann, G., Kraus, E., Lee, S.E., Schar, P., and Haber, J.E. (2001). NEJ1 controls non-homologous end joining in *Saccharomyces cerevisiae*. Nature *414*, 666-669.

Vernon, M., Lobachev, K., and Petes, T.D. (2008). High rates of "unselected" aneuploidy and chromosome rearrangements in *tel1 mec1* haploid yeast strains. Genetics *179*, 237-247.

Vialard, J.E., Gilbert, C.S., Green, C.M., and Lowndes, N.F. (1998). The budding yeast Rad9 checkpoint protein is subjected to Mec1/Tel1-dependent hyperphosphorylation and interacts with Rad53 after DNA damage. Embo J *17*, 5679-5688.

Vorechovsky, I., Luo, L., Dyer, M.J., Catovsky, D., Amlot, P.L., Yaxley, J.C., Foroni, L., Hammarstrom, L., Webster, A.D., and Yuille, M.A. (1997). Clustering of missense mutations in the Ataxia-Telangiectasia gene in a sporadic T-cell leukaemia. Nat Genet *17*, 96-99.

Wach, A., Brachat, A., Pohlmann, R., and Philippsen, P. (1994). New heterologous modules for classical or PCR-based gene disruptions in *Saccharomyces cerevisiae*. Yeast *10*, 1793-1808.

Wai, H.H., Vu, L., Oakes, M., and Nomura, M. (2000). Complete deletion of yeast chromosomal rDNA repeats and integration of a new rDNA repeat: use of rDNA deletion strains for functional analysis of rDNA promoter elements in vivo. Nucleic Acids Res *28*, 3524-3534.

Walmsley, R.W., Chan, C.S., Tye, B.K., and Petes, T.D. (1984). Unusual DNA sequences associated with the ends of yeast chromosomes. Nature *310*, 157-160.

Wang, B.D., Eyre, D., Basrai, M., Lichten, M., and Strunnikov, A. (2005). Condensin binding at distinct and specific chromosomal sites in the *Saccharomyces cerevisiae* genome. Mol Cell Biol *25*, 7216-7225.

Wang, H., Liu, D., Wang, Y., Qin, J., and Elledge, S.J. (2001). Pds1 phosphorylation in response to DNA damage is essential for its DNA damage checkpoint function. Genes Dev *15*, 1361-1372.

Warren, C.D., Brady, D.M., Johnston, R.C., Hanna, J.S., Hardwick, K.G., and Spencer, F.A. (2002). Distinct chromosome segregation roles for spindle checkpoint proteins. Mol Biol Cell *13*, 3029-3041.

Warren, C.D., Eckley, D.M., Lee, M.S., Hanna, J.S., Hughes, A., Peyser, B., Jie, C., Irizarry, R., and Spencer, F.A. (2004). S-phase checkpoint genes safeguard high-fidelity sister chromatid cohesion. Mol Biol Cell *15*, 1724-1735.

Weitao, T., Budd, M., and Campbell, J.L. (2003). Evidence that yeast *SGS1, DNA2, SRS2*, and *FOB1* interact to maintain rDNA stability. Mutat Res *532*, 157-172.

Westmoreland, J., Ma, W., Yan, Y., Van Hulle, K., Malkova, A., and Resnick, M.A. (2009). RAD50 is required for efficient initiation of resection and recombinational repair at random, gamma-induced double-strand break ends. PLoS Genet *5*, e1000656.

Wigge, P.A., and Kilmartin, J.V. (2001). The Ndc80p complex from *Saccharomyces cerevisiae* contains conserved centromere components and has a function in chromosome segregation. J Cell Biol *152*, 349-360.

Williams, B.R., and Amon, A. (2009). Aneuploidy: cancer's fatal flaw? Cancer Res *69*, 5289-5291.

Williams, B.R., Prabhu, V.R., Hunter, K.E., Glazier, C.M., Whittaker, C.A., Housman, D.E., and Amon, A. (2008). Aneuploidy affects proliferation and spontaneous immortalization in mammalian cells. Science *322*, 703-709.

Williams, G.L., Roberts, T.M., and Gjoerup, O.V. (2007). Bub1: escapades in a cellular world. Cell Cycle *6*, 1699-1704.

Wyatt, H.R., Liaw, H., Green, G.R., and Lustig, A.J. (2003). Multiple roles for *Saccharomyces cerevisiae* histone H2A in telomere position effect, Spt phenotypes and double-strand-break repair. Genetics *164*, 47-64.

Xu, B., Kim, S., and Kastan, M.B. (2001). Involvement of Brca1 in S-phase and G(2)-phase checkpoints after ionizing irradiation. Mol Cell Biol *21*, 3445-3450.

Xu, Y., Ashley, T., Brainerd, E.E., Bronson, R.T., Meyn, M.S., and Baltimore, D. (1996). Targeted disruption of *ATM* leads to growth retardation, chromosomal fragmentation during meiosis, immune defects, and thymic lymphoma. Genes Dev *10*, 2411-2422.

Yazdi, P.T., Wang, Y., Zhao, S., Patel, N., Lee, E.Y., and Qin, J. (2002). SMC1 is a downstream effector in the ATM/NBS1 branch of the human S-phase checkpoint. Genes Dev *16*, 571-582.

Yuen, K.W., Warren, C.D., Chen, O., Kwok, T., Hieter, P., and Spencer, F.A. (2007). Systematic genome instability screens in yeast and their potential relevance to cancer. Proc Natl Acad Sci U S A *104*, 3925-3930.

Zhang, T., Nirantar, S., Lim, H.H., Sinha, I., and Surana, U. (2009). DNA damage checkpoint maintains CDH1 in an active state to inhibit anaphase progression. Dev Cell *17*, 541-551.

Zhao, X., Muller, E.G., and Rothstein, R. (1998). A suppressor of two essential checkpoint genes identifies a novel protein that negatively affects dNTP pools. Mol Cell *2*, 329-340.

Zhao, X., and Rothstein, R. (2002). The Dun1 checkpoint kinase phosphorylates and regulates the ribonucleotide reductase inhibitor Sml1. Proc Natl Acad Sci U S A *99*, 3746-3751.

Zhao, X.L., Georgieva, B., Chabes, A., Domkin, V., Ippel, J.H., Schleucher, J., Wijmenga, S., Thelander, L., and Rothstein, R. (2000). Mutational and structural analyses of the ribonucleotide reductase inhibitor Sml1 define its Rnr1 interaction domain whose inactivation allows suppression of *mec1* and *rad53* lethality. Mol Cell Biol *20*, 9076-9083.

Zhou, B.B., and Elledge, S.J. (2000). The DNA damage response: putting checkpoints in perspective. Nature *408*, 433-439.

Zou, L., and Elledge, S.J. (2003). Sensing DNA damage through ATRIP recognition of RPA-ssDNA complexes. Science *300*, 1542-1548.

Biography

Jennifer Lynn McCulley was born to Charles Robert McCulley and Judith Ann McCulley on June 16, 1981 in Port Jefferson, NY. She has two brothers, Mark Stewart McCulley and Ryan Douglas McCulley.

EDUCATION

Ph.D. in Molecular Cancer Biology
Duke University, Durham, NC. May 2010

Bachelor of Arts in Chemistry and Biological Sciences
Degree with Distinction
Goucher College, Baltimore, MD. May 2003

ACADEMIC AWARDS AND FELLOWSHIPS

National Science Foundation Graduate Student Fellowship	2005-2008
James B. Duke Fellowship, Duke University	2003-2007
Conference Travel Fellowship, Duke University	2007
NCAA Postgraduate Scholarship	2003
Phi Beta Kappa National Honor Society	2003
Stimson-Duvall Graduate Fellowship, Goucher College	2003
The Jessie L. King Prize in Biology, Goucher College	2003
The Hilda Gabrilove '48 and Dr. Janice Gabrilove Dirzulaitis '73 Chemistry Prize, Goucher College	2003
Senior Leadership Award, Goucher College	2003
Milly Bielaski Prize in Chemistry, Goucher College	2002
Scholar-Athlete Award, Goucher College	2002
Claasen Award for Chemistry Research, Goucher College	2001
Goucher College Dean's Scholarship, full tuition to Goucher College	1999-2003
Goucher College Dean's List	1999-2003
Maryland Distinguished Scholar Award	1999